Structural design of a reinforced concrete tsunami-resistant building for vertical evacuation structure in Bo. Espinal-Aguada, Puerto Rico

By

ARIEL ANDRÉS MARRERO-IRIZARRY

A thesis submitted in partial fulfillment of the requirements for the degree of
MASTER OF SCIENCE
IN
CIVIL ENGINEERING

UNIVERSITY OF PUERTO RICO
MAYAGÜEZ CAMPUS
2015

Approved by:

Luis E. Suárez-Colche, PhD Member, Graduate Committee	Date
Miguel F. Canals-Silander, PhD Member, Graduate Committee	Date
José A. Martínez-Cruzado, PhD President, Graduate Committee	Date
Aurelio Mercado-Irizarry, PhD Representative of Graduate Studies	Date
Ismael Pagán-Trinidad, MSCE Chairperson of the Department	Date

ABSTRACT

After the disasters caused by the Ocean Indian Tsunami (2004) and Tohoku Tsunami (2011), the society is much more aware of the necessity to have available vertical evacuation structures from tsunami. This situation has highlighted the need to incorporate the tsunami-resistant design in the building codes. For this reason, federal agencies and the academic sector have joined efforts to produce design guidelines such as FEMA P-646, to eventually incorporate them in future building codes. This study focused on the design of a reinforced concrete tsunami-resistant building to serve as a vertical evacuation structure for Bo. Espinal-Aguada, PR using the guidelines of FEMA P-646. Particular site data including, demographic information, tsunami risk evaluations, tsunami design hydrodynamic parameters, and FEMA P-646 tsunami load calculation provisions were required to perform the vertical evacuation structure design in this research work.

The vertical evacuation structure was designed to provide refuge area for little more than 85% of the residents. In addition, attributes of tsunami-resistant structures defined by FEMA P-646 were adopted. Since the computed tsunami hydrodynamic parameters were relative low for this particular area, the design was governed by the earthquake load combinations in many of the structural members. However, slab system were designed against the uplift effects from tsunami for the first two stories. Moreover, building displacement and inter-story drift curves were developed to compare the structure behavior due to tsunami and earthquake loads separately, where seismic loads resulted in higher displacements and higher drift values for this particular case. Suggested ideas to protect deep foundations from scouring were presented and a rough cost estimate of the vertical evacuation structure was performed. The present work could be considered as a methodology for the design of vertical evacuation structures in high risk coastal communities around the island of Puerto Rico.

RESUMEN

Luego de los desastres causados por el Tsunami del Océano Índico (2004) y el Tsunami de Japón (2011), la sociedad está mucho más consciente de la necesidad de diseñar estructuras para el desalojo vertical por tsunami. Esta situación ha resaltado la necesidad de incorporar el diseño tsunami-resistente en los códigos de edificación. Por esta razón, ciertas agencias federales y el sector académico han unido esfuerzos para producir guías de diseño como lo es el FEMA P-646, para eventualmente incorporarlas a los futuros códigos de edificación. Este estudio está enfocado en el diseño de un edificio tsunami-resistente en hormigón armado a ser catalogado como una estructura de desalojo vertical en el Bo. Espinal de Aguada, PR, utilizando las guías del artículo FEMA P-646. Datos particulares que incluyen población, evaluación de riesgos de tsunami, parámetros hidrodinámicos del tsunami de diseño, y las provisiones del cálculo de cargas de tsunami descritas en el FEMA P-646, fueron utilizados para realizar el diseño de la estructura de desalojo vertical en este proyecto de investigación.

La estructura de desalojo vertical fue diseñada para proveer refugio a un poco más del 85% de los residentes de dicha comunidad costera. En adición, fueron adoptados los atributos y consideraciones definidos por el artículo FEMA P-646 para estructuras tsunami-resistentes. Debido a que los parámetros hidrodinámicos del tsunami de diseño fueron relativamente bajos para esta área en particular, el diseño fue controlado por la carga de terremoto para la mayoría de los componentes estructurales del edificio. Sin embargo, para los primeros dos niveles del edificio los sistemas de losa, fueron diseñados para los efectos de levantamiento causados por el tsunami. Por otra parte, se desarrollaron curvas de desplazamiento del edificio y curvas de deriva entre pisos para comparar el comportamiento del edificio debido a cargas de tsunami y cargas de terremoto por individual. De estas, es notable que para este caso en particular, la carga de terremoto produce valores mayores, tanto de desplazamientos como de deriva entre pisos. Se presentan ideas sugeridas para la protección contra socavación de las fundaciones profundas, y además un estimado de costo aproximado de la estructura de desalojo vertical. Este trabajo puede ser considerado como una metodología para el diseño de estructuras de desalojo vertical en comunidades costeras con alto riesgo de tsunami alrededor de la isla de Puerto Rico.

Dedication

I dedicate this work to God, who has given me the life, and the opportunity to undertake an academic career. To my parents, my wife to be, and siblings, whom have been part of the support to accomplish this goal.

To the families and friends of the victims whom died for not having an appropriate vertical evacuation structure during previous tsunami events.

ACKNOWLEDGEMENTS

Firstly, I would like to express my gratitude to God for the blessings, the power of will, and lessons that I have received during my entire life. I also thank to all the people involved during my years of studies and development. Thanks to my parents, late Lucas Marrero-Berrios, and Lucybel Irizarry-Sierra for being my role models, and for teaching me to strive forward with faith to achieve any established goal, despite how hard it could be. Thanks to my wife to be and to my family for believing in me and for their disinterested support through these years.

I would like to thank to my advisor Dr. José A. Martínez-Cruzado for the opportunity to work on this investigation and for his commitment, support and guidance throughout our academic relationship. I would also like to thank to my graduate committee, Dr. Miguel Canals and Dr. Luis Suárez, for their help and assistance during my college experience and during this investigation.

I want to acknowledge the different members that help me out in gathering material to accomplish this work. I'm particularly grateful with Dr. Aurelio Mercado for tsunami simulation results and Roy Ruíz for the Census data. In addition, I would like to thank my colleagues Lionel Crúz, Miriam Romero, and Manuel Coll for their support and help in this research work.

Finally, I would like to thank the Chairperson of the Civil Engineering Department, Prof. Ismael Pagán, the General Engineering Department, and the Puerto Rico Strong Motion Program for the financial support during my Master's degree.

TABLE OF CONTENTS

LIST OF TABLES

LIST OF FIGURES

CHAPTER 1 - INTRODUCTION

1.1 Introduction and Justification

Tsunami are one of the more dangerous nature events known consisting in a series of waves with long wavelength caused by an impulsive disturbance that displaces a body of water. Tsunami is a Japanese word for “harbor wave,” which is sometimes mistakenly referred to as a tidal wave. Tsunamis usually are triggered by earthquakes, but with a less probability can also be generated by landslides, undersea slumps, volcanic eruptions or even an impact of a large object falling into the ocean (FEMA P-646, 2012).

In the deep ocean the tsunami waves, propagate at high velocities (hundreds of miles per hour) with an imperceptible water surface slopes. The sea bottom depth variations modify the height, velocity, and the direction of propagation. As the waves approach the coast, the shallow waters cause them to slow down while the height increases as a transformation of kinetic energy to potential energy takes place.

Tsunamis often appears as a quick rise in sea level or as a bore of turbulent water causing extensive flooding inland areas and carrying waterborne debris which eventually cause damage to structures. Tsunamis are classified by the location of the source and the time it takes to reach a given site. For a far-source tsunamis, there is usually a lead-time of two or more hours before its arrival, allowing for advance warning to distant coastal communities. For near-source tsunamis, however, the lead-time is reduced to 30 minutes or less where generally the effects of the triggering event are the first tsunami warning. Mid-source tsunamis is estimated to arrive between 30 minutes and two hours after the triggering event (Pacheco & Robertson, 2005). Coastal communities located in high risk seismic zones, as in the Caribbean, are mostly vulnerable to near-source tsunamis generated by a local earthquake.

In some locations, high ground may not exist, or tsunamis triggered by local events may not allow sufficient warning time for communities to evacuate low elevation areas. For this case, where horizontal evacuation out of the tsunami inundation zone is neither possible nor practical, a potential solution is vertical evacuation into the upper levels of structures designed and detailed to withstand the effects of a tsunami. "A vertical evacuation refuge from tsunamis is an earthen mound or a building that has sufficient height to elevate evacuees above the level of tsunami inundation, which is designed and constructed with the strength and resiliency needed to resist the effects of tsunami waves" (FEMA P-646, 2012).

Although there is significant damage and often total destruction of residential and light framed buildings during extreme flooding, there are also a number of examples of mid- to high-rise engineered structures that survived tsunami inundation. This justifies the consideration of vertical evacuation as a feasible option when horizontal evacuation out of the inundation zone is not promising. *The purpose of this work is to design a vertical evacuation structure able to withstand the effects of a tsunami event, providing an alternative evacuation solution to the coastal community for the particular case of Bo. Espinal at Aguada, PR.*

1.2 Research Objectives

The specific objectives of this research work can be summarized as follows:

- Evaluate the Bo. Espinal coastal community in terms of tsunami flood zone, tsunami evacuation zone, evacuation routes, road accesses, population, housing distribution, and a potential construction site.
- Determine the tsunami forces using tsunami simulation results from MOST[1] (PMEL) numerical model, performed by Mercado et al. (2011) and provisions in FEMA P-646.
- Evaluate the uses and applications of the proposed vertical evacuation structure (VES) when not serving as a refuge considering the Puerto Rico 2010 Census data. Determine the sizing and elevation considerations of the proposed structure, based on the characteristics of Bo.

[1] (MOST) Method of Splitting Tsunamis (Tang, 2009), developed by the Pacific Marine Environmental Laboratory (PMEL)

Espinal and using FEMA P-646 as a guide.

- Design a VES against wind, earthquake, and tsunami loadings following the structural design criteria and considerations presented in FEMA P-646 to provide a solution to mitigate the local tsunami risk.
- Compare the performance in terms of displacements and inter-story drifts of the designed building subjected to earthquake loads and to tsunami loads individually.
- Suggest the foundations design criteria based on previous geotechnical studies in or near the selected coastal community and provide a rough cost estimate of the structure.

1.3 Background

Information from historic tsunami events shows that tsunami behaviors cannot be inferred from common knowledge or perception due to its discrepancies in characteristics from other coastal hazards. The unique timescale associated with tsunami phenomena is the primary reason for this distinction. Wave periods in tsunamis can range from a few minutes to over one hour, distinct to typical wind-generated water waves that are characterized by periods between 5 and 20 seconds (FEMA, 2005). This timescale is also important because of the potential for wave reflection, amplification, or resonance within coastal features.

Tsunamis hydrodynamic properties are highly influenced by the tsunami waveform and the surrounding topography and bathymetry leading to a considerable uncertainty in its predictions. Even though there are exceptions, previous research and field surveys indicate that tsunamis have the following general characteristics: (1) the period of the resulting waves, and generally the damage potential are determined by the magnitude of the triggering event (FEMA, 2005). (2) A tsunami can travel more than several thousand kilometers without losing energy. (3) Tsunami energy propagation has strong directivity, meaning that the majority of its energy will be emitted in a direction normal to the major axis of the tsunami source. Hence the more elongated the tsunami source, the stronger the directivity (Okal, 2003; Carrier and Yeh, 2005). (4) The first leading wave is often a receding water level followed by an advancing positive heave (an elevation wave), for a locally-generated tsunami. (5) Tsunami run-up[2] height varies significantly

[2] Wave run-up is the maximum vertical extent of wave up-rush on a beach or structure above the still water level.

in neighboring areas, as the configuration of the continental shelf and shoreline affect tsunami impacts at the shoreline through wave reflection, refraction, and shoaling. Furthermore changes in offshore bathymetry and shoreline irregularities can focus or disperse tsunami wave energy along certain shoreline reaches, increasing or decreasing tsunami impacts (FEMA, 2005).

The frequency and distribution of recorded run-up, can characterize the relative tsunami hazard. Quantifying the severity of the tsunami hazard should be the first step given a known or perceived tsunami threat in a region. This can include a probabilistic assessment considering all possible tsunami sources, or a deterministic assessment considering the maximum tsunami that can reasonably be expected to affect a site. The design tsunami event is termed the Maximum Considered Tsunami (MCT). However, there is no methodology for setting a Maximum Considered Tsunami at a specified hazard level. For the design considerations, it is expected that the hazard level corresponding to the Maximum Considered Tsunami will be consistent with the 2500-year recurrence period associated with the Maximum Considered Earthquake (MCE) used in seismic design (FEMA P-646, 2012).

During a tsunami event, an efficient warning system and evacuation to high ground outside of the anticipated inundation area are the most important procedures for reducing loss of life. In the event of a tsunami triggered by a local-source earthquake, the severe ground-shaking serves as an immediate warning, preferably confirmed by successive official warnings. Public education and tsunami drills are essential to make known these procedures to the local population. However, there are some communities where evacuation to high ground outside the inundation zone is not possible in the time between the tsunami warning and inundation (Robertson, 2012).

During past damaging tsunami events, thousands of lives have been saved through people’s intuition to seek refuge in the upper floors of buildings and other structures in the inundation area. This was particularly evident in areas in Japan inundated by the Tohoku Tsunami. Many evacuees were able to make their way to elevated ground or into designated vertical evacuation structures with as little as 30 minutes between the ground-shaking and tsunami inundation. Japan has built a number of vertical evacuation structures and designated numerous existing buildings as tsunami refuges, because of their long history of damaging tsunamis (Fraser, 2012). Moreover, people often used any suitable mid- to high-rise building whether or not it was formally designated for tsunami evacuation. In most of the cases this vertical evacuation saved lives. Unfortunately, there were a number of cases where designated vertical evacuation structures were totally inundated, resulting in loss of life of those seeking refuge, becoming the building elevation parameter one of the major concerns regarding design of vertical evacuation structures.

Information on the response of the built environment to devastating tsunamis and coastal flooding were provided by damage studies from historic tsunami events, the 2004 Indian Ocean Tsunami and the 2011 Tohoku Japan Tsunami, and storm surge associated with Hurricane Katrina in 2005. The structural damages from tsunamis can be attributed to: (1) direct hydrostatic and hydrodynamic forces from water flood; (2) impact forces from water-borne debris; (3) fire spread by floating debris and any combustible liquids; (4) scour and slope/foundation failure; and (5) wave motion induced by wind forces. Building survivability varies with construction type and tsunami run-up height according to studies of damages from historic tsunamis (Yeh et al., 2005). Although observations show that some types of construction are largely damaged by high velocities in water flow, there is much evidence that suitably designed structural systems can survive tsunami inundation.

Evaluation of tsunami effects in high risk coastal communities in Aguada, PR was performed in the study "Tsunami Evacuation Routes for the Municipality of Aguada, PR" by Martínez-Cruzado (2012). This study consisted on determining the time needed to evacuate the tsunami inundation zone measured from the furthermost point on each of the seven tsunami risk coastal communities in Aguada (See Table 1.1). Some standard conditions used to quantify the time included setting a pedestrian velocity of 2 mph and considering 5 minutes as reaction time before starting to walk away from the evacuation zone. Routes selected had to comply with the following conditions: The suggested routes were delimited by existing roads, bridge crossings were minimized, walking time along coastline were minimized while walking away from the inundation zones were promoted. The results of this exercise are presented in Table 1.1.

Table 1.1: Seven coastal communities in Aguada, PR considered in Martínez-Cruzado (2012) field exercise study.

Communities in the inundation zone	*Distance (mi)*	*Time (min)*
Bo. Espinal	1.75	57.5
Sector Tablonal	0.55	21.5
Bo. Carrizal	1.1	38
Parcelas Novoa	0.8	29
Balneario Pico de Piedra	1.06	36.8
Asilo, PR-115	0.55	21.5
Parcelas Nieves	0.78	28.4

From this previous study results, Bo. Espinal (see Figure 1.1) is considered to have the tsunami highest risk within the municipality of Aguada, due to its critical evacuation time.

Figure 1.1: Coastal Community, Bo. Espinal in Aguada, PR.

1.4 Methodology

The activities to be performed as part of this research work involve:

(1) **Visit Bo. Espinal to evaluate site conditions:** A field visit to Bo. Espinal is proposed to determine the potential construction site of the VES based on housing distribution and existent

evacuation routes. From the particular characteristics of the population, obtained from the Puerto Rico 2010 Census data, some applications will be suggested.

(2) **Analyze tsunami simulation data:** Tsunami simulation results performed by Mercado et al. (2011) using MOST (PMEL) numerical model will be analyzed in MATLAB to obtain the design hydrodynamic parameters such as maximum run-up height, maximum flow velocity and maximum momentum flux. Tsunami force effects described in Section 2.4, its respective equation and considerations will be used to estimate the tsunami loads for which the structure will be designed.

(3) **Architectural and a preliminary structural design:** Once the maximum run-up height is known, a building layout will be selected using structural attributes that have demonstrated good behavior in past tsunamis and any other considerations detailed in FEMA P-646. For the selected structural layout a preliminary structural designed will be performed according to existent reinforced concrete pre-dimensioning rules.

(4) **Develop a numerical model of the proposed structural layout in order to analyze the structure:** A structural numerical model will be setup in the *ETABS* software to perform a structural analysis which includes tsunami load effects, earthquake loads, wind loads and gravity loads. By means of an iterative procedure of analysis and element dimensions adjustments, an efficient design of the structure will be obtained.

1.5 Organization of the Thesis

The thesis is divided in eight chapters. A brief description of the chapters is presented next:

- Chapter 2 summarizes the literature consulted for this investigation. A review of the FEMA P-646*: Guidelines for Design of Structures for Vertical Evacuation from Tsunamis*, is presented. Includes the historic tsunami activity and equations of tsunami loadings in structures.
- Chapter 3 presents the coastal community for which this project is intended, including general information and the proposed site to build the vertical evacuation structure.

- Chapter 4 shows the analysis of the tsunami numerical simulation results obtained by Mercado et al. (2011), used to determine the design hydrodynamic parameters, such as, maximum inundation depth, maximum flow velocity, and the maximum momentum flux for the site of interest selected in Chapter 3.
- Chapter 5 presents the proposed structural layout of the vertical evacuation structures and its applications based on the demographic information discussed in Chapter 3.
- Chapter 6 presents the computations of the design loads applied to the vertical evacuation structure, including dead loads, live loads, wind load, earthquakes load and tsunami load.
- Chapter 7 presents the structural model created in the *ETABS* software and the procedure taken for the design of the floor systems, columns, beams, and wall members. In addition, this chapter include a set of suggestions for the foundations design based on the geotechnical data available for the site of interest.
- Chapter 8 summarizes the conclusions based on the results from the vertical evacuation structure design described in Chapter 7. Several recommendations for future works are also presented in this chapter.

CHAPTER 2 - LITERATURE REVIEW

2.1 Introduction

In this chapter, a review of the tsunami activity along the history, including in Puerto Rico, and the most recent events of the Indian Ocean tsunami (2004) and Tohoku Japan tsunami (2011) is presented. Furthermore, tsunami effects on buildings based on surveying and field observations, vertical evacuation design implications, and tsunami loadings provisions from FEMA P-646 are discussed. With this review it is intended to present the reader with information about the tsunami behavior and previous research on vertical evacuation structures as a potential solution for coastal regions with high risk of being affected by a tsunami event.

2.2 Historic Tsunami Activity

In less than a decade, two of the worst tsunami events were recorded: the Indian Ocean Tsunami of December 25, 2004 and just over six years ago the Tohoku Japan Tsunami of March 11, 2011. Both events captured the world's attention leaving an unforgettable mark and leading to increased research activity in the tsunami's area.

Even though tsunamis are cataloged as rare events, observations have shown its occurrence to be fairly regular around the world. Yearly, there are on average 20 tsunami-genic earthquake events, where 25 percent of these large enough to generate tsunami waves capable of causing damage and fatalities. In the 1990's decade, more than 80 tsunamis were reported, 10 of which resulted in more than 4,000 fatalities (FEMA P-646, 2012).

A way to characterize the relative tsunami hazard is through the frequency and distribution of recorded run-ups. The National Oceanic & Atmospheric Administration (NOAA) provided an assessment of tsunami hazard for regions of the United States that are threatened by tsunamis using the last 200 years of data on recorded run-ups (see Table 2.1). This table shows that the

Caribbean is a region with a high hazard based on the frequency of the tsunami events and also by the high run-ups observed. Nevertheless, the Alaska and Hawaii regions have the highest tsunami hazard, with a very high frequency run-ups and very high to severe recorded run-ups.

Table 2.1: Qualitative tsunami hazard assessment for U.S. locations (FEMA P-646).

Region	Hazard Based on Recorded Run-ups	Hazard Based on Frequency Run-ups
Atlantic Coast	None to very low	Very low
Gulf Coast	None to very low	None to very low
Caribbean	High	High
West Coast	High	High
Alaska	Very high to severe	Very high
Hawaii	Very high to severe	Very high
Western Pacific	Moderate	High

2.2.1 Puerto Rico Tsunami Activity

Puerto Rico and the U.S. Virgin Islands are located along the northern boundary of the Caribbean plate, with the Puerto Rico Trench subduction zone (the deepest in the Atlantic Ocean) located at the north of the island. At the Puerto Rico Trench, the North American Plate is obliquely subducted beneath of the Caribbean Plate to the south. This oblique subduction is accommodated by a series of active fault zones, which lie very close to the Puerto Rico's northern coast. The existence of these large, active fault zones located offshore of the island creates a high risk from earthquakes, underwater landslides and consequently potential tsunami threat for the Puerto Rican coast.

Since 1530, more than 50 tsunamis of varying intensity have occurred in the Caribbean (FEMA P-646, 2012). In 1692, massive landslides in the Puerto Rican Trench generated a tsunami which reached the coast of Jamaica, causing an estimated 2,000 deaths (Lender, 1999). In November 18, 1867, twenty days after the passage of hurricane Narciso, an earthquake of 7.3 magnitude was registered with its greatest intensity felt in the U.S. Virgin Islands and in the eastern coast of Puerto Rico. The epicenter of the seismic event was localized in the Anegada Passage, between St. Thomas, St. Croix and Vieques islands. The resulting tsunami produced waves up to 20 feet height in St. Thomas and St. Croix, causing damage and 12 deaths in the two islands. In Yabucoa, PR, the water receded, causing a run-up of 450 feet inland.

On October 11, 1918, the island of Puerto Rico was hit by one of the most severe earthquakes in its history. The M_w 7.2 earthquake (Doser et al., 2005) had its epicenter in the Mona Passage, at 25 miles from Aguadilla, PR. The tsunami caused an estimated 4 million dollars in property and other damages to the coastal communities of Puerto Rico. According to official numbers, 116 people were killed by the earthquake, and 40 of those were victims of the resulting tsunami (FEMA P-646, 2012).

At all locations, eyewitnesses to the tsunami indicated that the event was marked first by a large retraction of water from the shore, followed by a large wave. The eyewitnesses indicated that this pattern was then repeated one or two more times, but at a smaller scale.

In addition to causing widespread destruction across Puerto Rico, the 1918 earthquake generated a tsunami that produced run-up as high as six meters along the western coast of the island. A description of the tsunami's effects at several locations along Puerto Rico's coast are discussed using the Figure 2.1, which includes the tsunami run-up values at these locations.

Figure 2.1: Description of the effects of the 1918 tsunami at several locations along Puerto Rico's coast (USC-Tsunami Research Center)

The maximum run-up values were registered at the closest locations to the earthquake epicenter and probable tsunami source. The highest value occurred at Point Agujereada with 6 meters, followed by Point Higuero with 5.2 meters and Point Borinquen with 4.5 meters. Point Borinquen is a low-lying area, and as a result the tsunami inundation reached as far as 100 meters inland. At Point Agujereada, eight people died and many houses were destroyed.

The town of Aguadilla experienced run-up values of 2.4 to 3.4 meters, which were not as great as those elsewhere, but tsunami waves swept a village of wooden houses located along the beach, causing 32 deaths. Several 1000 kilogram limestone blocks were moved up to 75 meters inland from their original location, providing an indication of the energy carried by the tsunami waves.

At Mayagüez a tsunami run-up of 1.5 meters was registered which flooded the lower stories of buildings at the coastal areas and destroyed numerous light-frame residences located near the shore. A two meters run-up was reported in the town of Isabela. On Mona Island a pier was destroyed by a run-up height of four meters.

Tsunami's energy was rapidly dissipated as a function of the distance from the source area. For instance, one meter waves were reported in Boquerón, located near the southwestern corner of Puerto Rico. Guánica, and Isla Caja de Muertos both located on the southern shore of the island received only 0.5 and 1.5 meters of run-up, respectively. At Arecibo, the run-up value was 0.6 meters, while in San Juan Harbor, the tsunami was not noticed.

In Puerto Rico, efforts to mitigate the effects of this phenomenum have been channeled through the Tsunami Ready Program, under which tsunami evacuation maps have been developed, improvements in the local education and government agencies preparedness to respond in a fast way against seismic activity threatening Puerto Rico region. However, the people by itself plays an integral role in its own safety. A tsunamigenic event close to Puerto Rico would not allow much time to the agencies to take action in organizing an evacuation out of the expected inundation areas. For this reason, it is of great importance that people understand this phenomenum, especially the residents of coastal communities areas.

2.2.2 Indian Ocean Tsunami (2004) and Effects on Buildings

The Indian Ocean Tsunami was generated by a magnitude-9.3 underwater earthquake, one of the strongest recorded in the modern seismology, which devastated coastal areas around the northern Indian Ocean. It took from 15 minutes to 7 hours to hit the different affected coastlines. It is estimated that the tsunami caused over 220,000 deaths among 14 countries around the Indian Ocean. Certainly, this tragedy highlighted the high vulnerability of coastal communities bordering high risk seismic zones. Subsequently, there have been major advances in understanding, preparedness and action to this unexpected events.

Observations from historic data on tsunami effects were confirmed by the damage observed as a result of the 2004 Indian Ocean tsunami. Moreover the event provided new evidence on previously observed effects, such as foundations scour, waterborne debris impact and structural failure with the uplift of the precast panels in buildings and docks. Figure 2.2 shows a damaged unreinforced masonry house in Devanaanpattinam, India. Severe scour was experienced in the foundations, and the hydraulic pressure due to inundation inside the house.

As observed in past tsunamis, numerous engineered buildings survived the 2004 Indian Ocean Tsunami. There was damage to structural and non-structural elements at the lower levels, but rarely to a point that led to the collapse of the entire structure. For instance, a remaining structure is a mosque located in Uleele, Banda Aceh, (see Figure 2.3) which experienced inundation depths of around 10 meters. As shown in Figure 2.3, the building experienced significant damage but remained in place while the immediate structures were totally collapsed. In Khao Lak, Thailand, the maximum scour depth registered onshore was 3 meters, according to data collected by various survey teams (see Figure 2.4).

Figure 2.2: Damage masonry beach house in Devanaanpattinam, India (FEMA P-646)

Figure 2.3: Reinforced concrete mosque in Uleele, Banda Aceh that survived the tsunami (FEMA P-646)

Figure 2.4: Scour around spread footing in Khao Lak area (FEMA P-646)

Impact from debris caused damages to structural components of non-engineered reinforced concrete buildings (see Figure 2.5). Some of the debris observed in the assessment included fishing vessels and cars. In Figure 2.6 it can be observed how the debris damming effect produced damaged to structural elements.

Figure 2.5 Examples of waterborne debris (FEMA P-646)

Figure 2.6: Damage to corner column due to debris damming effect (FEMA P-646)

As shown in Figure 2.7, concrete panels were lifted by the effects of uplift forces that were large enough to break attachments between the panels and the supporting members. A combination of the buoyancy force effects, trapped air effects, and vertical hydrodynamic forces caused by the rising water alone caused net uplift forces high enough to fail these members.

Figure 2.7: Uplift damage to precast concrete floor panels and harbor piers (FEMA P-646)

2.2.3 Tohoku Japan Tsunami (2011) and Effects on Buildings

On March 11, 2011 the magnitude 9.0 Great East Japan Earthquake was the source of the Tohoku Japan Tsunami where inundation heights exceeded all historical records for the coast of the main Japanese island of Honshu. The tsunami defensive systems were overtopped in most of the coastal communities along the Tohoku coastline. More than 19,000 persons missing or dead, and the widespread destruction of all kind of structures and coastal infrastructure were the results caused by the tsunami.

The Tohoku tsunami led to inundation heights of over 30 meters. Light-frame constructions collapsed in nearly 100 percent of the affected areas, while 75%-95% of the low-rise buildings located in commercial and industrial areas also collapsed. This collapsed rate was higher in areas where the tsunami reached run-ups of around 30 meters. Despite the high percentage of structure collapse, there was an amount of multi-story buildings that resisted the tsunami effects without experiencing significant damage.

The coastal region of Minamisanriku, Japan, had a coastal building with a designated evacuation area as shown in Figure 2.8. This structure was built for residence purposes, but the design included vertical evacuation characteristics. For instance, the design provided an external staircase and elevator for vertical ingress to a rooftop level evacuation area. This evacuation area of 660 square meters secured by a 2 meter high fence provided refuge to the only survivals that reached the roof elevation, since the building was overtopped by the inundation for about 0.7 meters.

Opposite to the moderate performance in terms of evacuation of the building shown in Figure 2.8, many others designated vertical evacuation buildings did not provide any safe area for the evacuees. Although the structures remained standing, those buildings were not designed for the inundation depths experienced. For this reason it is imperative that a designated vertical evacuation structure should have both, structural resistance against the tsunami forces and enough height to refuge evacuees above the maximum inundation depth.

Figure 2.8: Designated coastal evacuation building in Minamisanriku, Japan (FEMA-P-646).

In West of Sendai port in Japan, a soil berm in a park area was used as a refuge area during the tsunami event. The inundation level reached about a half of the mound as shown in Figure 2.9. Some of the effects were controlled erosion on the sides. Based on the resulting performance, it could be concluded that this idea can be a solution for evacuation from tsunamis.

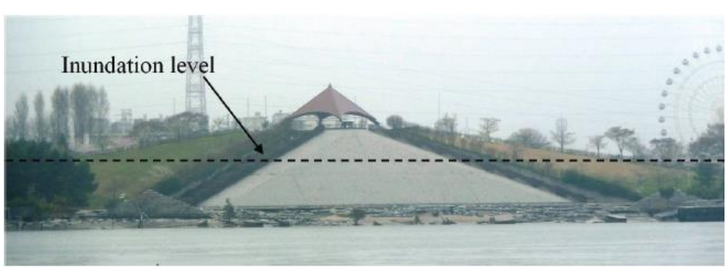

Figure 2.9: Soil berm used as evacuation area at West of Sendai port (FEMA P-646).

As in previous tsunami events, during the Tohoku tsunami, all of the typical effects such as hydrostatic forces, hydrodynamic forces, impacts from debris, debris damming forces, and scour, were observed. Low to mid-rise building elements failed due to the effects of these forces alone or in combination. Moreover, the performance of those buildings was not only based on the structural material or the structural system, but in the strength to resist lateral forces and the impact resistance. As shown in Figure 2.10, a few low to mid-rise reinforced concrete buildings survived the tsunami effects. Many of these structures experienced maximum hydrodynamic forces, since solid concrete walls were oriented perpendicular to the incoming flow direction.

Figure 2.10: Surviving low to mid rise damaged reinforced concrete buildings in Minamisanriku, Japan (FEMAP-646).

In Onagawa, Japan, the tsunami inundation reached depths of over 18 meters which overtopped almost all the buildings only excluding some located on a hillside. Nevertheless, many low-rise steel and concrete buildings survived. According to the observations, more than six of the failed buildings were overturned and displaced. These buildings were subjected to hydrostatic forces and hydrodynamic forces, and those effects were function of the openness of the buildings.

One of the failed buildings was a two-story cold storage building made of reinforced concrete, designed and constructed as a closed structure except for doors and second floor windows due to its functionality (see Figure 2.11). It was affected by the tsunami buoyancy effect which lifted the structure off its pile foundation which did not had tensile capacity. The building was overturned and displaced over 15 meters inland. In Figure 2.12 is shown an overturned and displaced three story building made of reinforced concrete with a frame system composed of shear walls, seated on a mat foundation of about 0.9 meter thick. These observations from

Onagawa, left uncover that a vertical evacuation structure should be founded using deep foundations with tensile capacity.

Figure 2.11: Overturned and displaced two-story cold storage building in Onagawa, Japan (FEMA P-646)

Figure 2.12: Overturned and displaced three-story building on mat foundation in Onagawa, Japan (FEMA P-646)

2.3 Vertical Evacuation Design Implications

Vertical evacuation solutions must have the ability to receive a large number of people in a short time frame and proficiently transport them to areas of refuge that are placed above the level of flooding to provide refuge from tsunami inundation. Potential vertical evacuation solutions can include areas of naturally occurring elevated ground, areas of artificial elevated ground built through the use of soil berms, new structures particularly designed to be tsunami-resistant, or existing structures proven to have sufficient strength to resist expected tsunami effects. In theory, new or existing structures can serve as vertical evacuation structures, but in general, it will be more complex to retrofit an existing structure than to build a new one that is tsunami-resistant.

Vertical evacuation structures can be single purpose (facilities for refuge only), or multi-purpose facilities in regular use when not serving as a refuge. The failure of lower level walls, nonstructural components, and contents should be taken into account in the design of the facility and selection of possible alternative uses, if the building is required to remain functional in the event of a disaster.

Vertical evacuation structures should be positioned such that all persons designated to take refuge can reach the structure within the time available between tsunami warning and tsunami inundation. Travel time must take into consideration vertical ingress within the structure to levels above the inundation depth.

To establish the required number and spacing of tsunami vertical evacuation structures, the critical factors are warning time and ambulatory capability of the nearby community. According to FEMA P-646, the average speed at which a healthy person can walk is approximately 4 mph. Some people in a community, however, may have restricted capability due to age, health, or disability. The average pace for mobility-impaired populations can be assumed to be about 2 mph (FEMA P-646, 2012). The maximum distance from any given starting point and distance between structures depend on the warning time associated with the source distance, as shown in Table 2.2. A sample layout of vertical evacuation structures in a hypothetical coastal community is shown in Figure 2.13.

Table 2.2: Maximum spacing evacuation structures based on travel time (FEMA P-646, 2012).

Warning Time	Ambulatory Speed	Travel Distance (miles)	Maximum Spacing (miles)
2 hr	2 mph *	4	8
30 min	2 mph *	1	2
15 min	2 mph *	1/2	1

* Based on the average pace for a mobility-impaired population.

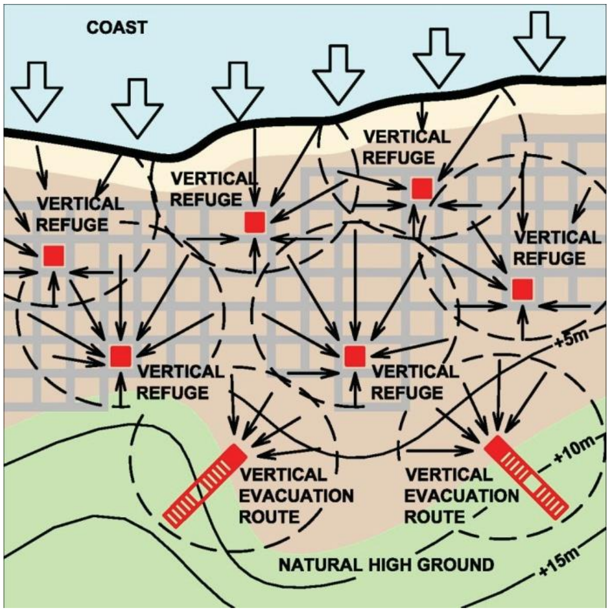

Figure 2.13: Vertical evacuation refuge locations considering travel distance, evacuation behavior, and naturally occurring high ground. Arrows show anticipated vertical evacuation routes (FEMA P-646, 2012)

Special hazards in the vicinity of each site must be considered in the design of vertical evacuation structures. Potential site hazards include sources for large waterborne debris, and sources of waterborne hazardous materials.

Based on previous tsunami events which included several cycles of waves, it is suggested that evacuees should stay in the refuge until the second high tide. Since the second high tide after the first tsunami wave could occur up to 24 hours later, a considerable minimum square footage per occupant for a tsunami refuge is 10 square feet per person. This number concur with the square footage recommendations employed in the design of shelters for other hazards. This number should be higher or lower depending on the specific occupancy needs of the refuge under consideration.

It is fundamental that the area of refuge be located above the maximum tsunami inundation level anticipated at the proposed site, in order to serve well as a vertical evacuation structure. Determination of an appropriate elevation for tsunami refuge should consider the uncertainty intrinsic in estimation of the tsunami run-up elevation, possible splash-up during impact of tsunami waves, and the anxiety level of evacuees seeking refuge in the structure. To consider this uncertainty, the maximum tsunami run-up elevation is amplified by 30% from the values predicted by numerical simulation modeling or obtained from tsunami inundation maps. It is recommended that an additional allowance for freeboard of 3m or 10ft (or one story height) be provided, because of the inundation potential of the refuge area. The recommended minimum elevation for a tsunami refuge area is, therefore, the maximum tsunami run-up elevation anticipated at the site, plus 30%, plus a freeboard allowance of 10 feet (3 meters) (see Figure 2.14).

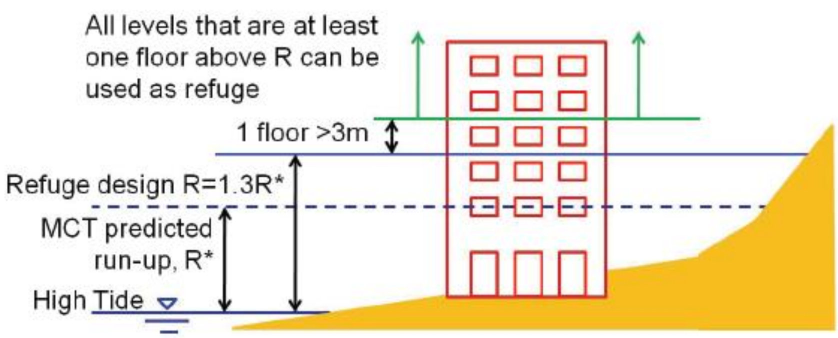

Figure 2.14: Graphical illustration of FEMA P-646 refuge elevation guide (Robertson, 2012)

In order for a tsunami refuge to serve its purpose in locations threatened by near-source tsunamis, it must first withstand the large magnitude earthquake responsible for the tsunami. FEMA P-646 recommends that the refuge be designed for seismic performance consistent with that of code-defined essential facilities. The design can be evaluated using performance-based seismic design techniques such as ASCE/SEI 41-06 Seismic Rehabilitation of Existing Buildings (ASCE, 2006b), to obtain a higher level of assurance that improved seismic performance is achieved. FEMA P-646 recommends that the performance objectives should be at least Immediate Occupancy performance for the Design Basis Earthquake (DBE) and Life Safety performance for the Maximum Considered Earthquake (MCE) (see Figure 2.15). The structure must then be designed for all likely tsunami loads and effects. Using these design conditions, it is expected that the refuge structure will survive the earthquake with limited structural and non-structural damage, and have adequate remaining strength to resist all tsunami induced loads and foundation scour avoiding the collapse.

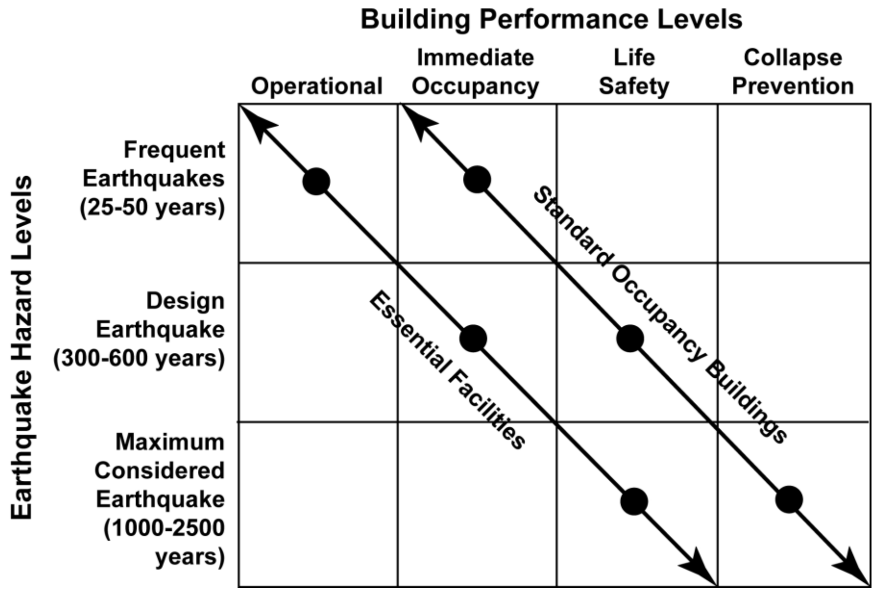

Figure 2.15: Seismic performance objectives linking building performance to earthquake hazard levels (FEMA P-646, 2012).

Many common structural systems can be engineered to resist tsunami load effects. Some of the structural characteristics that have demonstrated good performance in past tsunamis include: (1) open systems that allow water to flow through with low resistance; (2) well-built systems with reserve capacity to resist extreme forces; (3) ductile and resilient systems that withstand extreme forces with no collapse; and (4) redundant systems that can experience localized failure with no progressive collapse. Reinforced concrete and steel moment frame systems, and reinforced concrete shear wall systems have exhibit such properties. Moreover, the use of deep foundations should be considered for resistance to scour and breakaway wall systems to minimize hydrodynamic forces.

2.4 Tsunami Loading According to FEMA P-646

Tsunami loading provisions presented in FEMA P-646 are based on a number of general assumptions. For instance, the water density is taken as 1.1 times that of freshwater to take into consideration the density of seawater and the impending sediment transported within the tsunami flow. Depending on the complexity of the bathymetry and topography at the site under analysis, tsunami flow depths vary notably. Figure 2.16 depicts how the potential tsunami inundation could behave as a function of the local topography. FEMA P-646 assumes the condition (b) in Figure 2.16, where $T_E = R$, being T_E the tsunami elevation at a site of analysis, and R the ultimate inland run-up elevation, unless a well-defined tsunami inundation simulation is performed for the specific site under study.

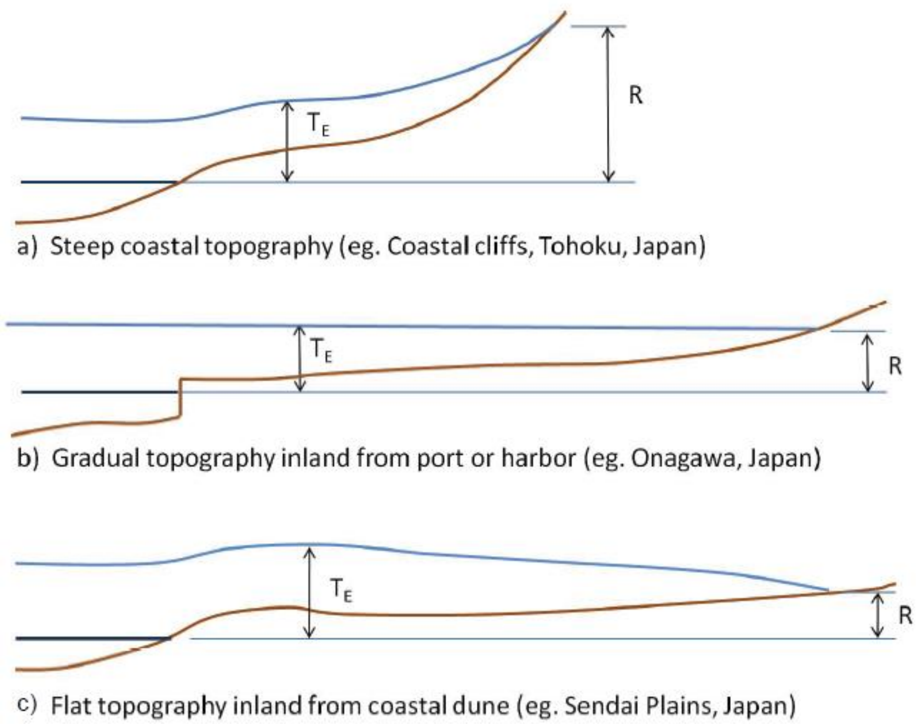

Figure 2.16: Topographical effect on coastal inundation such that the tsunami elevation (T_E) at a site of interest could be less than, equal to, or greater than the ultimate inland run-up elevation (R) (FEMA P-646, 2012).

2.4.1 Hydrostatic Forces

Hydrostatic forces are a result of the water pressure difference among opposite sides of components such as a wall. It is generated when the base floor of the structure is sufficiently impermeable causing an interruption or delay of water entrance. Figure 2.17 displays the hydrostatic pressure distribution, including its resultant and Equation 2.1 shows the mathematical expression to calculate such force.

$$F_h = P_h A_w = \frac{1}{2}\rho_s g b_w h_{max}^2 \tag{2.1}$$

where:

F_h = horizontal hydrostatic force,

P_h = hydrostatic pressure,

A_w = wetted area of the panel,

ρ_s = fluid density including sediment, taken as 1.1 ρ_w (2.13 slugs/ft^3),

g = gravitational acceleration (32.2 ft/s^2),

b_w = breadth (width) of the wall, and

h_{max} = maximum water height above the base of the wall at the structure location.

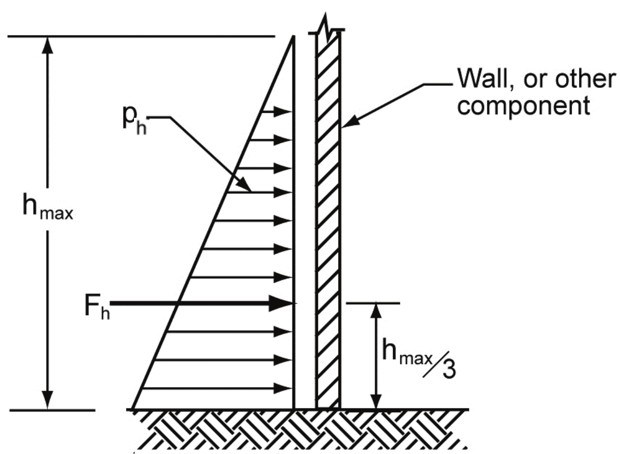

Figure 2.17: Hydrostatic force distribution and location of the resultant (FEMA P-646).

2.4.2 Buoyant Forces

Buoyant forces act upward and are equal to the weight of the displaced water. They are a major concern for light-weight structures, building with basements and components designed only to carry gravity loads, since they are opposed only by the weight of the building or component.

Figure 2.18 presents an example of the buoyant force distribution, while Equation 2.2 shows the expression to calculate buoyant forces.

$$F_b = \rho_s g V \tag{2.2}$$

where:

F_b = buoyant force, and

V = volume of water displaced by the building.

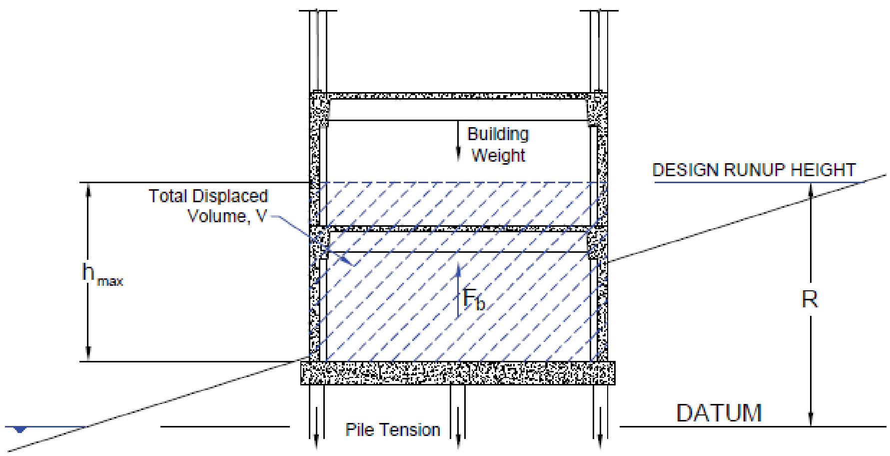

Figure 2.18: Buoyant forces (FEMA P-646, 2012).

2.4.3 Hydrodynamic Drag Forces

Hydrodynamic drag forces are a combination of the lateral forces caused by the pressure forces from the moving water and the friction forces generated as the water flows around the structure or component. These forces are a function of water density, flow velocity and the geometry of the structural component. The hydrodynamic drag force distribution is shown in Figure 2.19, and it can be calculated with Equation 2.3.

$$F_d = \frac{1}{2}\rho_s C_d B (hu^2)_{max} \tag{2.3}$$

where:

F_d = hydrodynamic force,

C_d = drag coefficient taken as C_d = 2, following the work of Yeh (2007).,

B = width of the component,

h = flood depth, and

u = flow velocity.

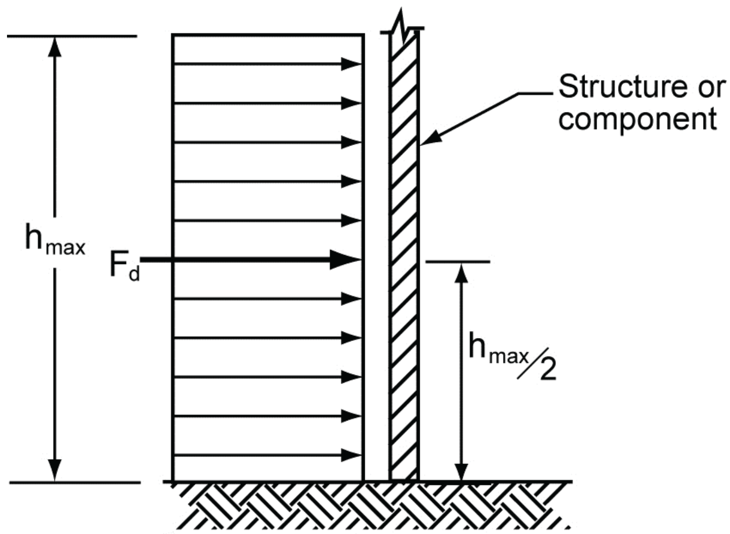

Figure 2.19: Hydrodynamic forces (FEMA P-646, 2012).

The maximum hydrodynamic force is obtained when the combination hu^2, known as the momentum flux per unit mass per unit width, is maximum. The maximum velocity, u_{max}, generally occurs at the leading edge of the tsunami surge when h is small. When the flow depth reaches a maximum, h_{max}, the flow velocity, u_{max}, is generally very low. Therefore, it is important to note that $(hu^2)_{max}$ is not equal to $h_{max}u^2_{max}$.

It is extremely difficult to measure flow depth and flow velocity in a real time event, since tsunamis are unpredictable. Therefore, these measurements have not been made during past tsunamis. According to FEMA P-646, a detailed numerical model might be constructed for the building site using previous run-up data. This model can then be used to approximate the flow velocity and the flow depth at the building location. However, in case that a more detailed analysis is not available, FEMA P-646 suggests that $(hu^2)_{max}$ can be estimated using Equation 2.4. This equation is based on an analytical solution for a one dimensional nonlinear shallow water theory for a constant beach slope with no friction, and no lateral topographical variation. In

Appendix E of FEMA P-646, provides two equations from studies performed by Yeh (2007) which can be solved to obtain flow depth and velocity at any location between the shoreline and maximum run-up for a frictionless surface (see Equations 2.5 and 2.6).

These equations do not have an analytical solution for flow depth and velocity, but they can be solved numerically using the ground elevation at the base of the structure and the maximum expected run-up from the previous records at the given location.

$$(hu^2)_{max} = gR^2\left[0.125 - 0.235\frac{z}{R} + 0.11\left(\frac{z}{R}\right)^2\right] \tag{2.4}$$

$$\eta = \frac{1}{36\tau^2}\left(2\sqrt{2}\,\tau - \tau^2 - 2\zeta\right)^2 \tag{2.5}$$

$$\upsilon = \frac{1}{3\tau}\left(\tau - \sqrt{2}\tau^2 + \sqrt{2}\zeta\right) \tag{2.6}$$

where:

$$\eta = \frac{h}{R} \tag{2.7}$$

$$\upsilon = \frac{u}{\sqrt{2gR}} \tag{2.8}$$

$$\tau = t\ tan\alpha\sqrt{\frac{g}{R}} \tag{2.9}$$

$$\zeta = \frac{z}{R} \tag{2.10}$$

where:

h = the water depth,

R = the ground elevation at the maximum penetration of tsunami run-up, measured from the initial shoreline,

u = the flow velocity,

g = the gravitational acceleration,

α = the beach slope,

t = the time: 0 when the bore passes at the initial shoreline, and

z = the ground elevation of the location of interest, measured from the initial shoreline: this identifies the location of interest along a uniformly sloping beach.

2.4.4 Impulsive Forces

Impulsive forces are caused by the initial impact to the structure of the leading edge of the surge. According to Ramsden (1993), experiments on impulsive forces show that there is no significant initial impact force in dry-bed surges, but a significant increase was observed in surges that occur when the site is initially inundated. Since tsunamis come in sets of waves, the first wave might not cause any impulsive forces, while the ensuing waves would be traveling over flooded terrain and may cause impulsive forces on structures. According to laboratory data obtained by Arnason (2005) the significant increase is approximately 1.5 times the hydrodynamic force. Therefore to calculate impulsive forces and consistent to previous data, FEMA P-646 conservatively recommends using Equation 2.11.

$$F_s = 1.5F_d \tag{2.11}$$

As shown in Figure 2.20, impulsive forces are applied on components at the leading edge of the tsunami surge, at the same time as hydrodynamic forces will be acting on all components that have already passed by the leading edge.

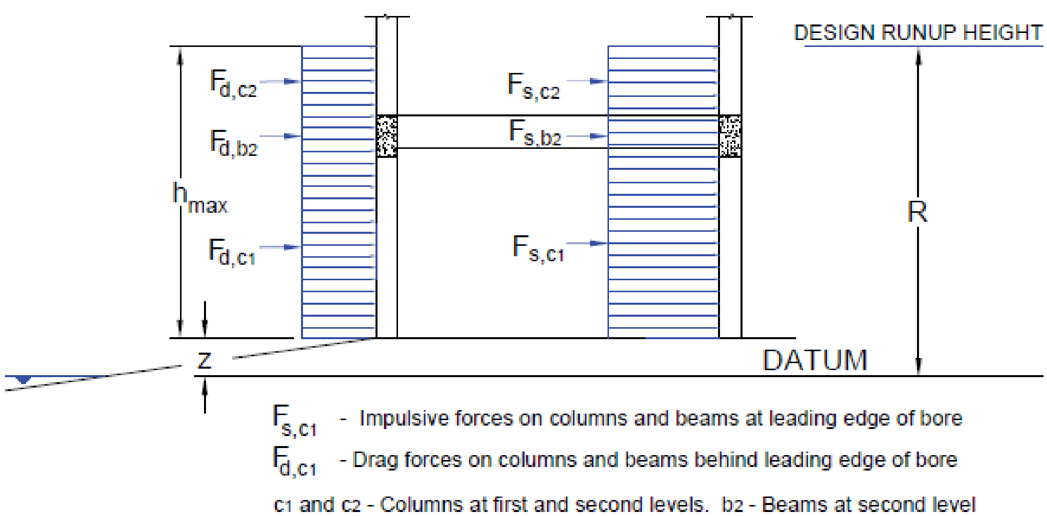

Figure 2.20: Impulsive and drag forces on structural components (FEMA P-646, 2012).

2.4.5 Floating Debris Impact Forces

Debris impact forces are caused by impact of floating objects traveling with the tsunami surge. Objects such as driftwood, lumber, shipping containers, boats, automobiles and different other debris get washed away during the initial inundation, and then behave as projectiles when subsequent waves come onshore. FEMA P-646 recommends Equation 2.12 which uses the stiffness of the debris to calculate the impact force.

$$F_i = 1.3 u_{max} \sqrt{k m_d (1 + c)} \tag{2.12}$$

where:

F_i = debris impact force,

c = added mass coefficient,

u_{max} = maximum flow velocity,

k = effective stiffness of debris, and

m_d = mass of debris.

When a numerical model is unavailable, the maximum flow velocity at the site can be estimated using Equation 2.13. This same equation is used to estimate the maximum flow velocity carrying lighter debris requiring little or no draft, traveling at higher velocities than heavier which requires much larger depth to float.

$$u_{max} = \sqrt{2gR\left(1 - \frac{z}{R}\right)} \tag{2.13}$$

where:

g = the gravitational acceleration,

R = the design run-up height that is 1.3 times the ground elevation R^* at the maximum tsunami penetration, and

z =the ground elevation at the structure (the datum must be at the sea level). Background information on the development of this equation is provided in Appendix E of FEMA P-646.

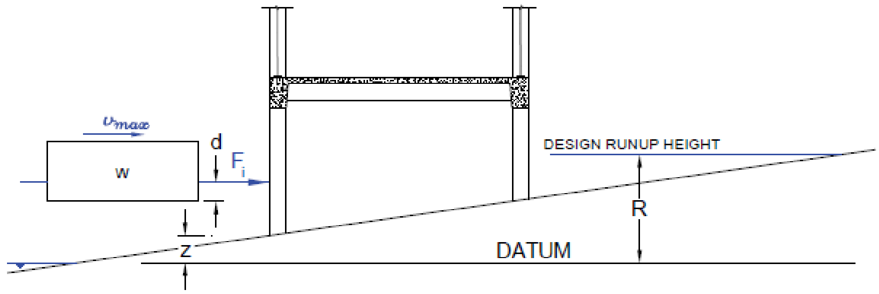

Figure 2.21: Floating debris impact force (FEMA P-646).

For larger (heavier) debris with draft *d*, the ratio of the draft to the maximum run-up height can be computed, and Figure 2.22 can be used to estimate the maximum flow velocity. Draft *d* can be calculated with Equation 2.14:

$$d = \frac{W}{\rho_s g A_f} \tag{2.14}$$

where:

W = the weight of the debris,

ρ_s = the fluid density including sediment (1100 kg/m3 = 2.13 slugs/ft^3),

g = the gravitational acceleration, and

A_f = the cross-sectional area parallel to the water surface such that the product d x A_f = the volume of water displaced by the debris.

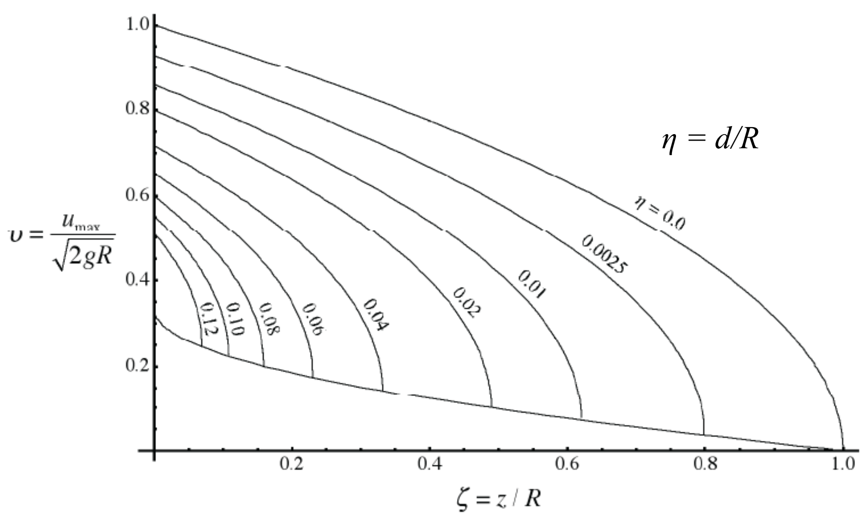

Figure 2.22: Maximum flow velocity of a debris with draft, d, as a function of z/R variation (FEMA P-646).

The maximum velocity for Equation 2.12 is to be computed using Figure 2.22 from FEMA P-646 based on Equations 2.5 and 2.6. Since the debris requires a certain depth of water in order to float, it is impossible that it would be floating at the leading edge of the bore. Figure 2.22 provides a relationship between velocity and the draft that is required to carry the debris, and is to be used in the absence of a detailed numerical model. FEMA P-646 also provides a table of common debris with the appropriate mass and stiffness. This information is provided in Table 2.3.

Table 2.3: Mass and stiffness of common waterborne floating debris (FEMA P-646, 2012)

Type of Debris	Mass *(m_d)* [slugs]	Hydrodynamic Mass Coefficient *(c)*	Debris Stiffness *(k)* [Kip/in]
Lumber or Wood Log - oriented longitudinally	30.83	0	13.70
20 ft Standard Shipping Container - oriented longitudinally	150.75 (empty)	0.30	485.36
20 ft Heavy Shipping Container - oriented longitudinally	164.45 (empty)	0.30	531.04
40 ft Standard Shipping Container - oriented longitudinally	260.38 (empty)	0.20	342.61

2.4.6 Damming of Accumulated Waterborne Debirs

During a tsunami, various debris may form a dam against the face of the structure. This could potentially add to the effective breadth of the structure and subject it to higher hydrodynamic loads. FEMA P-646 recommends using a minimum debris dam width of 40 ft that is representative of a 40-ft shipping container wedged against the structure. The effects of these forces should be assessed at all critical locations in the structure. In the same way as hydrodynamic forces, the damming of waterborne debris forces is estimated using Equation 2.15.

$$F_{dm} = \frac{1}{2}\rho_s C_d B_d (hu^2)_{max} \tag{2.15}$$

where:

F_{dm} = force due to damming of waterborne debris,

C_d = drag coefficient, and

B_d = breadth of the debris dam.

2.4.7 Uplift Forces on Elevated Floors

Uplift forces will be applied to floor levels of a building that are submerged by tsunami inundation. In addition to standard design for gravity loads, these floors must also be designed to resist uplift due to buoyancy and hydrodynamic forces. When computing the buoyant forces with Equation 2.16 on a floor slab, consideration must be given to the potential for increased buoyancy due to the extra volume of water displaced by air trapped below the floor framing system. Moreover, exterior walls at the upper floor level will keep out water until their lateral resistance is surpassed by the applied hydrostatic pressure. This can significantly increase the displaced volume of water contributing to the buoyancy, as shown in Figure 2.23.

$$F_b = \rho_s g A_f h_b \tag{2.16}$$

where:

F_b = total buoyant force,

A_f = area of the floor panel, and

h_b = water height displaced by the floor.

During rapid inundation, rising water also creates uplift forces on floor slabs as shown in Figure 2.23. Experiments have shown that when rapidly moving water encounters resistance, such a wall, there will be significant uplift forces. However, since no detailed research has been published on this topic, FEMA P-646 recommends using Equation 2.17 to calculate the hydrodynamic uplift force on the slab.

$$F_u = \frac{1}{2} C_u \rho_s A_f u_v^2 \tag{2.17}$$

where:

F_u = total hydrodynamic uplift,

A_f = area of the floor panel,

C_u = 3.0, (suggested by FEMA P-646),

u_v = vertical water velocity (u_v = u tan α), and

α = average slope of grade at the site.

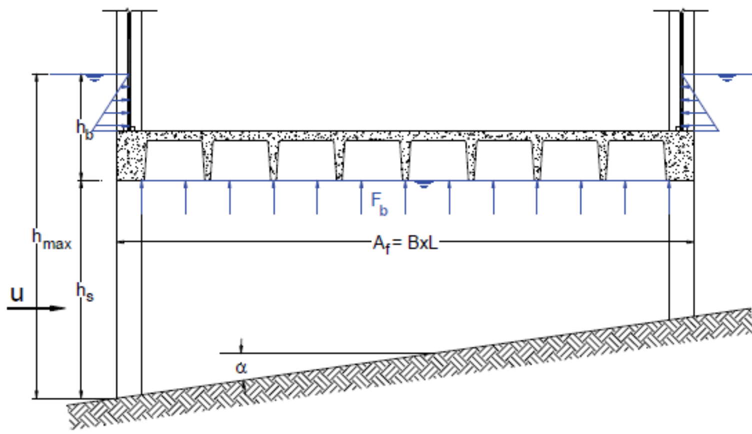

Figure 2.23: Uplift and buoyant forces acting on elevated floor systems (FEMA P-646).

2.4.8 Additional Retained Water Loading on Elevated Floor

During a tsunami event, inundation is followed by drawdown, where all of the water rapidly recedes back into the ocean. If the inundation was high enough to flood elevated floors, it is possible that during the drawdown, water will be trapped on elevated floors and increase gravity loads on all of the structural members as shown in Figure 2.24. The maximum additional force due to trapped water can be calculated using Equation 2.18.

$$F_r = \rho_s g h_r \tag{2.18}$$

where:

F_r = maximum potential gravity force per unit area, and

h_r = maximum potential depth of water on the elevated floor.

$$h_r = h_{max} - h_1 \leq h_{bw} \tag{2.19}$$

where:

h_{max} = maximum inundation level predicted at the site, h_1 is the floor elevation above grade, and

h_{bw} = maximum water depth that can be retained before failure of a significant portion of the wall due to internal hydrostatic pressure of the retained water.

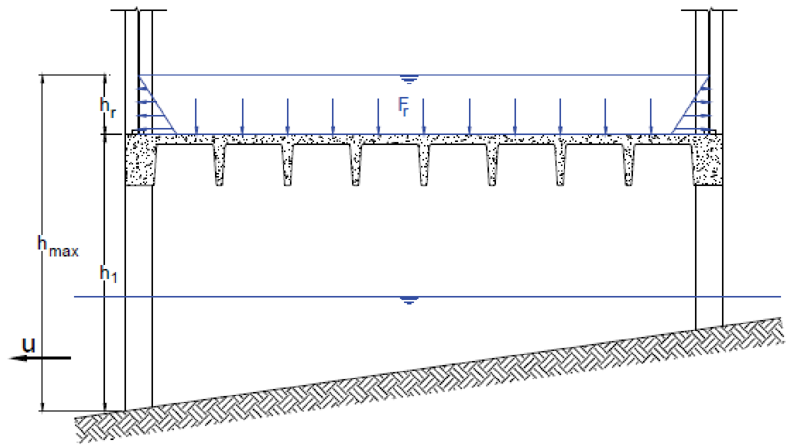

Figure 2.24: Retained water gravity loading on elevated floor during tsunami drawdown (FEMA P-646).

2.5 Load Combinations

The tsunami forces described above will not occur simultaneously, and will not necessarily affect a particular structural element concurrently. Furthermore, earthquake loads are not considered to take action at the same time with tsunami loads and there is a low probability of an aftershock with the same magnitude of the design earthquake to occur at the same time of the tsunami inundation. Following these considerations is necessary to describe the combinations of tsunami forces acting on the structure taken as a whole and on individual structural components. According to FEMA P-646, the recommended load combinations that should be considered for the entire structure are the following.

2.5.1 Tsunami Loads on the Structure

- Buoyant forces have a trend to decrease the weight of the structure affecting the structures' ability to oppose the overturning moments produced by lateral loads. Hence, buoyant forces should be taken into consideration in all load combinations.
- Impulse forces are produced by the leading edge of the tsunami surge and have an effect on the structure for only a short period of time. The surge impacts structural members sequentially, as the surge passes through the building, and as shown in Figure 2.25, the worst scenario occurs when the leading edge of the surge impacts the most closed off

section of the building and the hydrodynamic forces are acting on the rest of the frame components.

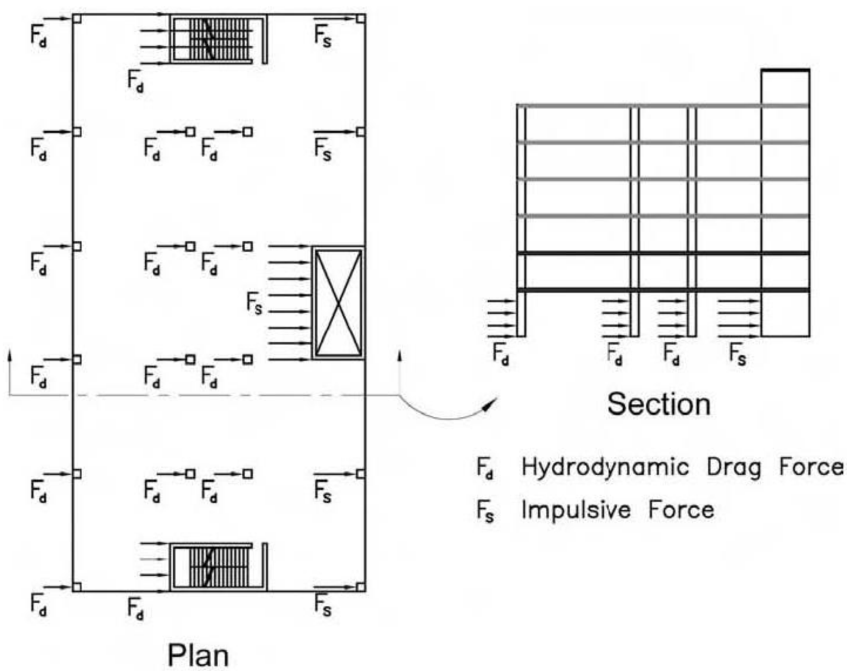

Figure 2.25: Impulsive forces in combination with drag forces (FEMA P-646).

- It is not possible for debris to impact the building in combination with impulsive forces, since debris impact forces require a certain depth of water to carry the debris. Moreover, while it is possible that a building could be impacted by various debris during the path of a tsunami, it is extremely improbable that it would be hit by more than one at the same time. Thus, a single debris impact force should be considered in combination with all the other forces except for the impulsive.
- Debris damming forces should be applied to the most vulnerable part of the whole structure in combination with hydrodynamic forces acting on the rest of the structural members.
- The following are the load combinations that were developed in FEMA P-646 with the guidance of ASCE 7-05:

Load Combination 1: $1.2D + 1.0T_s + 1.0L_{REF} + 0.25L$ (2.20)

Load Combination 2: $0.9D + 1.0T_s$ (2.21) where:

D = dead load,

T_s = tsunami load,

L = live load outside of the refuge area, and

$L_{REF} = L_{REF}$ is the live load in the refuge area.

2.5.2 Tsunami Loads on the Structural Elements

According to FEMA P-646, the tsunami effects that should be considered on individual structural components of the building are the following:

- Impulsive forces
- Hydrodynamic forces and the debris impact forces at the most vulnerable location of the building.
- Debris damming forces due to a minimum dam width of a 40 feet shipping container that causes the worst loading on the structural member.
- Hydrostatic pressure on walls that enclose watertight areas of the structure.
- A summation of buoyant and hydrodynamic uplift forces in combination with 90% of dead load and zero live load, as presented in Equation 2.21.

CHAPTER 3 - SITE DESCRIPTION

3.1 Introduction

In this chapter, the different community characteristics of Bo. Espinal, which includes the geographical information, actual tsunami risks based on its location, current evacuation routes, and time of evacuation away from the inundation area, is reported. To understand the population type of the coastal community, demographic characteristics according to the 2010 Puerto Rico Census are discussed. Furthermore, a proposed location for building the vertical evacuation structure within Bo. Espinal is displayed, and the coastal community housing distribution is analyzed with respect to this selected site.

3.2 Geographical Information

The coastal community of Bo. Espinal is located in the municipality of Aguada, in the northwest coast of Puerto Rico at Lat. 18°24'16"N and Lon. 67°10'01" W (see Figure 3.1). At the north it borders the town of Aguadilla, at the east borders Moca. Añasco and Rincón are to the south and southwest respectively, while the Mona Passage is at its west. It is located at the geographical region of Aguada-Hatillo which covers around 400 square miles of the west part of the North Coastal region, between the coastal valley of Aguadilla harbor and a sector of the floodplain of Culebrinas River and Caño Madre Vieja. The latter is an old outlet of the Culebrinas River which winds its way to the coast northwest of the Bo. Espinal area, in the Parque Colón sector of Aguadilla. The residential area of Bo. Espinal is located in the middle of the coastal valley and, in effect, break up the flood of Culebrinas River (Segarra-García, 2007). The topography in Bo. Espinal is mostly flat with elevations varying from two to five meters above mean sea elevation.

According to the Puerto Rico Planning Board, Bo. Espinal is composed of five different area classification (see Figure 3.2). Developed Area (AD) characterizes the area where the population and housing are established. Resource Conservation area (CR) is mostly around the developed area. The Preservation Resource area is located in the north region, along the Caño Madre Vieja. A Public Park is located in the center of Bo. Espinal, where the baseball park and basketball court are located, and a Public area, where the Martín Hernández elementary school is located.

Figure 3.1: Bo. Espinal location at the northwest part of the island

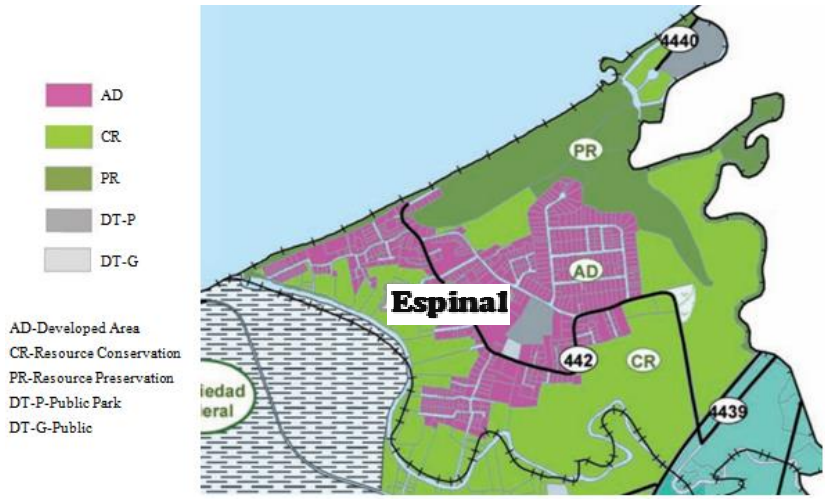

Figure 3.2: Bo. Espinal site classification according to Puerto Rico Planning Board

3.3 Tsunami Risk Assessment in Bo. Espinal

With a total area of 1.22 square miles, where 0.86 square miles correspond to land area, Bo. Espinal is located at north of the state road PR-115, and has only one access through the state road PR-442 (see Figure 3.3). Moreover, the segment of the road PR-115 that connects with PR-442, hold two bridges[3], BR-0581 (to Aguadilla), and BR-0582 (to Aguada). Both bridges were constructed in 1951. BR-0581 is a three span cast in place concrete slab, while BR-0582, which spans Culebrinas River, is a three span bridge with cast in place concrete T-beams in exterior spans and steel I-beams in middle span. According to the FEMA 339 (1999): *Building Performance Assessment Team Report - Hurricane Georges in Puerto,* Puerto Rico was identified as a seismic zone 3, requiring all new construction to be seismic resistant, as part of the 1987 Panning Regulation amendment. Since the year of construction of both bridges were prior to the 1987 amendment, there are high probabilities that the design not meet seismic requirements. This fact in combination with its low lying area put Bo. Espinal in a high risk during a tsunami event.

In Figure 3.4, is shown the tsunami inundation model and is observed that the tsunami run-up extension covers the entire coastal community and goes beyond (PR-115). Figure 3.5 shows the tsunami evacuation map of Bo. Espinal (Aguada Municipal Emergency Management Office, 2010). In this map is determined the path that evacuees should take in case of a tsunami event.

[3] Bridges numbers, BR-0581 and BR-0582, are according the Bridge Inventory Management Office of the Puerto Rico Highways and Transportation Authority

From the figure is possible to see that the whole community have to evacuate through PR-442 and any of the two previously mentioned bridges have to be crossed after to leave the evacuation zone.

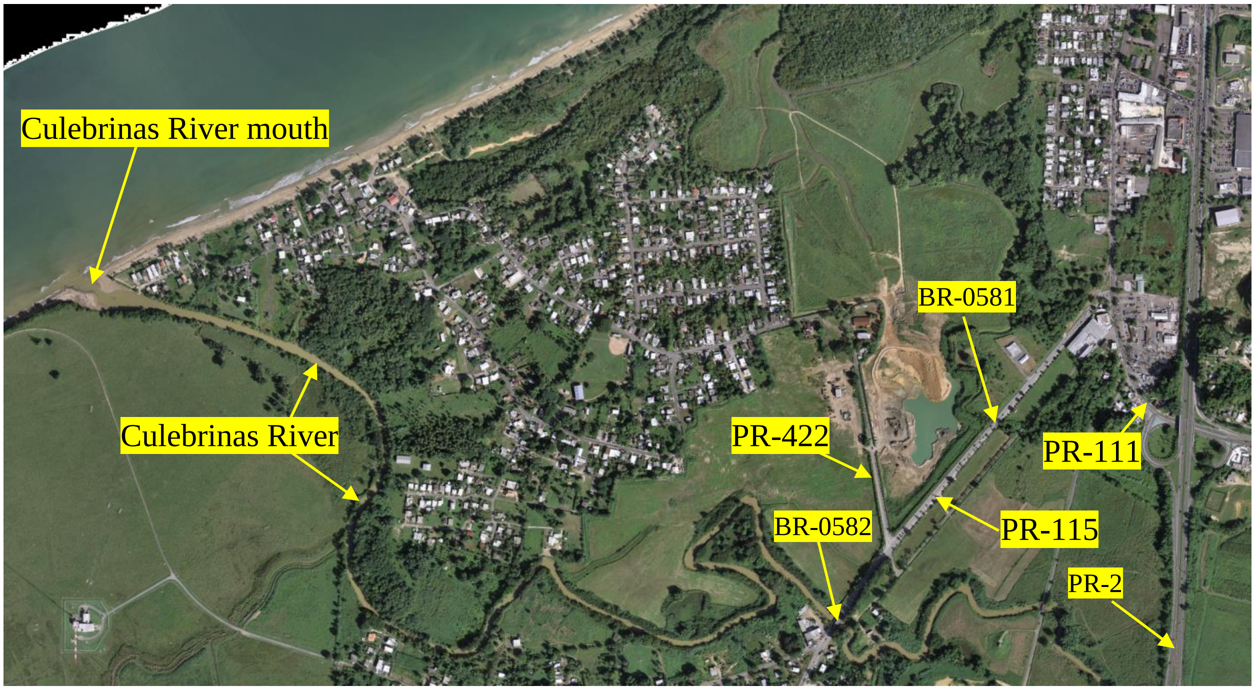

Figure 3.3: Road access to Bo. Espinal

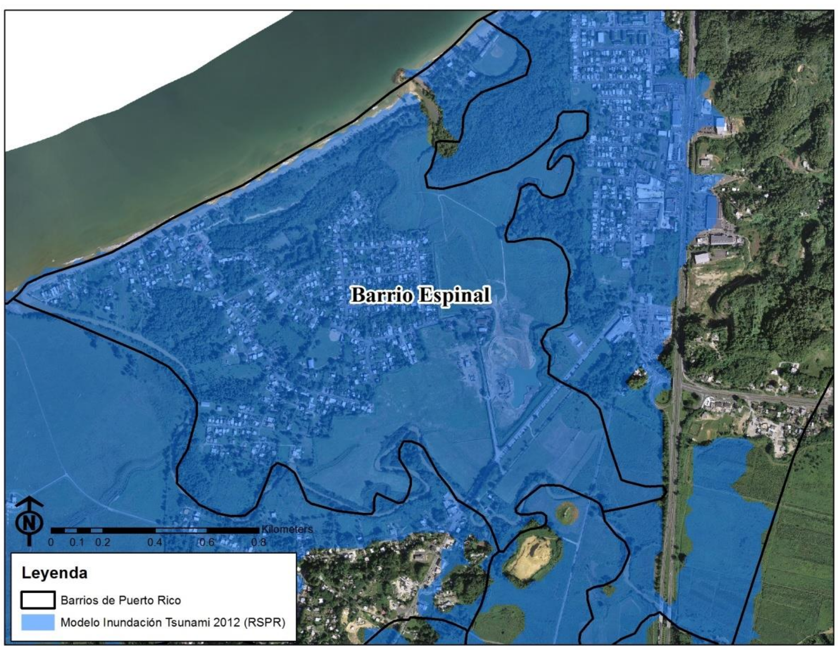

Figure 3.4: Tsunami inundation model, (RSPR, 2012)

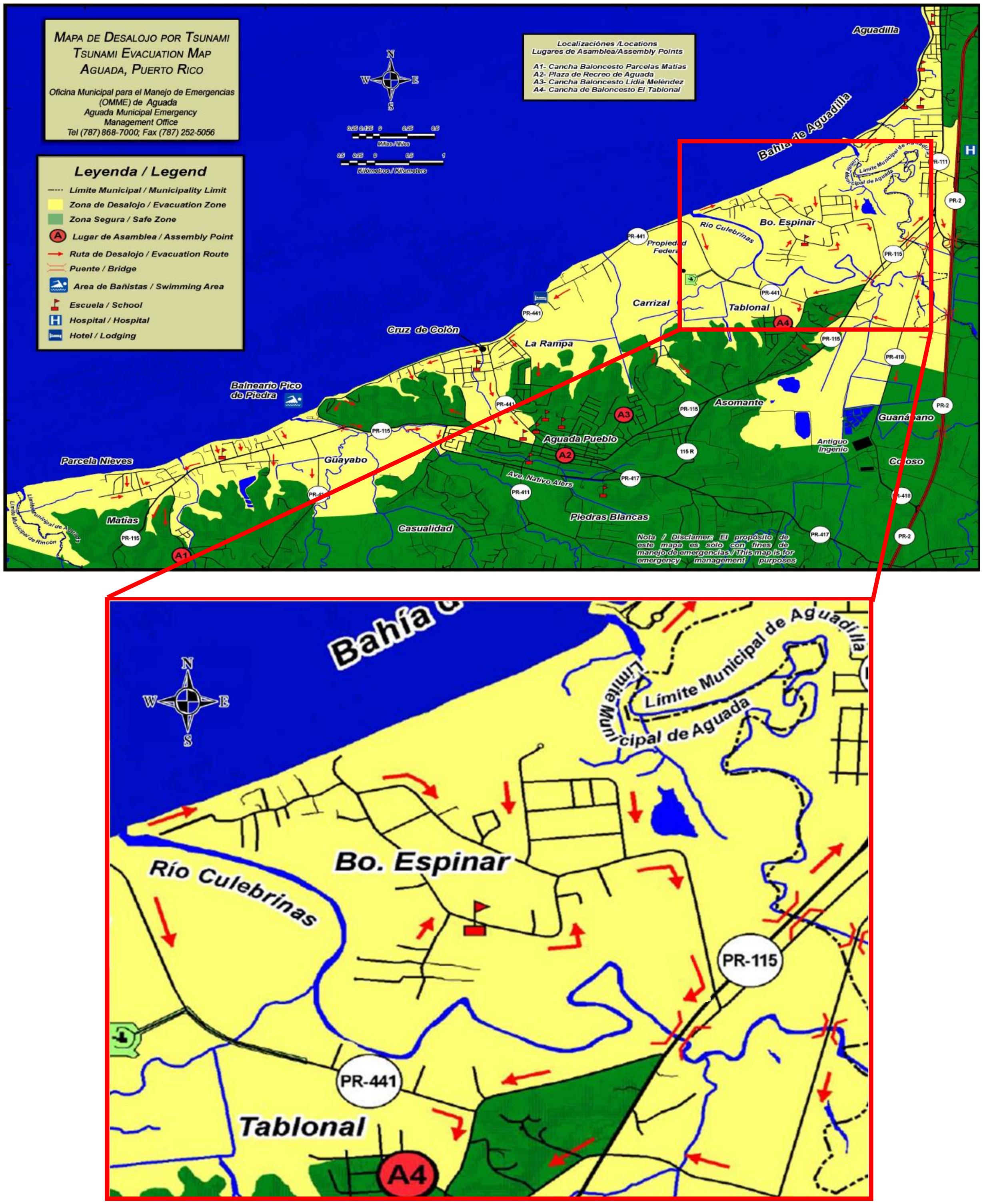

Figure 3.5: Bo. Espinal tsunami evacuation map

3.4 Demographic Characteristics

According to the Puerto Rico 2010 Census of Population and Housing, Bo. Espinal has a population of 1,281 people, and a population density of 1,489 people per square mile (average per square mile of land). Is composed with 626 housing units where only 469 are occupied and 66 are for seasonal recreational or occasional use. Figure 3.6, shows the age distribution for the total population at Bo. Espinal. From this results is notable that the higher age range is for 15-19 years while a high concentrations from 10 - 24 years, and 35 - 69 years for a median age of 42.

In Figure 3.7 and Figure 3.8 are shown the age distributions for both genders. The male population have a total of 644 people with a median age of 39.5, while female population consists of a total of 637 people with a median age of 43.5. From the results is noticed that the male quantities predominates the population up to the 19 years, beyond that age the females number start to get over in many of the age ranges.

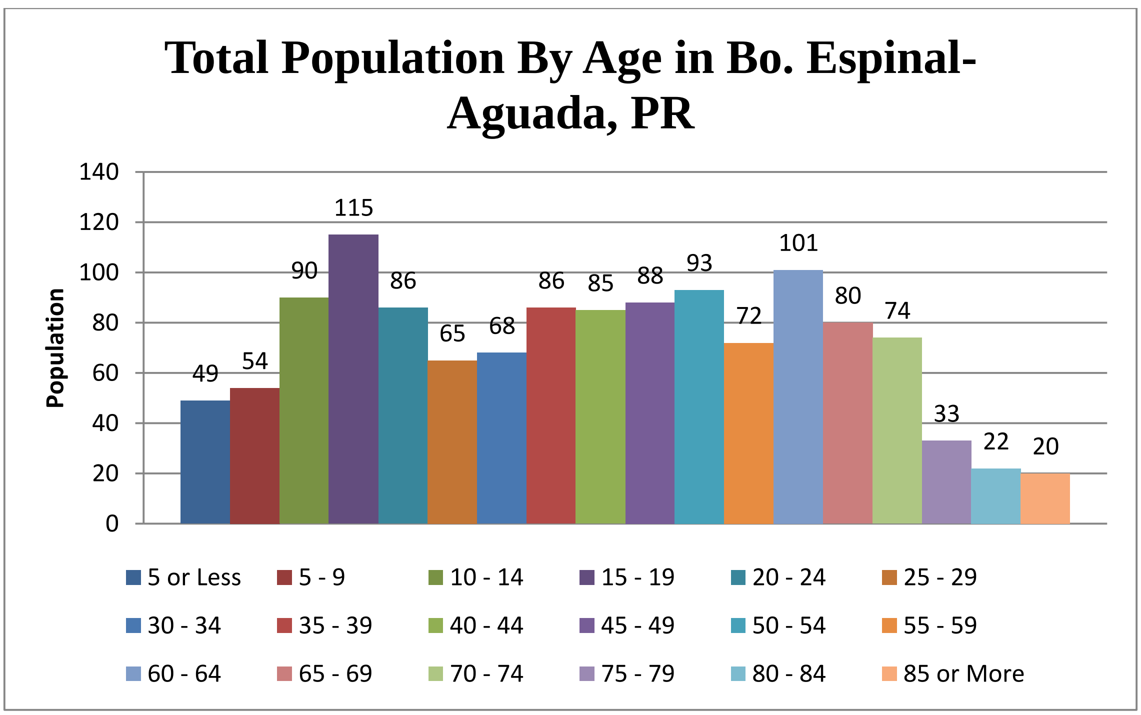

Figure 3.6: Age distribution in Bo. Espinal according Puerto Rico 2010 Census.

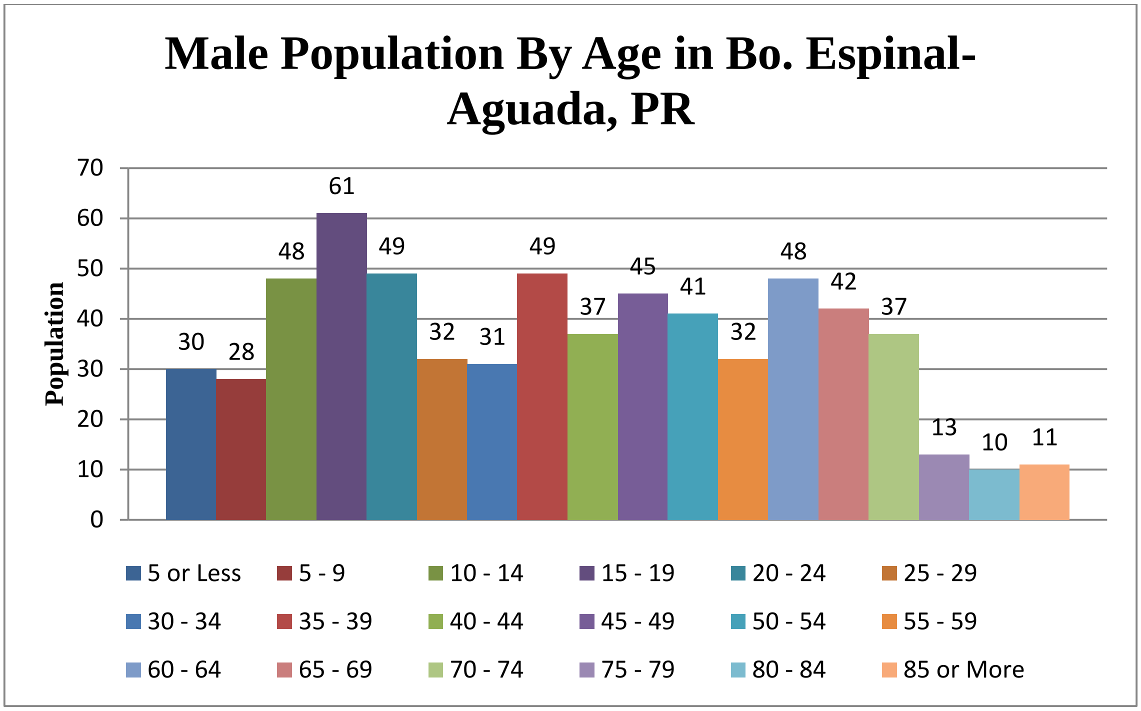

Figure 3.7: Male age distribution in Bo. Espinal according Puerto Rico 2010 Census. Median age of 39.5.

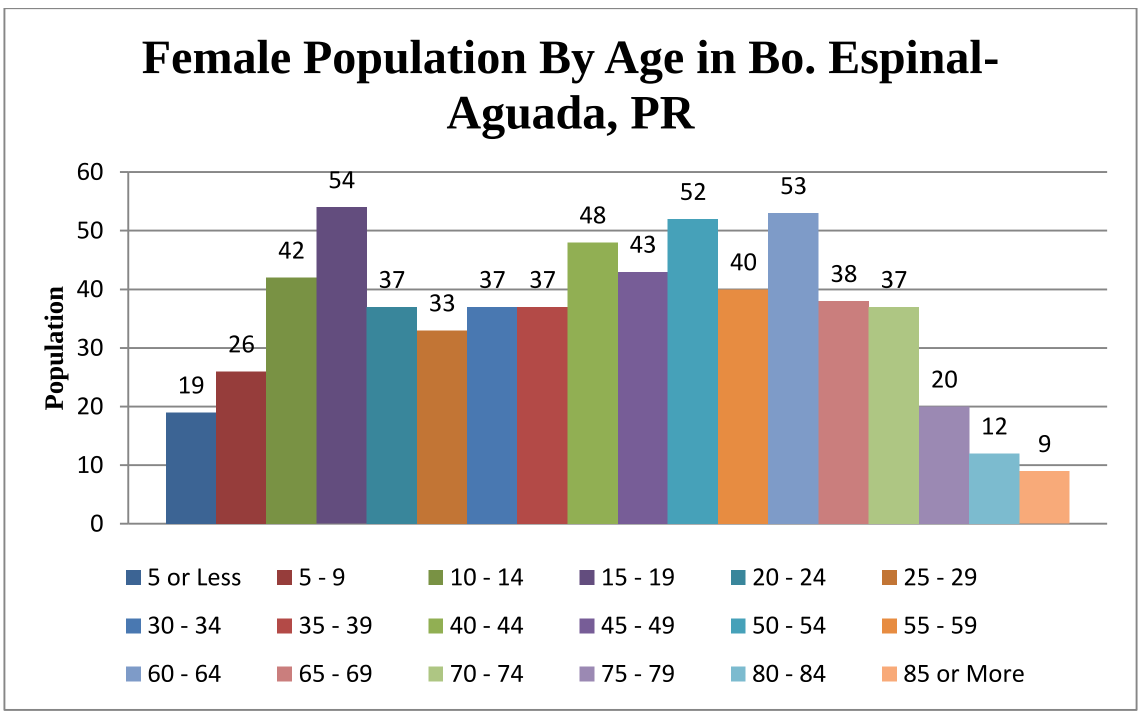

Figure 3.8: Female age distribution in Bo. Espinal according Puerto Rico 2010 Census. Median age of 43.5.

Table 3.1: Households by type of population for Bo. Espinal-Aguada, PR (2010 Puerto Rico Census).

Households by Type	Number	Percentage
Total households	469	100
Family households (families)	353	75.3
With own children under 18 years	120	25.6
Husband-wife family	235	50.1
With own children under 18 years	71	15.1
Male householder, no wife present	26	5.5
With own children under 18 years	11	2.3
Female householder, no husband present	92	19.6
With own children under 18 years	38	8.1
Nonfamily households	116	24.7
Householder living alone	104	22.2
Male	58	12.4
65 years and over	14	3
Female	46	9.8
65 years and over	26	5.5
Households with individuals under 18 years	159	33.9
Households with individuals 65 years and over	169	36
Average household size	2.73	N/A
Average family size	3.21	N/A

As a result of the 2010 Census, a households by type is obtained from Table 3.1. This data is important because it gave an idea of the composition of a family which can be correlated with the vulnerability in an evacuation process. For instance, there are 235 families (50.1%) in a husband-wife family, where 71 (15.1%) of them own children under 18 years. Furthermore, 26 (5.5%) male householders without wife, where 11 (2.3%) of them own children under 18 years. Female householder without husband present totaling 92 (19.6%), where 38 (8.1%) of children under 18 years. From this numbers is possible to know that 10.4% of the families with either a male or female householder have children under 18 years. This fact could complicate the evacuation, since they have to take care of their children without help from another adult.

Householder living alone are composed of 104 members (22.2%), where 40 (8.5%) are 65 year and over. Moreover there are 169 (36%) of households with individuals 65 years and over, representing possible difficulties at the time of the evacuation.

3.5 Vertical Evacuation Structure Proposed Site

Bo. Espinal counts with a green area in the center of the community with enough space, (Area = 26,750 m^2 = 6.6 acres) to accommodate a multistory structure and its location is appropriate since is closer for most of the population to meet there instead of leaving Bo. Espinal along PR-442. Since Bo. Espinal is a small coastal community only one VES is proposed, differing from FEMA P-646 which suggest an array of structures to provide refuge to the entire population for the critical tsunami arrival time. According to the Aguadilla topographic quadrangle digital elevation model (1996-1997) with a 1/3 arc-second resolution from the Municipal Revenue Collection Center (CRIM), the terrain elevation at the proposed VES site is 16.17 ft above the mean sea level.

Figure 3.9: Proposed site for VES

Figure 3.10: Plot of land of the proposed site for VES construction (Puerto Rico Digital Cadastre Office-CRIM, 2014)

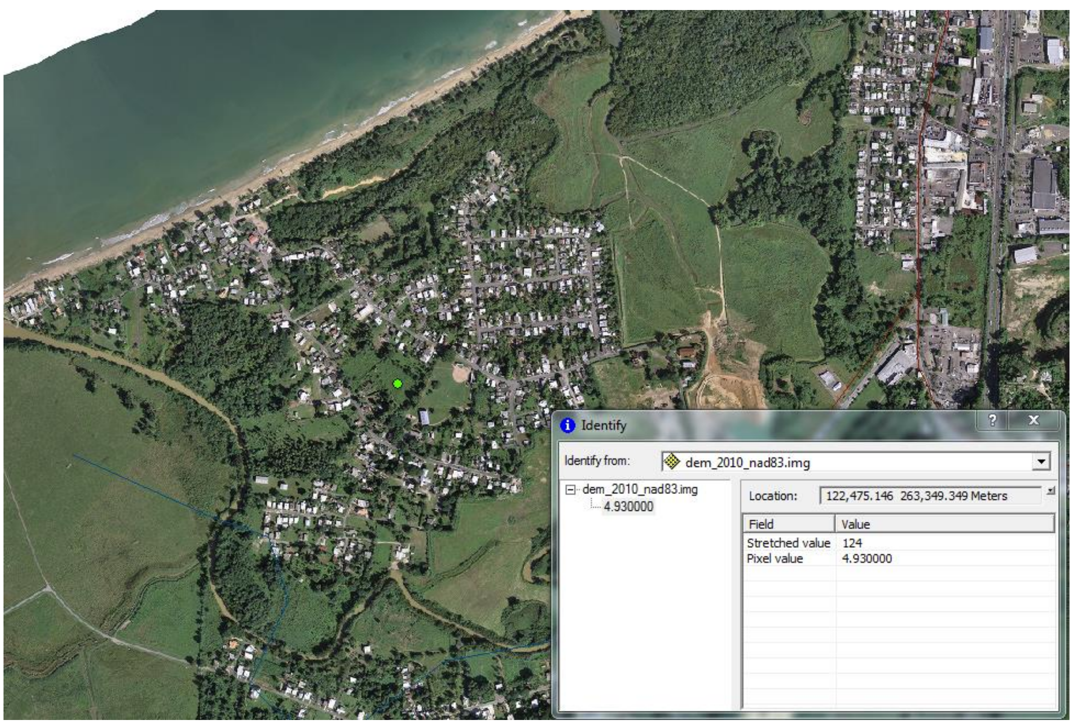

Figure 3.11: Terrain elevation in the proposed site, 4.93 meters (16.17 ft), above MSL.

3.6 Housing Distribution

An exercise was performed using an aerial image shown in Figure 3.12 to determine the distances of houses with respect to the proposed site in order to establish the number of refugees for a particular tsunami arrival time (t_T). Some assumptions were included. (1) Radial distances were used. (2) Reaction/recovery time after strong motion was set as five minutes. (3) Vertical ingress time to refuge area of VES was set to 3 minutes (recalling that the VES structural layout was intended to ascend one story per minute). (4) Pedestrians evacuation speed was set to 2 mph (according to FEMA-P646 guidelines). (5) Assuming that all the population are in their houses at the time of the evacuation event.

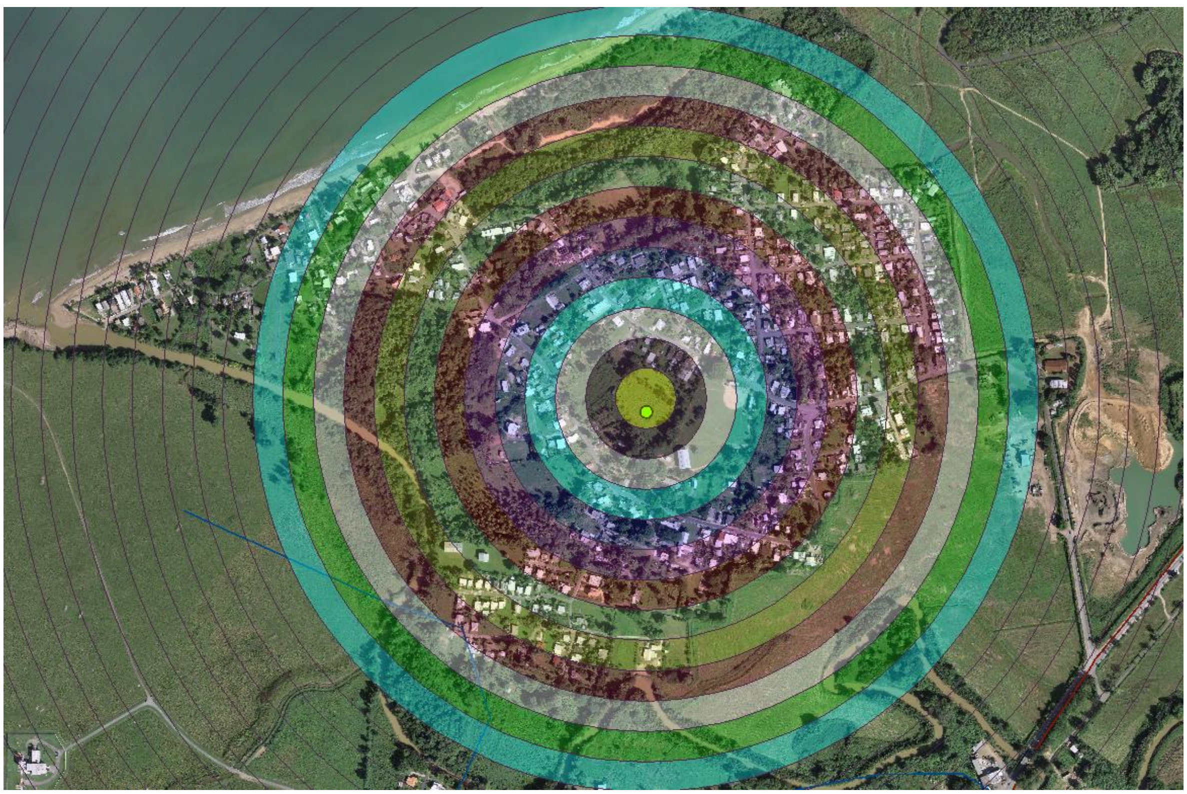

Figure 3.12: Aerial photo with sets of circle to determine radial distances.

Table 3.2: Results of the exercise and parameters used.

t_T (min.)	t_B (min.)	R (m)	Total of houses inside R(m)	Refugees
8	0	0	0	0
9	1	54	0	0
10	2	107	13	27
11	3	161	39	80
12	4	215	93	190
13	5	268	158	323
14	6	322	216	442
15	7	375	285	583
16	8	429	353	722
17	9	483	437	894
18	10	536	514	1052
19	11	590	566	1158
20	12	644	580	1187
21	13	697	589	1205
22	14	751	604	1236
23	15	805	606	1240
24	16	858	610	1248
25	17	912	618	1264
26	18	965	626	1281

t_R = Recovery time after strong motion
t_i = Ingress time to refuge area of VES
t_T = Tsunami arrival time since generated
t_B = Available time to arrive at base of VES; where $t_B = t_T - (t_R + t_i)$

According to the results obtained from this exercise, ten minutes are the minimum tsunami arrival time that allows first 27 evacuees reach the VES refuge area, starting in the roof of the third story at an elevation of 34.5 ft (see Table 3.2). As shown in Figure 3.13, every passed minutes after minute ten, the evacuees begin to arrive at the refuge area at a constant rate, reaching to accommodate around 500 people in 14.5 minutes and a 1,000 in less than 18 minutes. For a full evacuation, it would require about 26 minutes. This graph in conjunction with the aerial photo provides an idea on how close are the houses regarding the proposed vertical evacuation structure location, where little more than 75% of the houses are located within a radius of 500 meters away from this site.

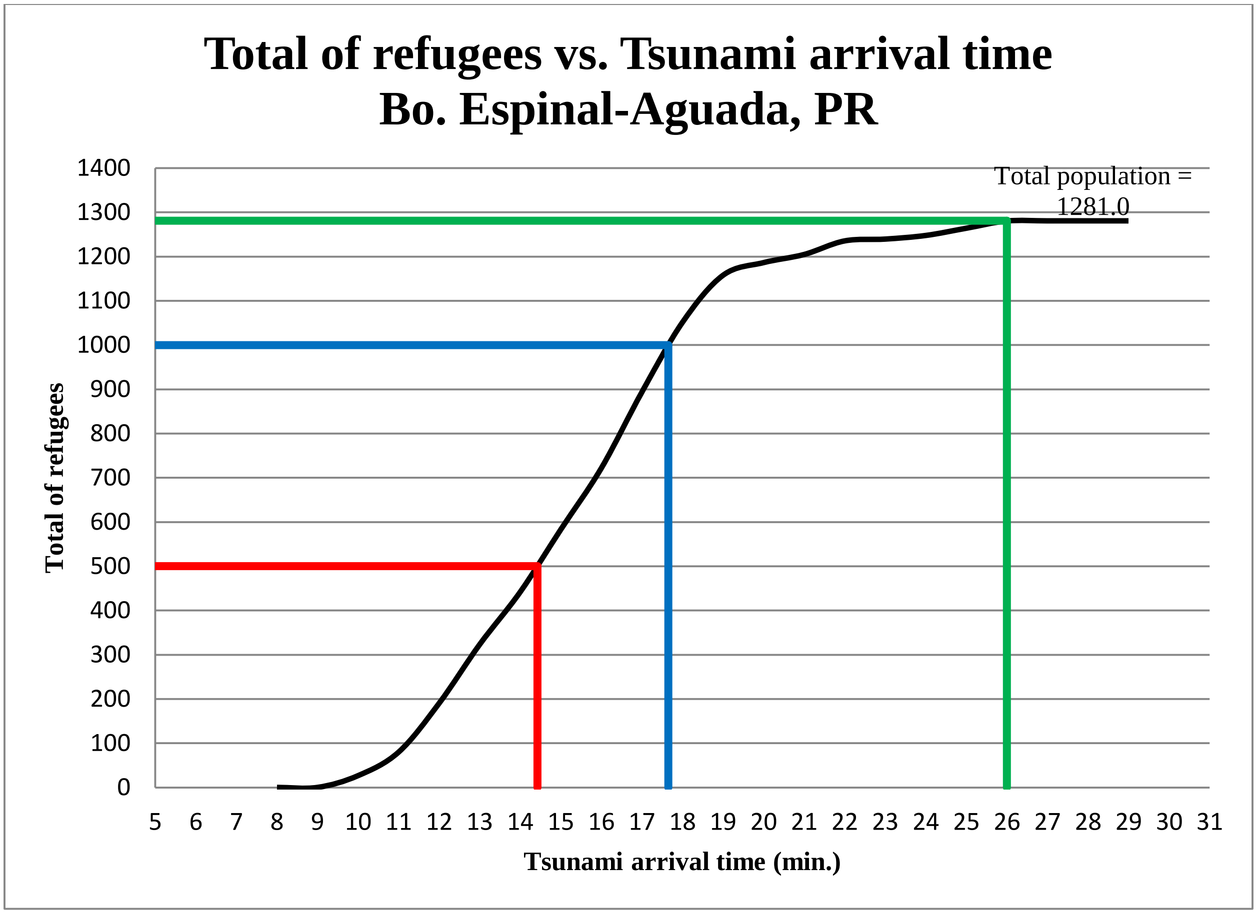

Figure 3.13: Population expected in the refuge area in function of the tsunami arrival time.

3.7 Soil Classification and Geotechnical Studies

At the east and northeast areas of Bo. Espinal coastal community, has been proposed a development of the Discovery Bay Resort & Marina, which in 2007, Advanced Soil Engineering-geotechnical consulting, conducted soil studies in the area. The results of the geotechnical studies are available in the report "*On the Preliminary Geotechnical Exploration Performed at the Site of the Proposed Discovery Bay Resort & Marina, Espinal Ward, Aguada, Puerto Rico"*. This results provides an idea of the soil type in the area of the proposed VES. In Appendix A, is presented a boring location map of the borings performed. Boring No. 11, is the most representative, since is the closest boring to the proposed site of the vertical evacuation structure, with a distance of approximately 1,200 feet apart.

According to the geotechnical study, boring No. 11, show a fill material composed of yellowish brown silt clay some limestone fragments trace sand, which extends to depths varying from 0.0 to 18.0 feet below existing ground elevation. Light brown sand trace silt extends from 18.0 to 28.0 ft. Light brown and gray silty clay trace sand that extends to depths varying from 28.0 to end of boring 40 feet. The ground water level for this particular boring at that particular date (06/19/07), was encountered at a depth of 12.0 ft below ground elevation. See Figure A.3 and Figure A.4 in Appendix A for details. According to the boring log presented, the Standard Penetration Test (SPT) N-values, were found to be lower than 15 blows/ft, which would result in a corrected average value below 15 blows/ft. By using Table B.7, the site could be classified as site class E – “soft clay soil”.

CHAPTER 4 - CALCULATIONS OF DESIGN HYDRODYNAMIC PARAMETERS

4.1 Introduction

By using the tsunami simulation results performed by Mercado et al. (2011) who used the MOST (Method of Splitting Tsunami) numerical model to simulate different tsunami events, it was possible to determine the design hydrodynamic parameters at the site of interest. The results from an idealized M 8.5 FEMA Catastrophic Scenario simulation in combination with a tsunami flood map were used to define the maximum inundation depth, maximum flow velocity and maximum momentum flux for the site of interest at Bo. Espinal. A comparison of the hydrodynamic parameters within the numerical simulation results and the FEMA P-646 provisions results is presented. The tsunami force effects described in Section 2.4, the respective equation and considerations will be used to estimate the tsunami loads for which the structure will be designed.

4.2 Method of Splitting Tsunamis (MOST)

MOST, developed by Titov (1997) of the Pacific Marine Laboratory (PMEL) and Synolakis of University of Southern California is the standard model used at the NOAA Center for Tsunami Research (NCTR). MOST is a suite of numerical simulation codes based on finite difference method to divide its computational domain and capable of simulating three processes of tsunami evolution: earthquake, transoceanic, and inundation of dry land. On local spatial scales, nonlinear shallow water (NSW) equations are solved numerically. Propagation on regional and transoceanic spatial scales requires equations that are expressed in spherical coordinates. Propagation solutions are obtained by a numerical technique that involves a mathematical transformation known as splitting. Tsunami modeling using MOST proceeds in three distinct stages: (1) Deformation phase which generates the initial conditions for a tsunami by simulating ocean floor changes due to a seismic event. (2) Propagation phase which propagates the generated tsunami across deep ocean using (NSW) wave equations. (3) Inundation phase which simulates the shallow ocean behavior of tsunami by extending the (NSW) calculations using a multi-grid run-up algorithm to predict coastal flooding and inundation (NOAA-MOST Software Manual, 2006).

4.3 Tsunami Event Simulation Data

4.3.1 M 8.5 FEMA Catastrophic Scenario

FEMA Catastrophic Scenario is an idealized 8.5 magnitude earthquake that the Federal Emergency Management Agency established as the triggering event for a tsunami simulation. The main reason for this study was to quantify the tsunami hazard in terms of fatalities and economic losses in northern Puerto Rico. With an epicenter at Zone 19° fault location, the north of Puerto Rico and the Virgin Islands would expect strong shaking intensity and potential damages due to an expected tsunami. The MOST numerical model was used by Mercado et al. (2011) to perform the tsunami simulation.

General Simulation Parameters

A. **Deformation and Propagation Phase Input Data:**

- Fault origin or epicenter is in Aki-Richards convention
- Minimum depth for offshore (Depth threshold for propagation, vertical wall is set at this point): 20 meters
- Time step (Based on CFL-Courant-Friedrichs-Lewy stability condition): 5.5 sec.
- Amount of steps (Total time for simulation based on "input time step", 2 hours for this case): 1963
- P-wave velocity: Default value of 8.11 Km/s
- S-wave velocity : Default value of 4.49 Km/s
- Size of deformation area in X and Y: 1,000 [units]
- X-integration: Default value of 41[units]
- Y-integration: Default value of 21[units]
- Number of Fault Planes: 4

Table 4.1: Fault parameters used for the four segments defined (Mercado et al., 2011).

Fault Parameters	Segment 1	Segment 2	Segment 3	Segment 4
Longitude (Deg.)	-64.80	-65.40	-66.50	-67.00
Latitude (Deg.)	19.00	19.00	19.25	19.25
Length (Km)	66.92	63.08	118.9	52.49
Width (Km)	72.59	72.59	72.59	72.59
Dip (Deg.)	45.0	45.0	45.0	45.0
Rake (Deg.)	90.0	75.0	85.0	75.0
Strike (Deg.)	109.0	90.0	103.0	90.0
Slip (m)	5.473	5.473	5.473	5.473
Depth (Km)	10.0	10.0	10.0	10.0

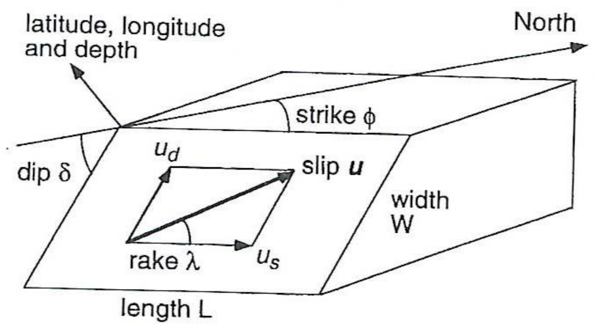

Figure 4.1: Earthquake fault parameters and geometry system (NOAA-MOST Software Manual, 2006)

B. Inundation Phase Input Data:

- Minimum amplitude of input offshore wave: 0.0050 meters
- Minimum depth of offshore: 5.0 meters
- Dry land depth of inundation: 0.1 meters
- Manning coefficient of friction (resistance to run-up): 0.03
- Outer grid run-up: 1
- Maximum wave height before blow-up: 100.00 meters
- Time step: 0.16 sec.

- Total number of time steps in run (2 hrs): 90,000
- Time steps between A-grid computations: 36
- Time steps between A-grid computations: 36
- Time steps between B-grid computations: 6
- Time steps between output steps (18 sec.): 180

4.3.2 Maximum of the Maximums: Local Sources

As an effort to develop the tsunami flood map for Puerto Rico, the National Tsunami Hazard Mitigation Program (NTHMP) and Mercado et al. (2011), simulated a total of 269 faults scenarios from 12 different seismic fault all around the island to represent a fraction of all possible tsunami floods and inundation depths in every coastal area of Puerto Rico (see Figure 4.3). Each of the fault scenarios were modeled using the MOST numerical model.

Table 4.2: Twelve seismic faults considered for tsunami flood map development (Mercado et al., 2011).

Seismic Fault	Total of Faults
Anegada Passage	28
Eastern Dominican Republic	9
Leeward Islands	11
McCann's Faults	31
Muertos Trough	23
Mona Canyon	24
Zone 19°	16
North Platform	25
Puerto Rico Trench	28
West to Southeast Puerto Rico	36
Septentrional	14
Sombrero	24

Figure 4.2 presents the inundation grids for every tsunami simulation performed by Mercado including the M 8.5 FEMA Catastrophic Scenario and all of the Maximum of the Maximums simulations sets. The inundation outer grid has 60 arc sec resolution. The inundation intermediate grid has 9 arc sec resolution. For the inundation inner grids the island was broken down into three parts: West, Central, and East. Each has a computational cell size of 1 arc second (approximately 30 x 30 meters), (National Geophysical Data Center PR DEM, 2007). Results are output for each part, and then a mosaic is created based on joining the three parts.

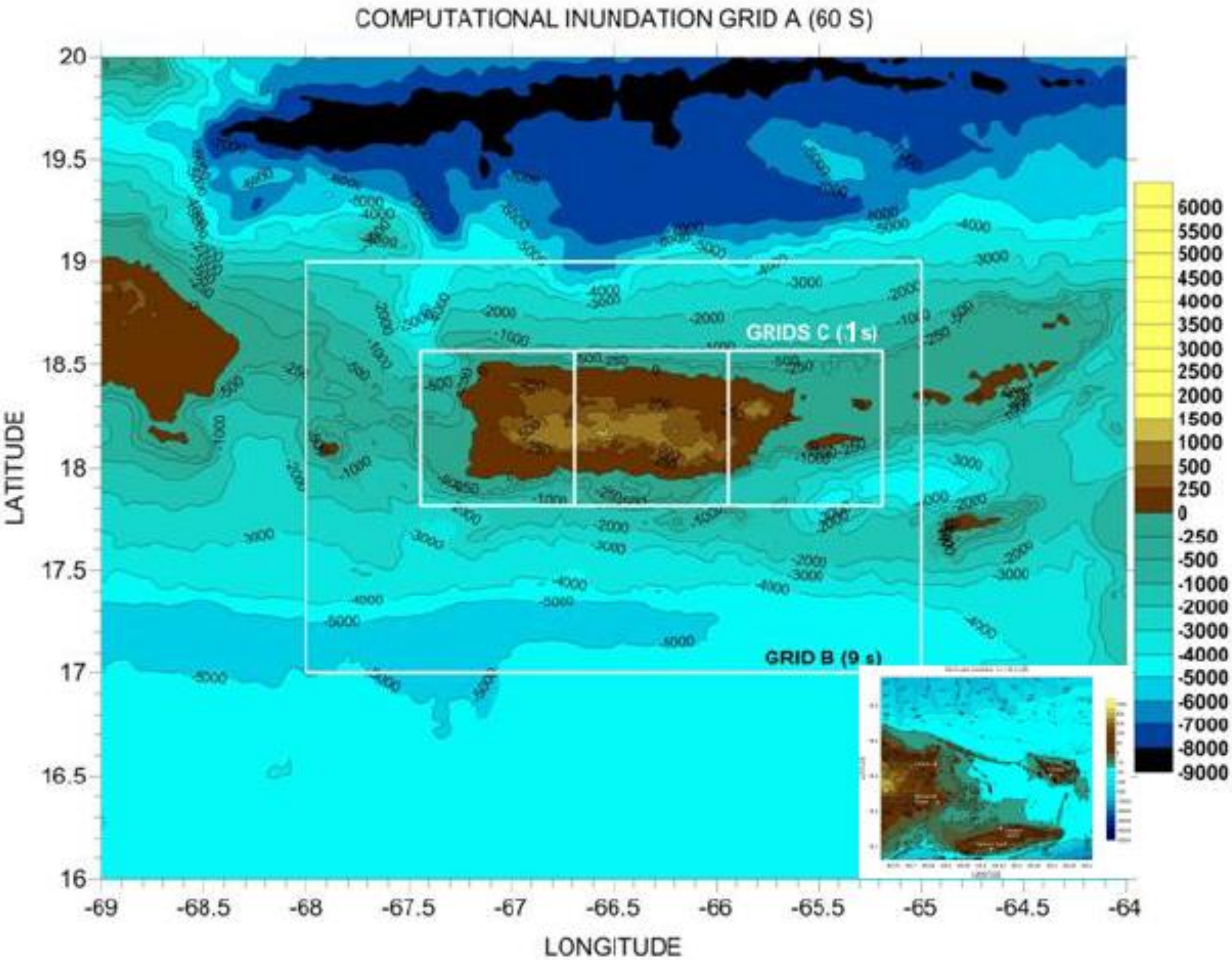

Figure 4.2: Inundation grids used for tsunami simulation (Mercado et al., 2011).

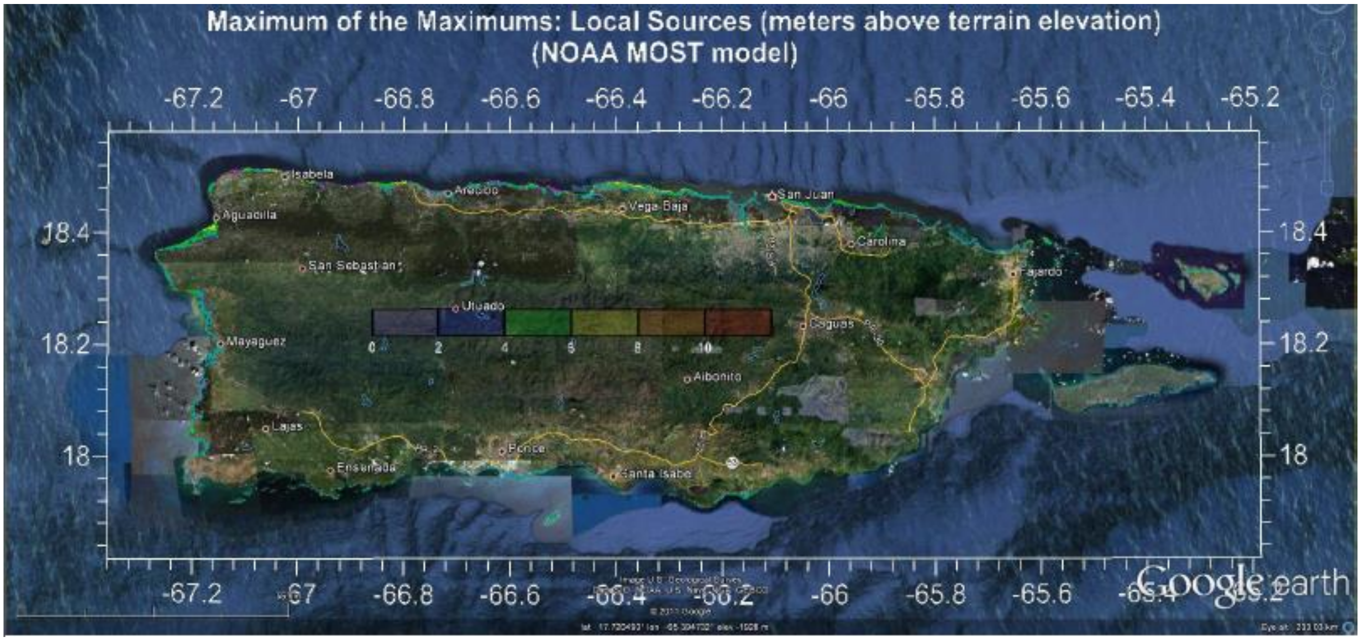

Figure 4.3: 2011 Puerto Rico NTHMP tsunami flood map (Mercado et al., 2011).

4.4 Tsunami Simulation Results

To determine the design parameters such as maximum inundation, velocity magnitude and maximum momentum flux for the vertical evacuation structure design, it was intended to use the available tsunami simulation results of the M 8.5 FEMA Catastrophic Scenario previously discussed. After analyzing and plotting the results of the maximum inundation depth, as shown in Figure 4.4, it is perceived that the resultant tsunami run-up does not reach the vertical evacuation proposed site (see Figure 4.5). This was to be expected since the source of this event is located in the north of Puerto Rico. As a result of this, it is the northern coastal communities the ones that will be most affected. As a matter of fact, in Figure 4.4 it is shown that the town of Aguadilla will experience run-ups of five meters or higher for this particular event.

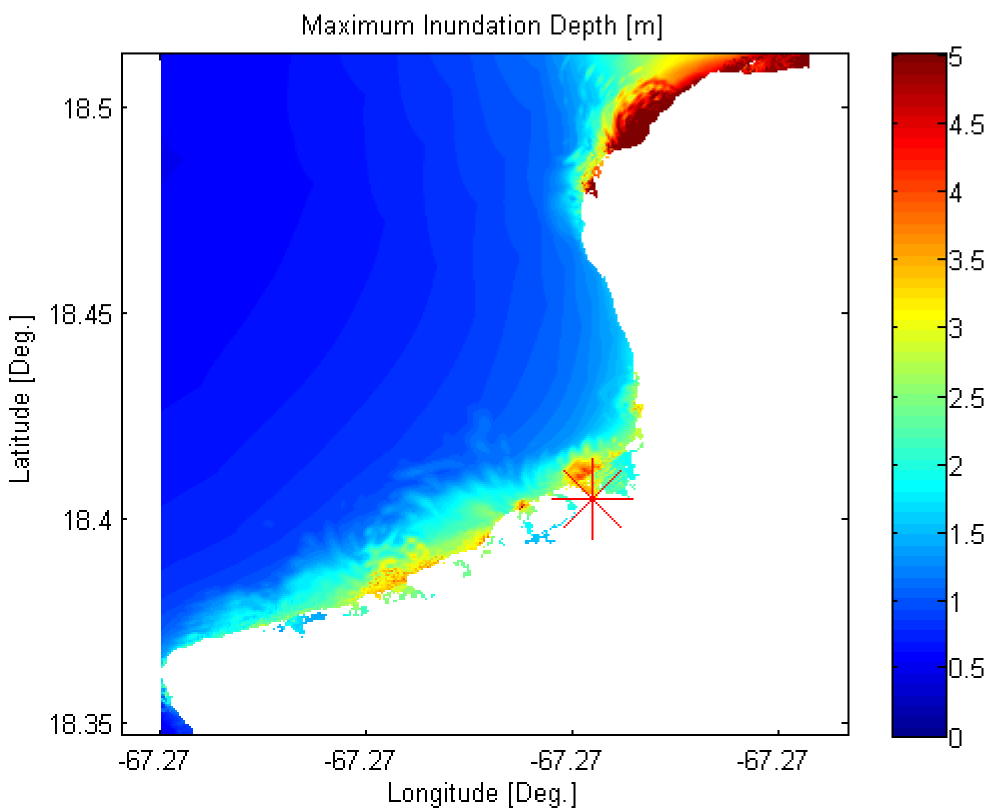

Figure 4.4: Bo. Espinal maximum inundation depth [meters] for 8.5, FEMA Catastrophic Scenario, (Red star locate the vertical evacuation structure site).

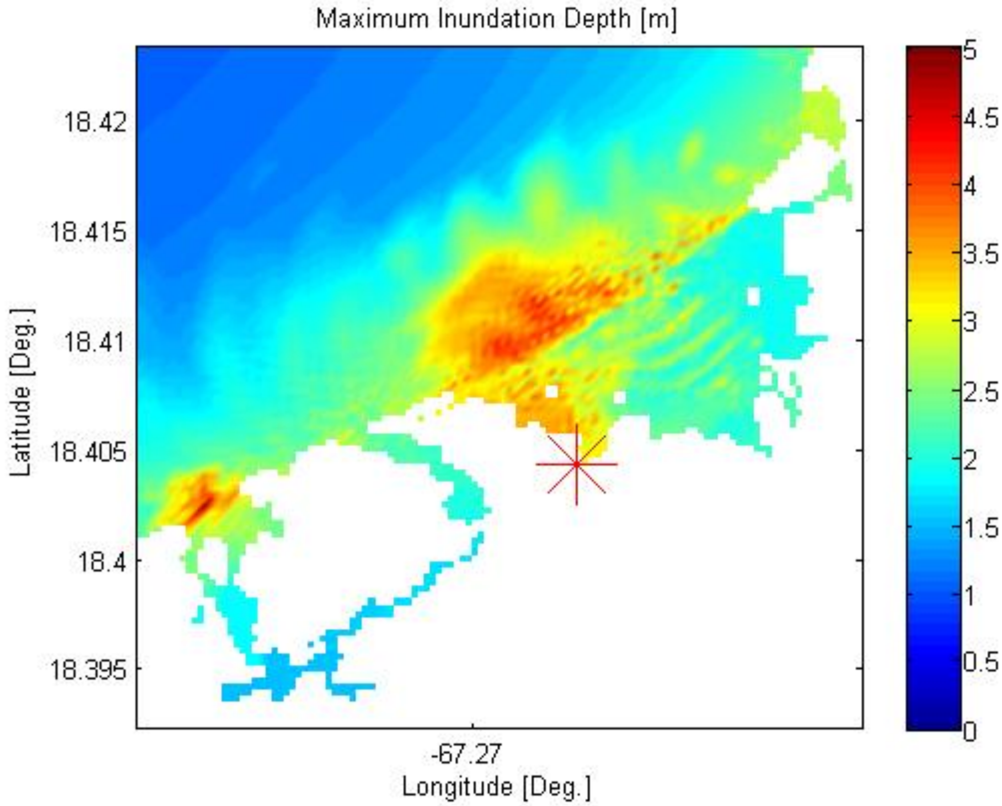

Figure 4.5: Zoomed area of previous figure.

Since the M 8.5 FEMA Catastrophic event does not fully affect the Bo. Espinal, the Maximum of the Maximums flood map was used to determine the maximum inundation depth at the proposed location of the vertical evacuation structure. As shown in Figure 4.6 and Figure 4.7, the maximum inundation depth in the site of interest is among 3-4 meters. Hence, for design purposes, 4 m will be used.

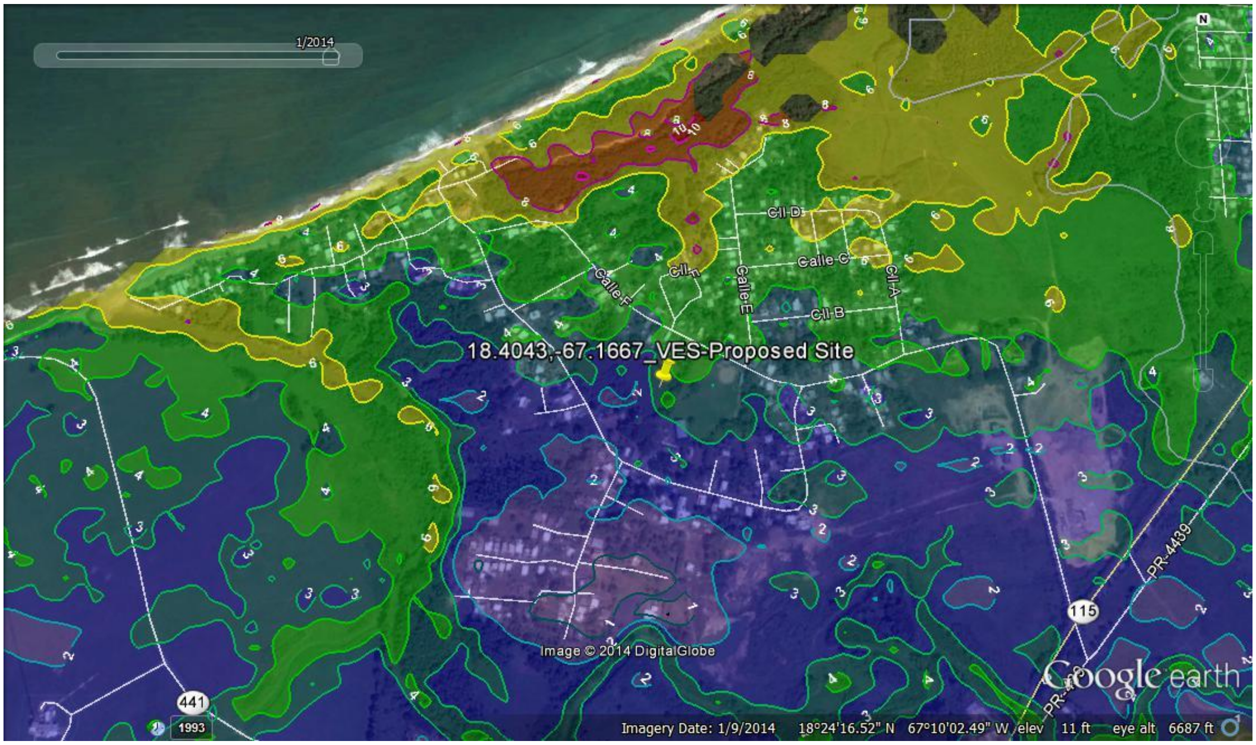

Figure 4.6: Bo. Espinal tsunami flood map with depth values [meters].

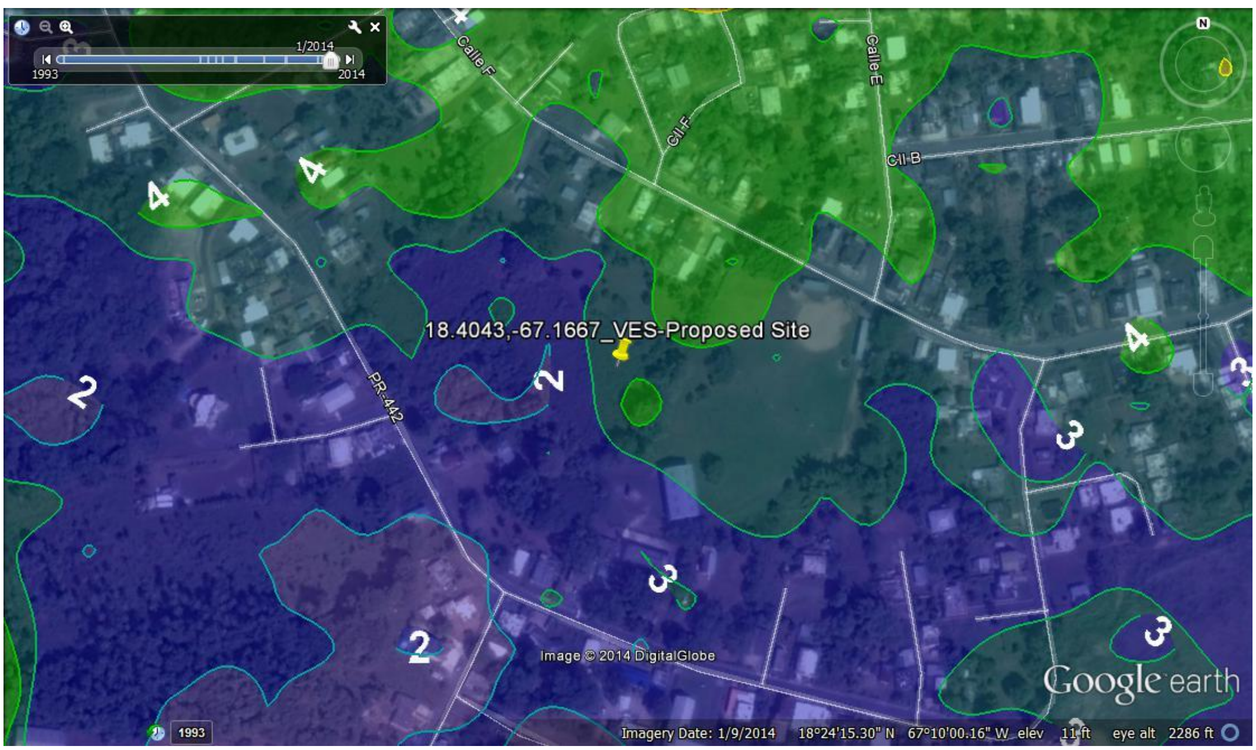

Figure 4.7: Proposed site flood map with depth values [meters].

Since there is a relationship between the inundation depth and velocity magnitude for a given constant Manning roughness factor, a reference point was used to obtain the maximum velocity and maximum momentum flux. The reference point selected had to meet three conditions: (1) same inundation depth as the site of interest as shown in Figure 4.8, (2) located near the site of interest, which feels the same wave transformation effects, (3) run-up expected for the M 8.5 FEMA Catastrophic Scenario.

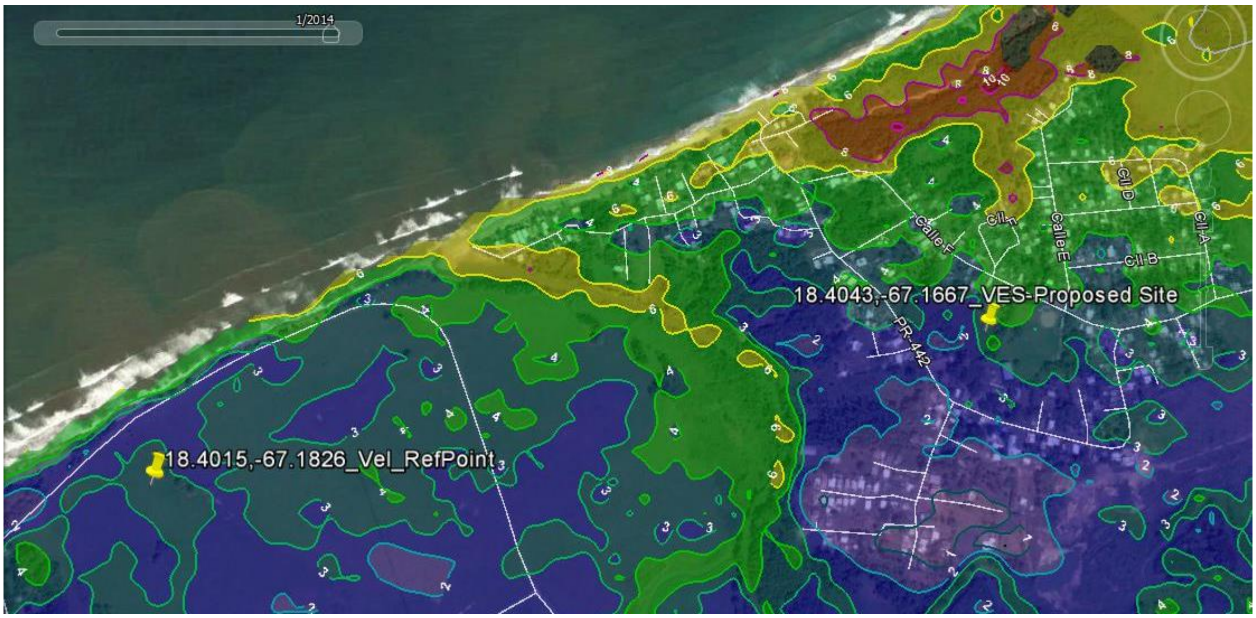

Figure 4.8: Velocity reference point with same inundation depth as the proposed site location.

By using the results of the FEMA event at the reference point, according to Figure 4.9 through Figure 4.12, a velocity magnitude of 3 m/s and a momentum flux of 20 m^3/s^2 are to be expected at the vertical evacuation proposed site. The momentum flux values are important for engineering design purposes or re-assessment of existing structures to verify their capability to resist tsunami loads. In addition, this parameter can assist coastal managers in assessing the relative vulnerability of some infrastructure by identifying the nature and location of major tsunami flows.

It has been noted that numerical predictions of flow velocities and consequently the momentum flux, are less accurate than predictions of inundation depths, and the grid size for numerical simulations in the run-up zone should be very fine in order to obtain sufficient accuracy in both predictions (FEMA P-646). Because of the uncertainty involved in even accurate numerical simulations, it is recommended that a safety factor be applied to the computed flow velocity, depending on the level of confidence in the numerical model simulations.

According to FEMA P-646, it is recommended for conservatism that the design inundation elevation be increased at the structure site by 30% over the computed inundation elevation. In addition, the design flow velocity should be increased by 15% and the momentum flux $(hu^2)_{max}$ must be increased by 70% over the computed values. These safety factors are basically a guideline based on the 30% error band in modeled tsunami run-up heights compared with observed run-up heights from historic tsunami survey data.

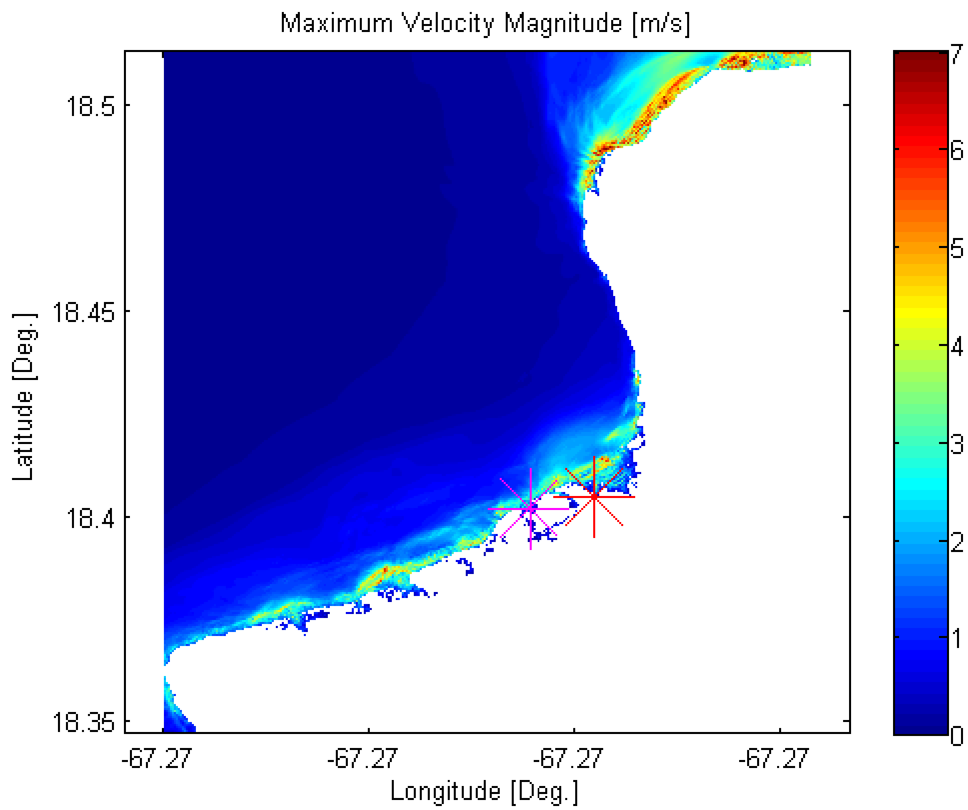

Figure 4.9: Bo. Espinal maximum velocity magnitude [m/s] for 8.5, FEMA Catastrophic Scenario, (Red star locates the vertical evacuation structure site and magenta star locates the reference point).

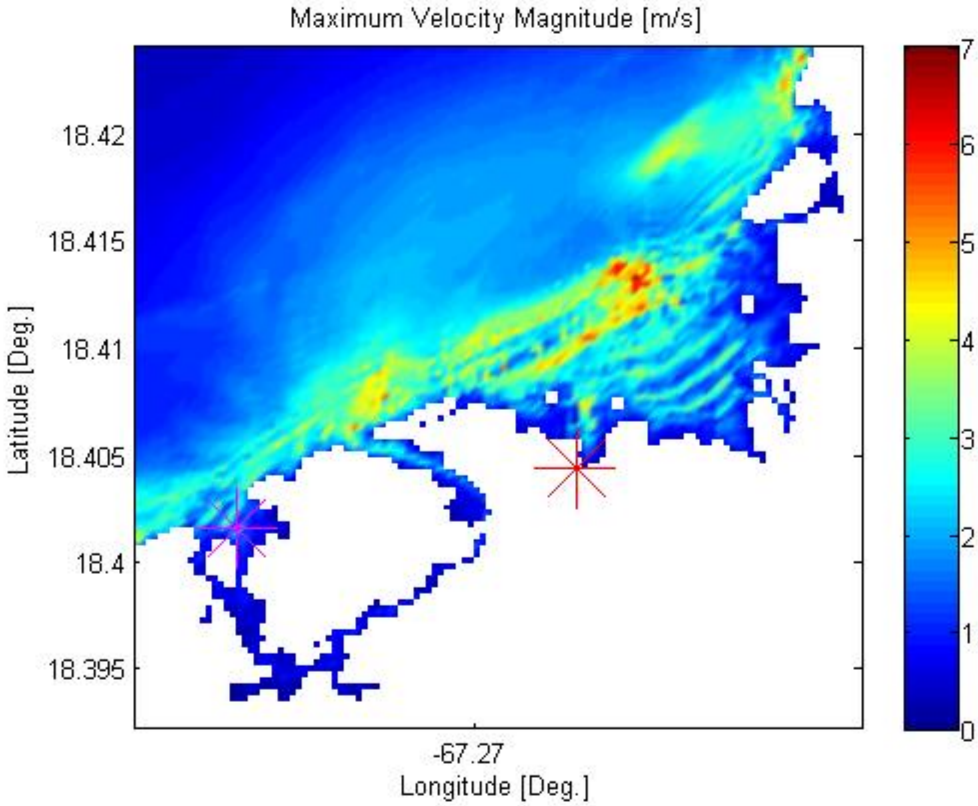

Figure 4.10: Zoomed area of previous figure.

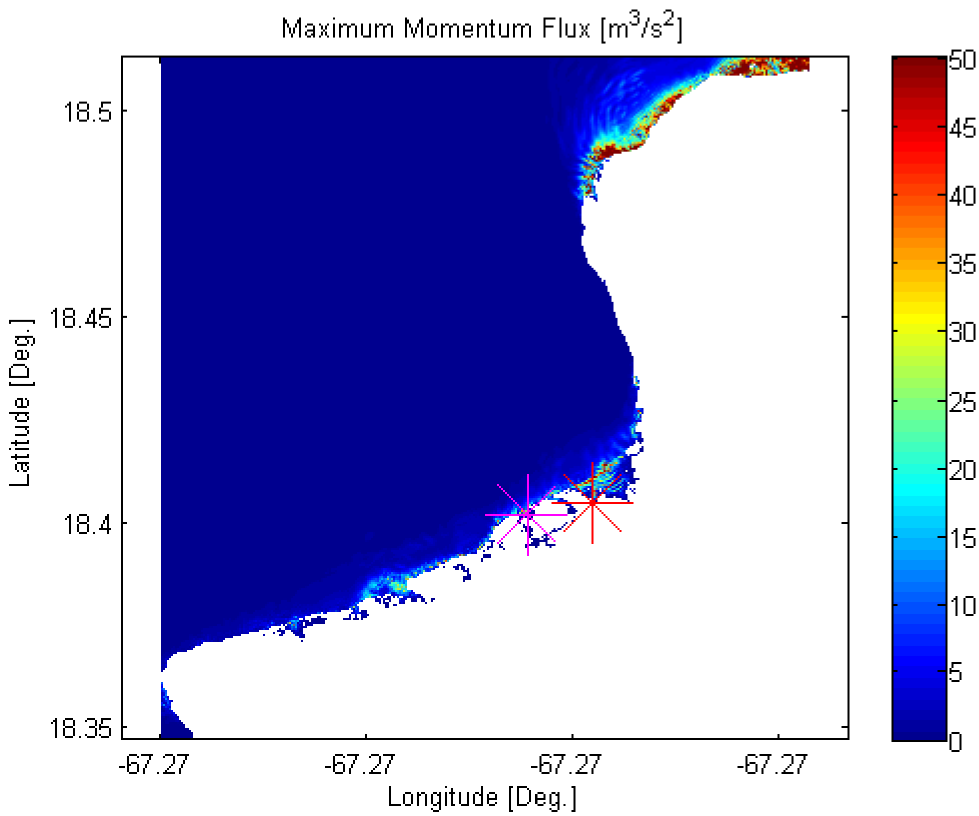

Figure 4.11: Bo. Espinal maximum momentum flux [m^3/s^2] for 8.5, FEMA Catastrophic Scenario, (Red star locates the vertical evacuation structure site and magenta star locates the reference point).

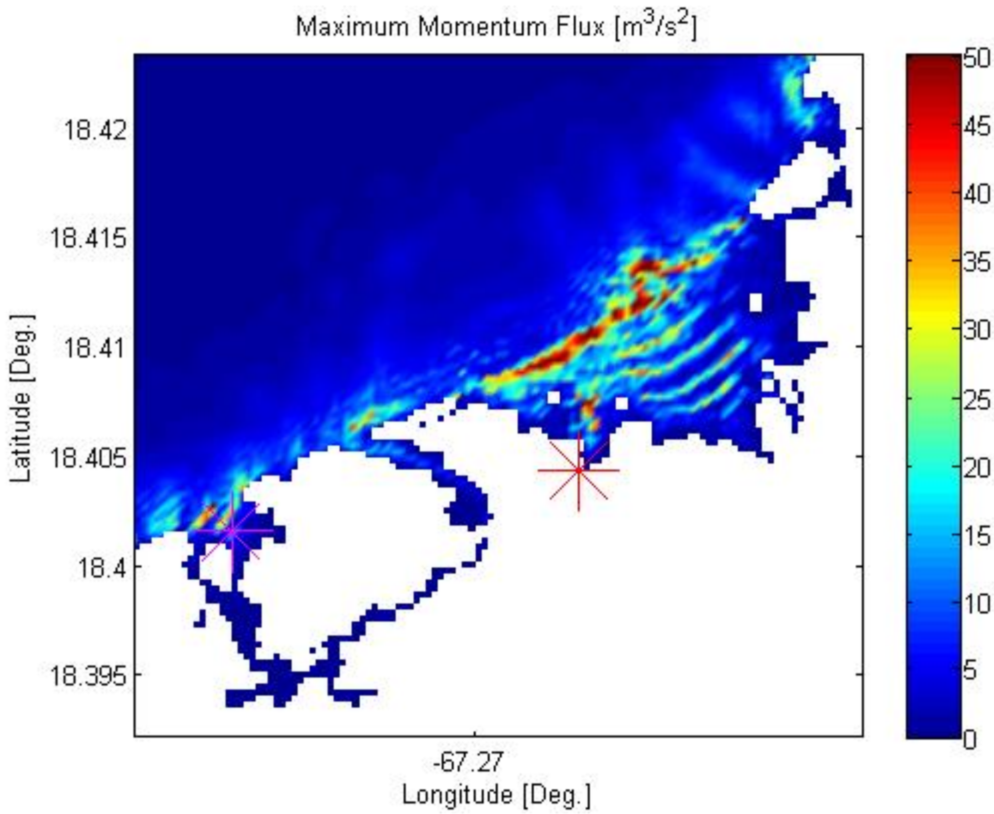

Figure 4.12: Zoomed area of previous figure.

4.5 Comparison and Analysis Between the Simulation Results and FEMA P-646 Provisions

In the previous section the hydrodynamic parameters such as maximum flow velocity magnitude and momentum flux were determined by the tsunami simulations results. As described in Section 2.4 (Tsunami Loading According to FEMA P-646), there is a set of equations to determine in a conservative way these hydrodynamic parameters.

The maximum flow velocity and the momentum flux at the site are estimated using, R^* = 8.93 m, $R = 1.3R^*$, z = 4.93 m and g = 9.81 m/s^2

Maximum velocity magnitude at the site using Equation 2.13:

$$u_{max} = \sqrt{2gR\left(1-\frac{z}{R}\right)} = \sqrt{2 * 9.81\frac{m}{s^2} * 11.61m * \left(1-\frac{4.93m}{11.61m}\right)} = 11.45\frac{m}{s}$$

Maximum momentum flux at the site using Equation 2.4:

$$
\begin{aligned}
(hu^2)_{max} &= gR^2\left[0.125 - 0.235\frac{z}{R} + 0.11\left(\frac{z}{R}\right)^2\right] \\
&= 9.81\frac{m}{s^2} * (11.61m)^2 * \left[0.125 - 0.235\frac{4.93m}{11.61m} + 0.11\left(\frac{4.93m}{11.61m}\right)^2\right] \\
&= 59.56\frac{m^3}{s^2}
\end{aligned}
$$

In Figure 4.13 is shown the variation of momentum flux for a given z/R ratio using Equation 2.4, where the red star indicates the value of 59.56 m^3/s^2, previously computed for this particular case.

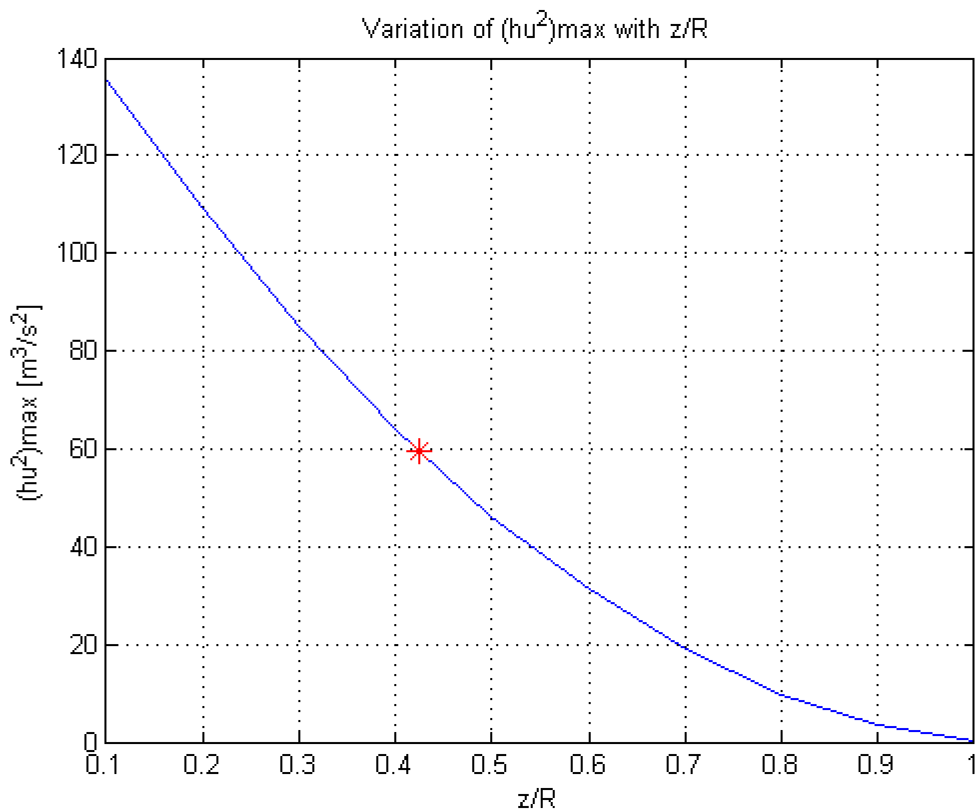

Figure 4.13: Variation of momentum flux with z/R

Table 4.3: Results of the design hydrodynamic parameters from three different sources.

Design Hydrodynamic Parameter	**Tsunami Simulation Results by Mercado et al., (2011)**	**FEMA P-646 provisions**
Maximum Velocity (m/s)	3.00*1.15 = 3.45	11.45
Maximum Momentum Flux (m^3/s^2)	20.00*1.7 = 34	59.56

The results in Table 4.3 shows the maximum values of velocity and momentum flux to be expected in the site of interest at Bo. Espinal. Factors of amplification were used according to FEMA P-646 for the numerical simulation results. Results from Mercado et al. (2011) are validated with the publication "Advanced Tsunami Numerical Simulations and Energy Considerations by use of 3D-2D Coupled Models: The October 11, 1918 Mona Passage Tsunami" by López et al. (2014). For the FEMA provisions the maximum inundation depth parameter was increased by 30%, which has an effect in the maximum velocity and momentum flux, since both are a function of the inundation depth. According to the results, the FEMA provisions produced higher values than the simulation output, implying that it is a conservative method to approximate these hydrodynamic parameters. In fact, the flow velocity calculated using Equation 2.13 does not include the effects of friction and the maximum flow velocity occurs at the leading run-up tip, where the flow depth is zero.

It is important to highlight that the maximum velocity and maximum momentum flux used for the design procedure are representative for the M 8.5 FEMA or similar events. However a tsunami event originated closer to the West coast of Puerto Rico having a north-south fault alignment could produce a direct hit resulting in higher magnitudes of velocities and momentum flux. A final design must verify the velocity magnitude in the site with the maximum of the maximums set of scenarios map which are in current development.

CHAPTER 5 - VERTICAL EVACUATION STRUCTURAL LAYOUT AND APPLICATIONS

5.1 Introduction

A vertical evacuation structure could be as simple as a natural high ground/soil berm or as complex as a building intended for other uses when not being used as a refuge. Vertical evacuation structures could be developed to satisfy specific community needs; for instance, community centers, recreational facilities, sport complex, libraries, etc. Some of the advantages of selecting a building instead of a man-made mound of earth includes, the ease to justify a constantly used facility due to its multiple applications in contrast to a single purpose structure. Moreover, a building could provide storage areas for first aid supplies, water and many other resources. A drawback of using a multi-purpose building as an evacuation structure is that the vertical ingress could be affected by the furniture or any other object blocking the access to the refuge area. For this reason a solution to mitigate such problem is adding to the structural layout an exterior access which allows the vertical ingress at any time and without obstructions.

As mentioned in Section 2.3, some of the structural characteristics that have demonstrated good behavior in past tsunami activities are: (1) open systems that allow water to flow through with low resistance; (2) well-built systems with reserve capacity to resist extreme forces; (3) ductile and resilient systems that withstand extreme forces with no collapse; and (4) redundant systems that can experience localized failure with no progressive collapse. All of these characteristics should be taken into consideration for the development of the vertical evacuation structure layout.

In this Chapter the methodology used to assign preliminary sections to the structural members of the proposed vertical evacuation building is discussed.

Furthermore an objective of this study is to determine other potential use and applications of the proposed building. Some suggestions are presented based on the demographic characteristics discussed in Section 3.4.

5.2 Proposed Structural Layout Description

5.2.1 Sizing Details

The proposed vertical evacuation structure is a five story building made of reinforced concrete. The amount of stories is based on the results obtained in Section 4.4. With a maximum inundation depth, h_{max} of 13.12 ft (4 meters), and a ground elevation at the site of interest, z of 16.17 ft (4.93 meters), the maximum tsunami run-up elevation anticipated at the site, R^*, is 29.30 ft (8.93 meters). After amplifying the run-up by 30%, and adding a freeboard allowance of 10 feet (3 meters), the refuge area elevation above the terrain become to 31.92 ft (9.73 meters). Considering a typical story height of 11.5 feet, the refuge area should start at a height of 34.5 ft, corresponding to the plan of the fourth floor.

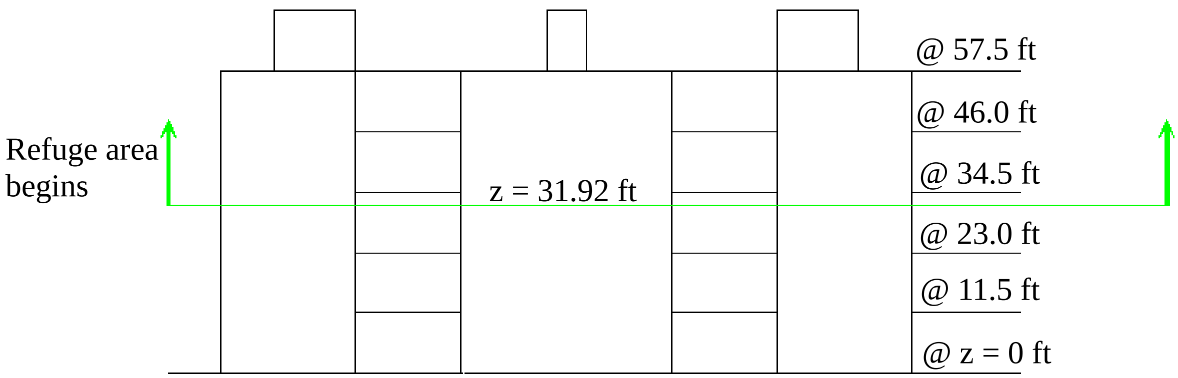

Figure 5.1: Delimited refuge area height.

As shown in Figure 5.3, the building plan is composed of a rectangular area (80ft x 50ft = 4,000ft^2) with 25 feet radius semicircles at each end, adding 1,963.5 square feet for a gross plan area of 5,963.5 square feet. The semicircular configuration at the ends was intended to help divert away and channel tsunami flow and potential waterborne debris from the structure. As part of the access features, an elevator core for day-to-day use is located at the center of the structure with dimensions of 12ft x 7ft. In addition one staircase in each semicircle with dimensions of 15ft x 12ft is provided. A third type of access is an external ADA compliant ramp, which goes around the building up to the roof top, with access to all stories. The vertical ingress ramp is a six feet wide, sloped at 8.33% (12:1), with supports spaced at approximately 20ft. In addition, this ramp include landings of at least five feet long each spaced at 28 ft. The stairs and the ramp systems could be used for both, daily or emergency access. After subtracting the elevator core area, staircase area, interior columns (assuming two square feet each), and 4.5% of the gross plan area for restrooms uses, the net floor area become 5,239.5 square feet.

According to FEMA P-646 and the International Code Council (*ICC 500 - 2008: Standard for the Design and Construction of Storm Shelters*), to determine the usable floor area of a shelter, some adjustments have to be considered: (1) in shelter areas with concentrated furnishings or fixed seating, usable floor area is 50 percent of gross floor area. (2) In shelter areas with un-concentrated furnishings and without fixed seating, usable floor area is 65 percent of gross floor area. (3) In shelter areas with open plan furnishings and without fixed seating, usable floor area is 85 percent of gross floor area.

It is intended that the applications/uses of the floors cataloged as refuge area do not have concentrated furnishing nor fixed seating, resulting in a 65% of the area to be considered for evacuation. Nevertheless, the rooftop will be deemed as an open plan furnishings without fixed seating for a usable area of 85%. Table 5.1 shows the adjusted floor areas for the specific refuge levels and Figure 5.2 the number of evacuees at a particular refuge story.

Table 5.1: Adjusted floor areas and number of evacuees for refuge levels.

Floor Level	Adjusted Area (ft^2)	Number of Evacuees
Refuge Area (with roof)	3,405.67	341
Refuge Area (roof top)	4,453.57	445

Providing two floor levels with roof and the roof top, a total number of 1,127 refugees could be accommodated. Since the probability that the entire population (1,281 people) are in the coastal community at the time of an event is low, the design will provide shelter for a little more than 85% of the total population at an area of 10 square feet per person.

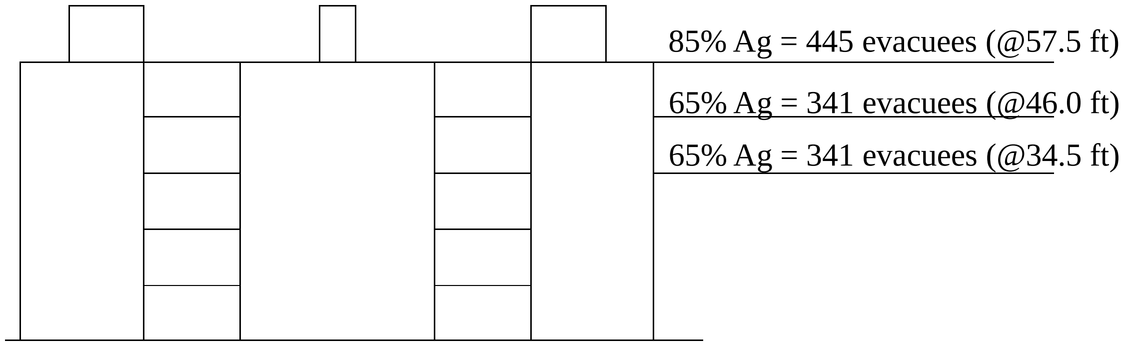

Figure 5.2: Number of evacuees at a particular refuge story.

5.2.2 Structural System Details

The building consists of special reinforced concrete shear walls. The building will have an orientation so that the convex side of the semicircular walls face the expected incoming wave direction. Two semicircular walls, with a length of 78.54 ft, are expected to protect against tsunami hydrodynamic forces and provide seismic resistance in both direction. Two other walls with a length of 40 ft parallel to the expected direction of the tsunami inundation flow do reduce the drag forces. Reinforced concrete slabs are proposed as the floor system supported by the beams and columns arrangement (see Figure 5.3). Twenty four rectangular section beams are located in the rectangular area, 12 spanning 20 ft and 12 spanning 16.67 ft in the long and short direction respectively. Two more beams in each semicircle area with a length of 23.6 ft, connects the beam and column frame to the curved walls. To keep the hydrodynamic forces to a minimum, ten round circular shaped columns were assigned as the interior columns, and eight at the edge of each wall member. In addition, rectangular columns are considered at intermediate locations of the wall systems to support the beams for each case, for a total of six more columns.

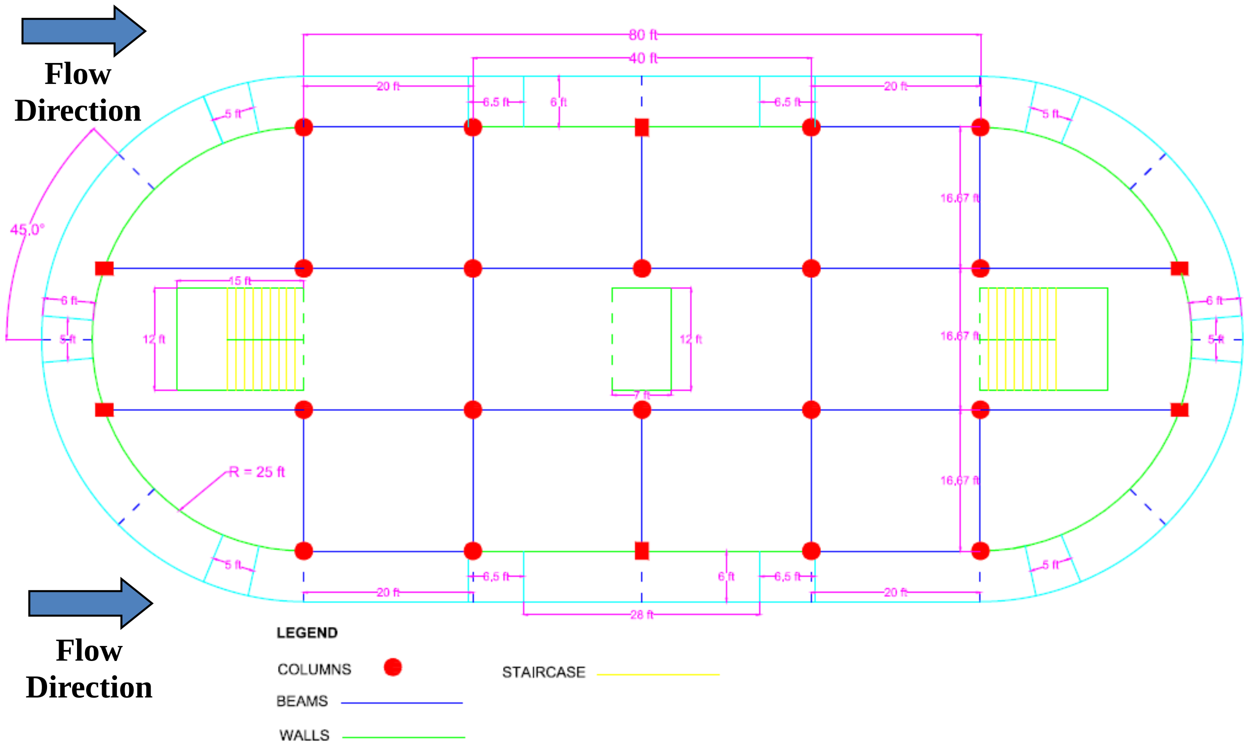

Figure 5.3: Structural layout of the proposed vertical evacuation structure.

For the selected structural layout a preliminary structural design was performed according to elementary rules of thumb design.

5.2.3 Structural Elements Pre-Dimensioning

Floor System (Slab)

In Figure 5.4 is shown the structural layout which identifies the slab panels in the floor plan. The initial slab thickness was determined using Figure 5.5*: Minimum Slab Thickness for Two-Way Slab Systems*, (ACI 318-05 & PCA Notes on 318-05) Table 5.2 shows the thickness values for a given β, which is the ratio between the longer to the shortest side of the slab panel.

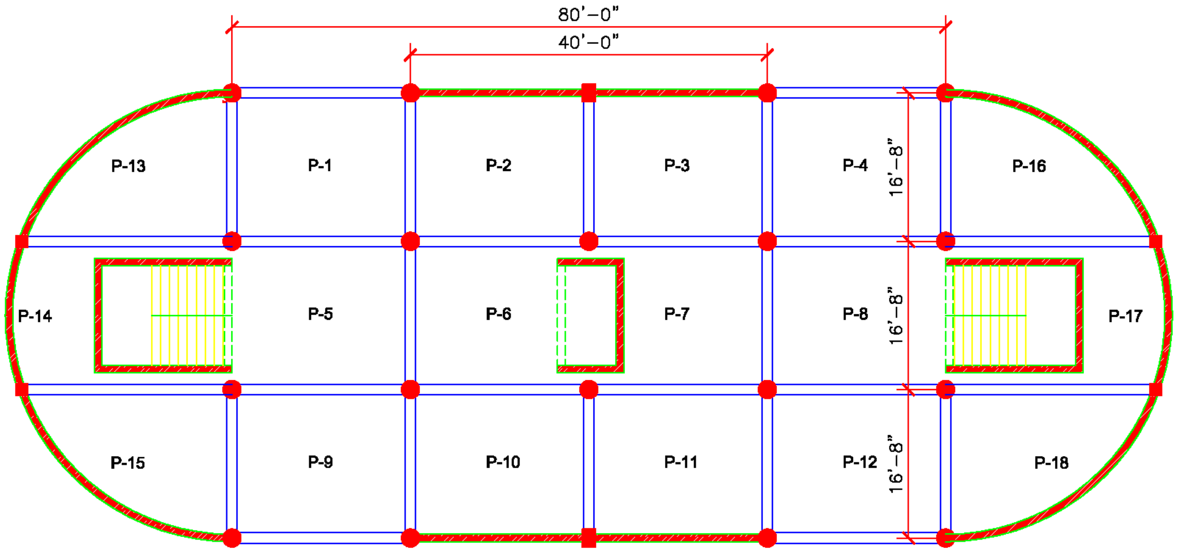

Figure 5.4: Slab panel identification.

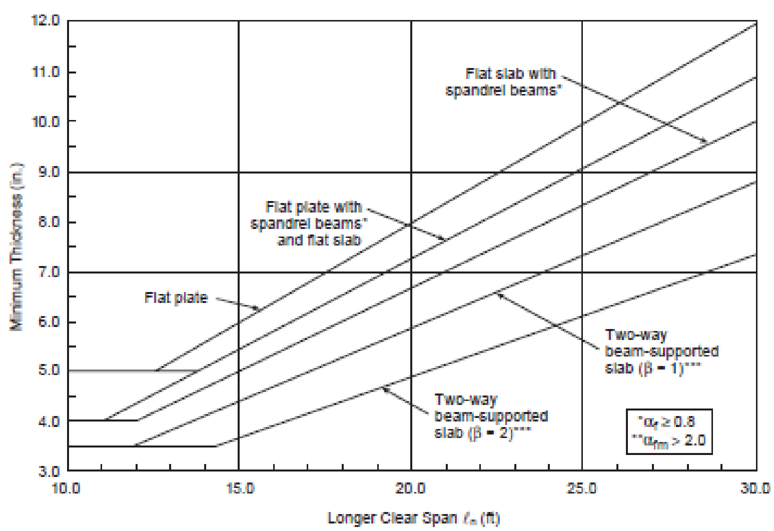

Figure 5.5: Minimum slab thickness for two-way slabs systems, (ACI 318-05 & PCA Notes on 318-05).

Table 5.2: Thickness for a given β value

Slab Panel	L_{higher} (ft)	L_{lower} (ft)	$\beta = L_{higher} / L_{lower}$	Thickness (in)
P-1	20.0	16.7	1.2	5.7
P-6	16.7	16.5	1.0	5.0
P-13, P-14	23.6	16.7	1.4	6.0

According to Table 5.2, all of the slab panels meet the requirements with a six inches thickness as a minimum. Hence to be consistent, for preliminary sizing, this value is selected for all panels.

Beams

Beam members in the typical floor plan are identified in Figure 5.6. To determine the preliminary cross section dimensions, the following relation between the span length and beam depth was considered: one inch per foot of beam length. Table 5.3 presents the preliminary depths. On the other hand, the width was established using a relation among the beam width, *b*, and the effective depth, *d*, where $d = 1.6*b$, and $h = d + 3$ *inches*. Both, depth and width dimensions, were forced to even numbers and using 10 inches as a minimum.

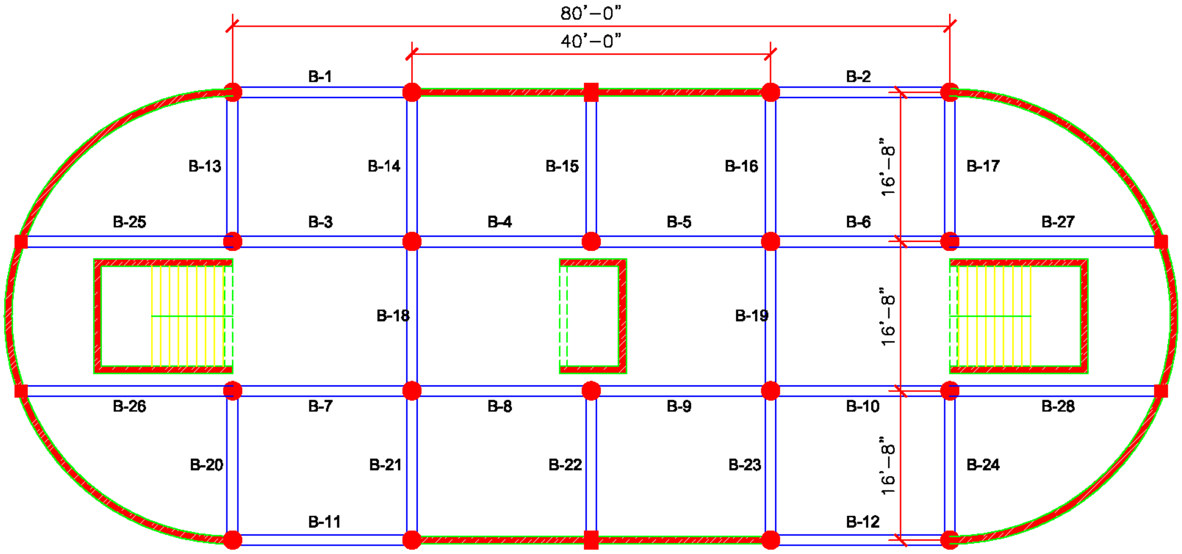

Figure 5.6: Beam elements identification

Table 5.3: Beam cross section preliminary dimensions.

Beam	Span Length (ft)	Depth, h (in)	Effective depth, d (in)	Width, b (in)
B-1	20.0	20	17	12
B-13	16.7	18	15	10
B-25	23.6	24	21	14

Since beam section 24 in X 14 in govern the trial, is to be assigned in all beams.

Columns

The column distribution is presented in Figure 5.7. To determine the columns preliminary sections, the following trial was considered. For interior columns, the diameter is chosen such that $d > h_w / 10$, where h_w is the story height in inches. For edge columns, the diameter is taken as $d > h_w / 9$, and for corner columns, $d > h_w / 8$. It is recalled that the story height is 11.5 feet. The resulting diameters were forced to even numbers and higher than 12 inches. For the rectangular columns the same trial was considered, for both, height and width dimensions, resulting in a square section (see Table 5.4 and Table 5.5).

Table 5.4: Circular column preliminary sections

Column	Column Type	d (in)
C-1	Edge	16
C-6	Interior	14

Table 5.5: Rectangular column preliminary sections

Column	Column Type	h (in)	b (in)
C-3	Edge	16	16
C-21	Edge	16	16

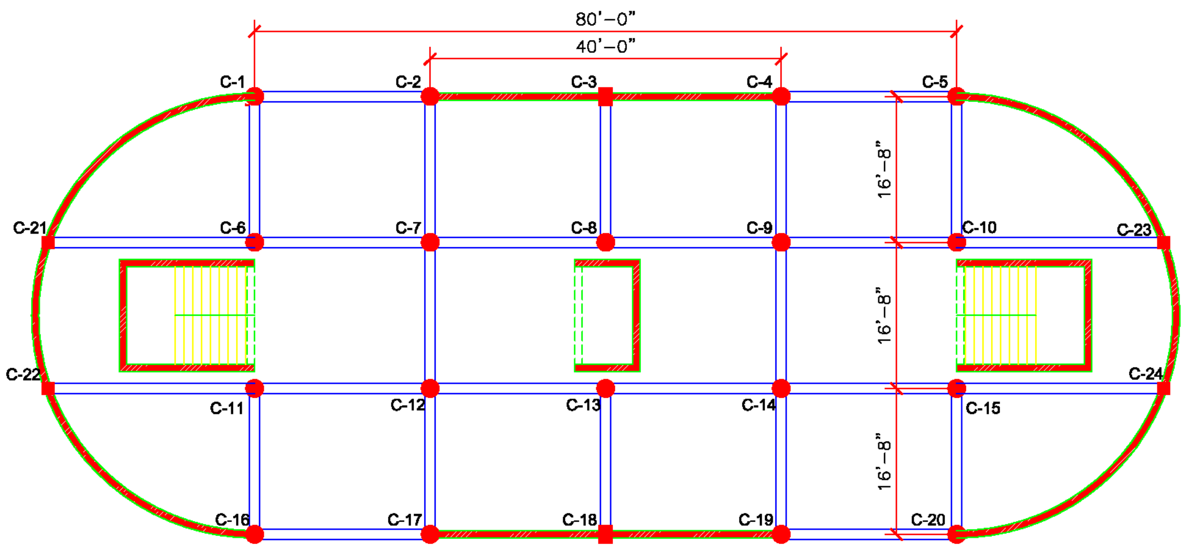

Figure 5.7: Column distribution and identification

To homogenize the design, the highest area section was assigned for all the columns.

Walls

The wall members are identified in Figure 5.8. To estimate the minimum thickness, t_w, of each wall, different options were considered. For instance, $t_w \geq 4$ *inches*, according to Chapter 14 of the ACI code, and $t_w \geq (h_w)_{inches} / 16$, where h_w is the story height. Using both criteria, and considering even numbers, the minimum wall thickness resulted in 10 inches, and it was assigned to all the walls members.

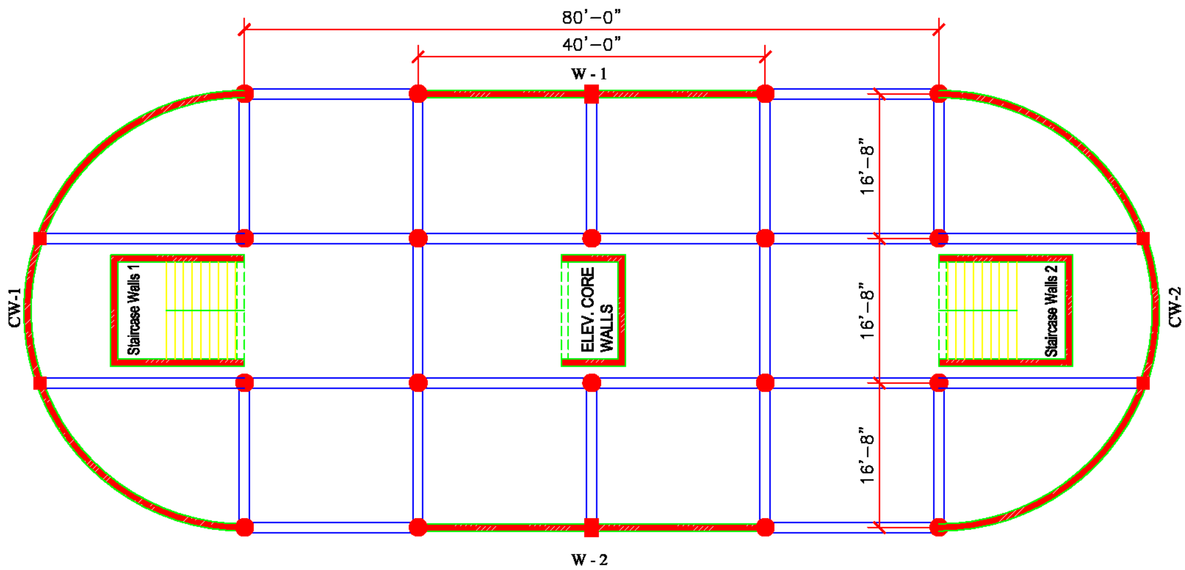

Figure 5.8: Walls identification

5.3 Suggested Applications

When not serving as a refuge area, a particular use for each floor level is presented below. These applications are based on the age distribution of the 2010 Census for Bo. Espinal-Aguada, which is discussed in Section 3.4.

First/Floor Base

As the building is located near an elementary school and highlighting that 144 children (11.2% of the population) are in the age range of 5-14 years, the first floor of this facility could be used as a children club, i.e., A place where children can spend their after school hours in a safe place while having fun.

Second Floor

The coastal community of Bo. Espinal has 848 people (66.2% of the population) within the ages of 10-59 years. Thus, an electronic library could be a useful facility established in one half of the second floor. The other half of this same level could be destined as a space to be used for community assemblies or any other common activity.

Third Floor/Fourth Floor

Since the coastal community studied has about 859 people (67% of the population) in the age range of 15-64 years, a fitness center which offers different amenities would be attractive. For instance a gym, including cardiovascular equipment and weight lifting machines, could be located in the third floor of the proposed building. Other fitness activities such as centers of aerobics, yoga, dancing, etc., which do not require concentrated furnishings nor fixed seating, could be located in the fourth floor, given that it is the level where the refuge area begins.

Fifth Floor

According to the census data, 229 people (17.9% of the population) are 65 year and over. For this type of population, a senior club with a variety of activities could be proposed. Similar to the fourth floor, the activities intended would not require concentrated furnishings nor fixed seating. The idea of locating the seniors in the highest level is that in case of an event, they would be at the refuge area already.

Roof Top

The roof top area could offer added space for special occasion of the activities mentioned in lower floors and in addition, serve as an open area to enjoy the Aguada-Aguadilla bay view. Above the staircase, an area of 12ft X 15ft is provided for emergency helicopter landing (see Figure 5.9). The dimensions for helipad marking pattern were established according the *Field Manual 5-430-00-2 Volume II, Chapter 13: Design and Construction of Heliports and Helipads, Figure 13-8.*

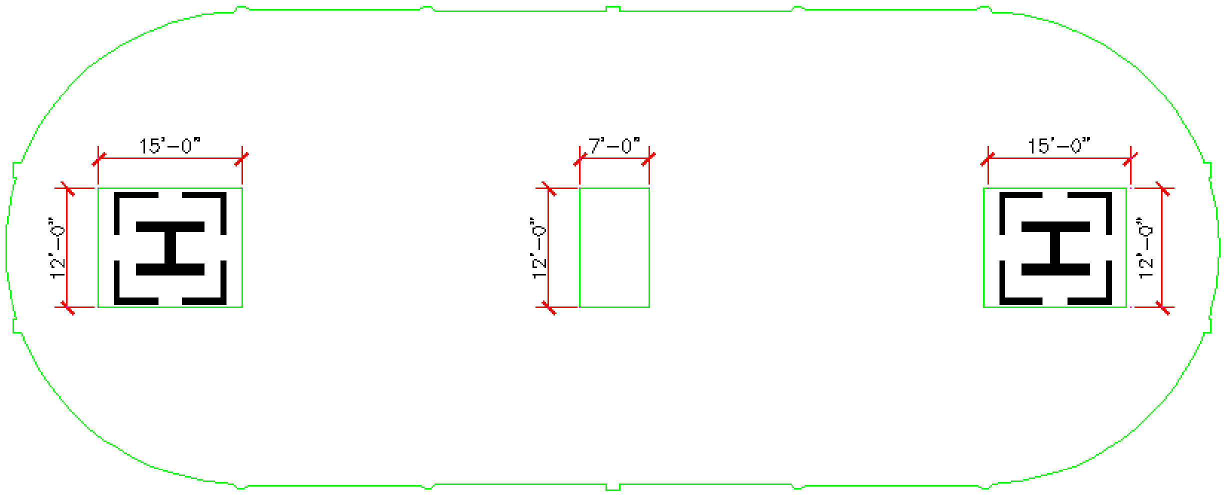

Figure 5.9: Helicopter emergency landing area above staircases.

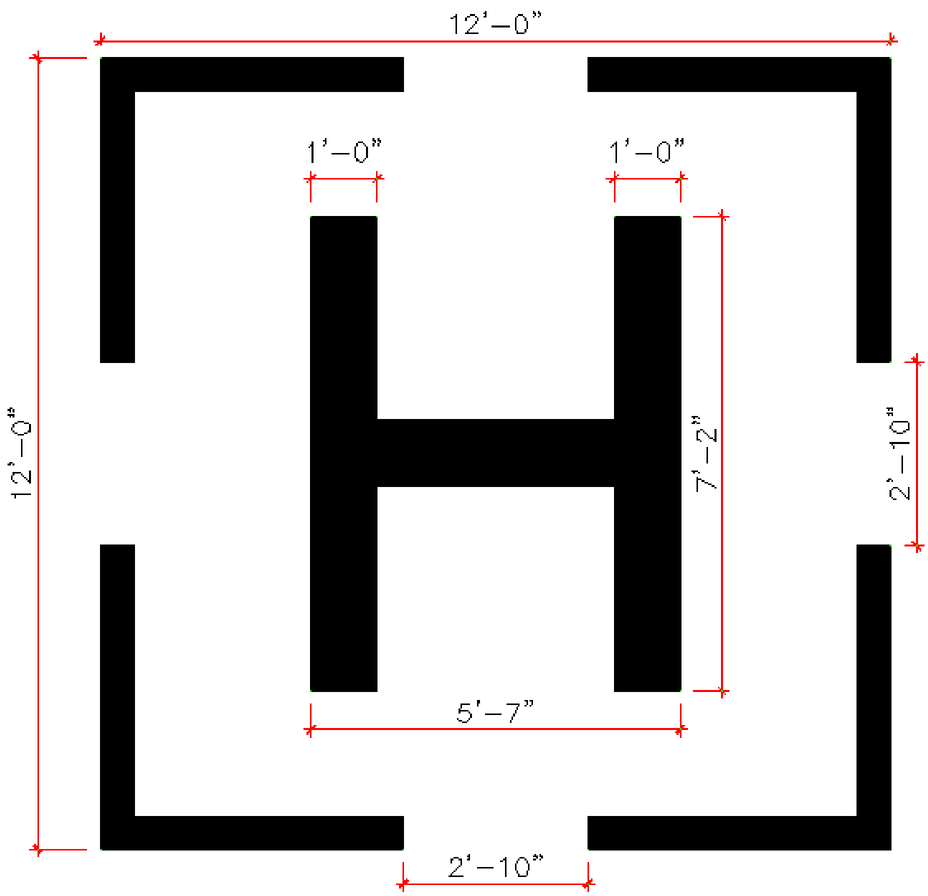

Figure 5.10: Helipad marking dimensions.

CHAPTER 6 - DESIGN LOADS ON VERTICAL EVACUATION STRUCTURE

6.1 Introduction

This chapter presents the computation of the different loads to which the structure will be designed for. These loads include, the dead loads, live loads, wind loads, earthquake loads, and tsunami loads. In addition, it is shown how the calculated load magnitudes are applied and located in the structural model of the building developed in the *ETABS* software. Dead loads, live loads and earthquake loads were determined using the *ASCE7-10*, while for tsunami loads the FEMA P-646 document was used as a guide. After the loads and applicable combinations were assigned and defined, the model was executed to obtain the internal forces on each element of the building. These were used later in the design, which is presented in Chapter 7.

6.2 Dead Loads

The dead loads to be assigned were taken from *Table C3-1: Minimum Design Dead Loads, (ASCE7-10)*. The applicable loads for the structure analyzed are presented in Table 6.1:

Table 6.1: Nonstructural dead loads considered.

Ceilings	**Weight (psf)**
Acoustical fiber board	1
Suspended steel channel system	2
Mechanical duct allowance	4
Floor and Floor Finishes	
Floor finishing (2 in, γ = 150 psf)	25
Plaster on concrete (0.5 in, γ = 150 psf)	6.25
Frame Walls	
Concrete masonry unit (6 in) with plaster in both sides for parapet walls	60
Windows / glass	8
Frame Partitions	
Movable Steel Partitions	4

The following dead loads were computed and assigned to the model as shown in Figure 6.1and Figure 6.2.

$$w_{D-slab} = w_{ceilings} + w_{f-f} + w_{f-w} = 7\,psf + 31.25\,psf = 38.25\,psf$$

$$w_{D-walls\,(stories\,1-4)} = w_{windows} * (h_{story} - h_{beam}) = 8\,psf * (11.5ft - 2ft) = 0.08\,Kip/ft$$

$$w_{D-frame\,walls\,(story\,5)} = w_{masonry} * h_{masonry} = 60\,psf * 4ft = 0.24\,Kip/ft$$

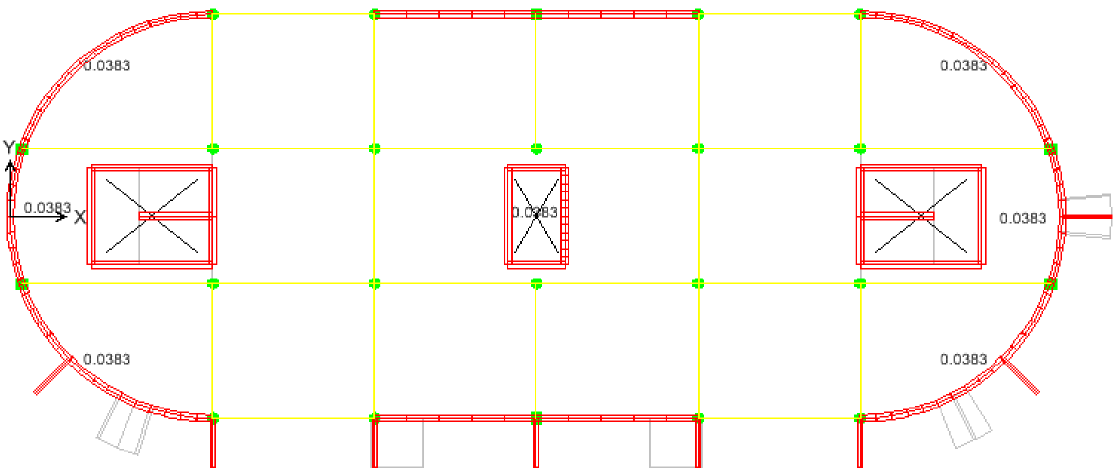

Figure 6.1: Dead load assignment in first floor

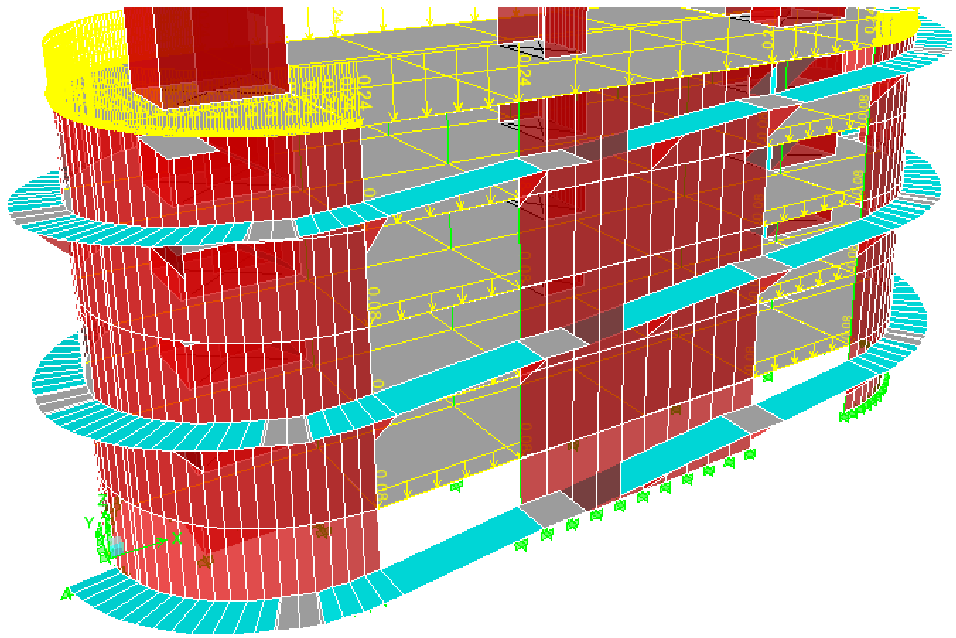

Figure 6.2: Dead loads assigned in frame members.

Table 6.2: Non-structural weights per story.

Stories 1-4	
Non-Structural Elements	**Weight (Kips)**
Ceilings	38.64
Floor and Floor Finishes	172.48
Windows/glass	5.67
Total	**216.80**
Fifth Story/Roof Top	
Non-Structural Elements	**Weight (Kips)**
Ceilings	38.64
Floor and Floor Finishes	172.48
Parapet walls	76.10
Total	**287.22**
Staircase and Elevator Core Roof	
Non-Structural Elements	**Weight (Kips)**
Floor and Floor Finishes	13.88
Total	**13.88**

Table 6.2 shows the non-structural weights per story according to the applicable dead loads from *ASCE7 -10*. The information and dimensions necessary to calculate the weight of the structural elements of the building is presented in Table 6.3. Table 6.4 and Table 6.5 shows the results of the structural weights per story and the total weight of the building respectively.

Table 6.3: Structural elements parameters to calculate the total weight of the structure.

Concrete specific weight	0.15 Kcf
Slab Area	5,519.50 ft^2
Preliminary Slab Thickness	6 in
Preliminary Beam Cross-Section Area	336 in^2
Plan Length of the Beams	527.73 ft
Circular Column Section Area	201.06 in^2
Number of Circular Column	18
Rectangular Column Section Area	256.00 in^2
Number of Rectangular Column	6
Plan Length of the Walls	355.75 ft
Preliminary Wall Thickness	10 in
Preliminary Stairs and Ramp Thickness	6 in

Table 6.4: Structural element weights per story.

Stories 1-4	
Structural Elements	**Weight (Kips)**
Slab	413.96
Beams	138.53
Columns	61.75
Walls	503.48
Stairs	15.01
Ramp	75.58
Total	**1,208.32**
Fifth Story/Roof Top	
Structural Elements	**Weight (Kips)**
Slab	413.96
Beams	138.53
Columns	30.88
Walls	343.74
Stairs	7.51
Ramp	37.79
Total	**972.41**
Staircase and Elevator Core Roof	
Structural Elements	**Weight (Kips)**
Slab	33.30
Walls	92.00
Total	**125.30**

Table 6.5: Total dead weight of the building

Story	Height (ft)	Weight (Kip)
1	11.5	1,425.12
2	11.5	1,425.12
3	11.5	1,425.12
4	11.5	1,425.12
5 / Top Roof	11.5	1,259.63
Staircase and Elevator Core Roof	11.5	139.18
Total	**69.0**	**7,099.27**

6.3 Live Load

Live loads to be assigned were taken from *Table 4-1: Minimum Uniformly Distributed live Loads, L0, and Minimum Concentrated Live Loads, (ASCE7-10)*.

Table 6.6 shows the uniform live load for each story based on the occupancy or use. It is noticed that all of the floor levels resulted in the same live load value of 100 psf. Since the layout does not specify a clear division between corridors and rooms, the live load corresponding to corridors was assigned to all the floor area. This consideration results in conservative live loads, but at the same time provides alternatives for changes in occupancy use areas.

Table 6.6: Uniformly distributed live loads for each story

Story	Suggested Application	Occupancy or Use (According *ASCE7-10*)	Uniform Load (psf)
1	Electronic Library	Computer use	100
1	Community Center Area	Corridors	100
2	Fitness Center (Gym)	Gymnasiums	100
3	Fitness Center (Others)	Gymnasiums	100
4	Senior Club	Corridors	100
5/Roof Top	Communal Activities	Roof used for assembly purposes	100
Staircases Roof	Helicopter Emergency Landing Area	Roof used for assembly purposes	100
Stairs	Access Feature	Stairs and exit ways	100
Ramp	Access Feature	Stairs and exit ways	100

6.4 Wind Load

According to FEMA P-646, the recommended basis for wind design of a vertical evacuation structure is the *International Building Code (IBC)*, which references *ASCE7-10: Minimum Design Loads for Buildings and Other Structures*, due to its wind requirements.

In Table 6.7 a summary of the wind load parameters determined for this particular area is presented. See Appendix B for wind load calculations procedure and details.

Table 6.7: Summary of wind load parameters

Occupancy Category	IV
Velocity pressure exposure coefficient, *Kz*	1.17
Topgraphic factor, *Kzt*	1
Exposure coefficient	C
Wind directionality factor, *Kd*	0.85
Basic wind speed, *V*	180 mph
Importance factor, *I*	1.15
Velocity pressure at height h, K_h	94.86 psf
Gust effect factor, *G*	0.85
External pressure coefficient for windward, C_p	0.8
External pressure coefficient for leeward, C_p	-0.5
Internal pressure coefficient, GC_{pi}	± 18
Net pressure in critical wind direction, p_{net}	104.82 psf
Area of considered wall surface, $A_{wall\text{-}surface}$	8,970 ft^2
Total base shear, V_{base}	940.2 Kips

6.5 Earthquake Load

Just as for wind loads, the *International Building Code (IBC)*, which references *ASCE7-10: Minimum Design Loads for Buildings and Other Structures*, shall be used for seismic design of vertical evacuation structures, due to its seismic requirements. Vertical evacuation structures, which are catalogued as essential facilities, should be designed using regulations for Risk Category IV buildings. Moreover, Seismic Design Category (SDC) D, as defined in *ASCE/SEI 7-10*, should be assigned to the structure, as a minimum, to guarantee sufficient capacity and ductility in the structure for resisting tsunami loads. Both criteria shall be considered even in the case that the site of interest is located in a region of low seismic risk.

In Table 6.8 a summary of the earthquake load parameters determined for this particular area is presented. See Appendix B for earthquake load calculations procedure and details.

Table 6.8: Summary of earthquake load parameters

$h_{building}$	69 ft	S_{DS}	0.738 g
$W_{building}$	7,099.27 Kips	S_{D1}	0.634 g
Risk Category	IV	R	2
Seismic Design Category	D	C_t	0.02
Importance Factor, *I*	1.5	x	0.75
S_s	1.23 g	T	0.48 s
S_1	0.39 g	T_L	12 s
Site Class - *"Soft clay soil"*	E	T_s	0.86 s
F_a	0.90	T_0	0.17 s
F_v	2.44	C_s	0.554
		V_{base}	3,929.4 Kips

A preliminary analysis of the lateral load shows that the earthquake lateral loads clearly predominates over the wind loads. This was expected for a low to mid-rise building made of reinforced concrete which is a heavy material and for a structure placed in alluvial soils where the seismic loads are amplified. It is recognized that wind loads could cause failures in non-structural elements, but this analysis is out of the principal scope of this project.

6.6 Tsunami Loading

6.6.1 General Data for Site of Interest

Fluid Properties:

$$\rho_s = 1.1\rho_w = 1.1 * 1.94\frac{slugs}{ft^3} = 2.13\frac{slugs}{ft^3}$$

$$g = 32.17\frac{ft}{s^2}$$

Site Elevation Properties:

$$R^* = Design\ Inundation\ Depth\ (DID) + z = 4.0\ m + 4.93\ m = 8.93\ m$$

$$R = 1.3R^* = 1.3 * 8.93\ m = 11.61\ m$$

$$h_{max} = 11.61\ m - 4.93\ m = 6.68\ m = 21.92ft$$

Hydrodynamic Properties:

Recalling from Chapter 4 results:

$$u_{max-design} = 1.15 * u_{max} = 1.15 * 3\frac{m}{s} = 3.45\frac{m}{s} = 11.32\frac{ft}{s}$$

$$(hu^2)_{max-design} = 1.7 * (hu^2)_{max} = 1.7 * 30\frac{m^3}{s^2} = 34\frac{m^3}{s^2} = 1200.70\frac{ft^3}{s^2}$$

Note: Although the expressions for the different forces presented in Chapter 2 and discussed in FEMA P-646 provide a point force value, the equations were rearranged to compute pressures or forces per unit length, depending on how they were assigned in the structural model.

6.6.2 Hydrostatic Forces

Since the maximum water height above the base of the building, h_{max}, is less than the height of any wall of the building, a triangular distribution of the hydrostatic pressures could developed (See Figure 2.17). The hydrostatic pressure at the bottom of the triangular distribution is:

$$P_h = \frac{F_h}{A_w} = \frac{F_h}{b_w * h_{max}} = \frac{1}{2}\rho_s g h_{max} = \frac{1}{2} * \ 2.13\frac{slugs}{ft^3} * 32.17\frac{ft}{s^2} * 21.92ft = 0.75\ Ksf$$

However, the architectural layout of the proposed structure is such that open areas are provided and the water can pass through avoiding any watertight areas inside the building. Therefore, the hydrostatic forces are not considered for this particular case.

6.6.3 Buoyant and Hydrodynamic Uplift Forces

The computed uplift pressure presented below were applied to the first and second stories, since the maximum inundation depth relative to the ground at the site of interest is 21.92 ft, the height of the second story is 23 ft. The pressure due to the effect of air trapped below the floor system with an area of A_f, considering a beam depth of 24 inches is as follows:

$$P_b = \frac{F_b}{A_f} = \rho_s g h_{beams} = 2.13 \frac{slugs}{ft^3} * 32.17 \frac{ft}{s^2} * \left(24in * \frac{1ft}{12in}\right) = 0.14\, Ksf$$

The other constituent of the uplift forces, which is based on the vertical velocity, was computed as follows:

Recalling that;

z = ground elevation at the site of the structure.

D_h = horizontal distance from the structure site to the point where ground elevation is z = 0.

tan (α) = average slope of grade at the site.

$$tan\,(\alpha) = \frac{z}{D_h} = \frac{16.17\, ft}{2{,}250\, ft} = 0.007$$

$$u_{max-des} = 11.32 \frac{ft}{s}$$

$$u_v = u_{max-des} * tan(\alpha) = 11.32 \frac{ft}{s} * 0.007 = 0.081 \frac{ft}{s}$$

Hence,

$$P_u = \frac{F_u}{A_f} = \frac{1}{2} C_u \rho_s u_v^2 = \frac{1}{2} * (3) * 2.13 \frac{slugs}{ft^3} * \left(0.081 \frac{ft}{s}\right)^2 * \frac{1\, Kip}{1{,}000\, lb} = 2.1x10^{-5} Ksf$$

Table 6.9: Summary of the uplift forces results

Element	tan (α)	u_v (ft/s)	P_b (Ksf)	P_u (Ksf)	$P_{Total-uplift}$ (Ksf)
Slab	0.007	0.08	0.14	$2.1x10^{-5}$	0.14
Ramp	0.091	1.02	0.034	$3.4x10^{-3}$	0.04

Table 6.9 displays the total uplift pressures which is the sum of the buoyant pressure and the vertical hydrodynamic pressure for both elements, the slab and the exterior access ramp. The term tan (α) represents the average slope as defined in Section 2.4.7, which for Bo. Espinal is around 0.007. For the exterior ramp the uplift force was computed in the same fashion, where tan (α) is based on a combination of the ramp slope and the slope of grade at the site.

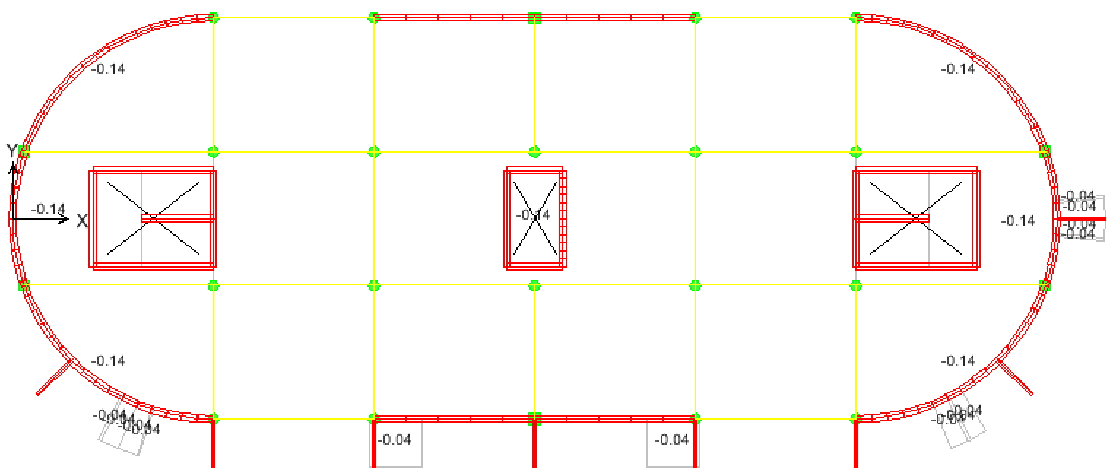

Figure 6.3: First story plan with uplift pressure assigned in the floor system and ramp.

6.6.4 Hydrodynamic and Impulsive Forces

Recalling Chapter 2, where C_d is defined as 2.0,

$$F_d/B = \frac{1}{2}\rho_s C_d (hu^2)_{max} = \frac{1}{2} * \ 2.13\frac{slugs}{ft^3} * 2.0 * 1200.70\frac{ft^3}{s^2} = 2.56\ Kip/ft$$

$$F_s/B = 1.5 * F_d/B = 1.5 * 2.56\frac{Kip}{ft} = 3.84\frac{Kip}{ft}$$

For column elements, the hydrodynamic force should be concentrated for a given width and distributed along the inundation height, 21.92 ft.

$$\frac{F_d}{L_{col}} = \frac{F_d/B}{h_{max}} * (b_{Column}) = \frac{2.56\ Kip/ft}{21.92ft} * (1.33ft) = 0.16\ Kip/ft$$

For wall members the load should only be distributed along the inundation height and assign to them as area loads. The impulsive force was assigned to the inland facing curved wall (CW) since it is considered the most closed off member of the building that the flow will experiment.

Element	$P_d = F_d/B/h_{max}$ (Ksf)	$P_s = F_s/B/h_{max}$ (Ksf)
CW-1	0.12	-
CW-2	-	0.18

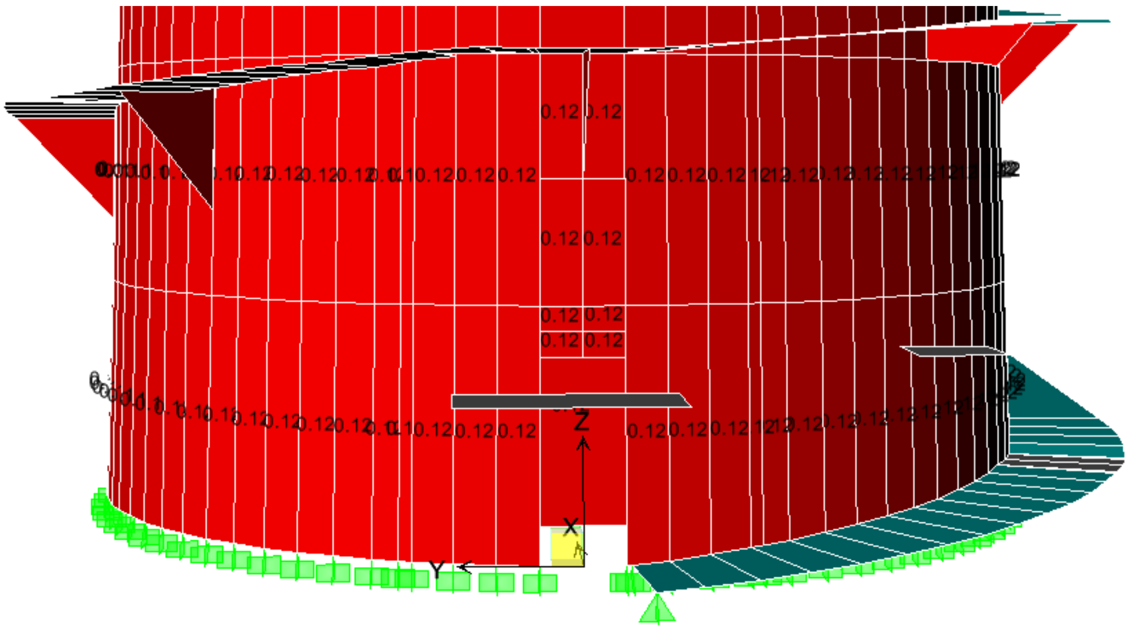

Figure 6.4: Hydrodynamic force on offshore facing walls assigned as an area load of 0.12 Ksf.

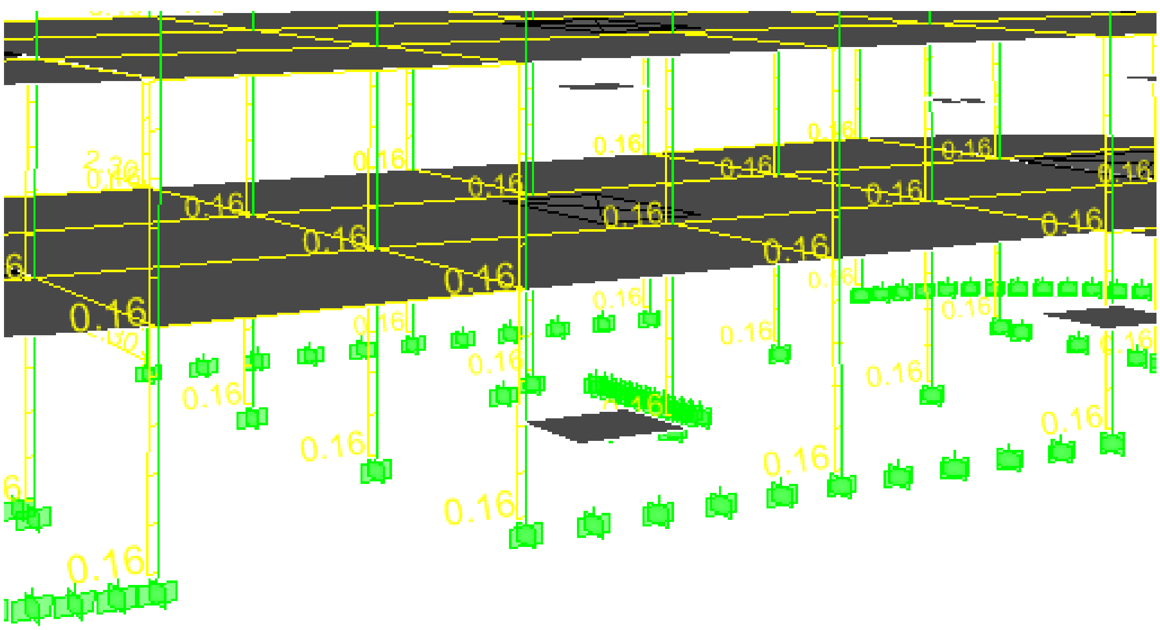

Figure 6.5: Hydrodynamic forces in column members assigned as distributed load of 0.16 Kip/ft.

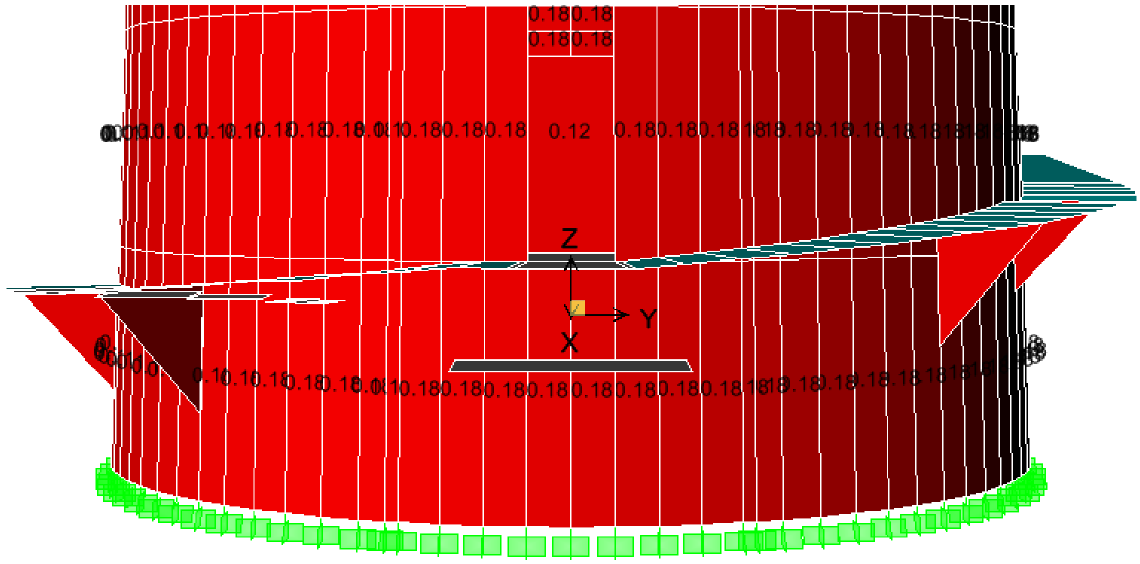

Figure 6.6: Impulsive force on inland facing walls assigned as an area load of 0.18 Ksf.

6.6.5 Floating Debris Impact Forces

Although Bo. Espinal is not a port area nor has neighboring ports, it will be assumed a standard shipping container 40 feet long and 8 feet wide as the debris to impact the structure at a height of h_{max} - d, (see Table 2.3 for m_d values), where,

$$d = \frac{W}{\rho_s g A_f} = \frac{m_d}{\rho_s A_f} = \frac{260.38\ slugs}{2.13\,\frac{slugs}{ft^3} * 40ft * 8ft} = 0.38\ ft$$

Considering a longitudinal strike with $k = 260.38\ Kip/in$ and hydrodynamic mass coefficient, $c = 0.2$ (see Table 2.3 for values), the impact force is as follows,

$$F_i = 1.3u_{max}\sqrt{km_d(1+c)}$$

$$= 1.3 * 11.32\frac{ft}{s} * \sqrt{342.61x10^3\,\frac{lb}{in} * \left(\frac{12in}{1ft}\right) * 260.38\ slugs * (1+0.2)}$$

$$= 527.4\ Kips$$

Hence, the impact force will be represented as a point load of 527.4 Kips. Even though the draft *d*, length was computed, the impact load was located in the middle of the first and second story at a height of 17.25 ft from the ground level, to consider the worst case scenario. Since the building will be oriented with the convex side of the curve wall facing the expected flow direction, therefore, the impact force was located in such wall.

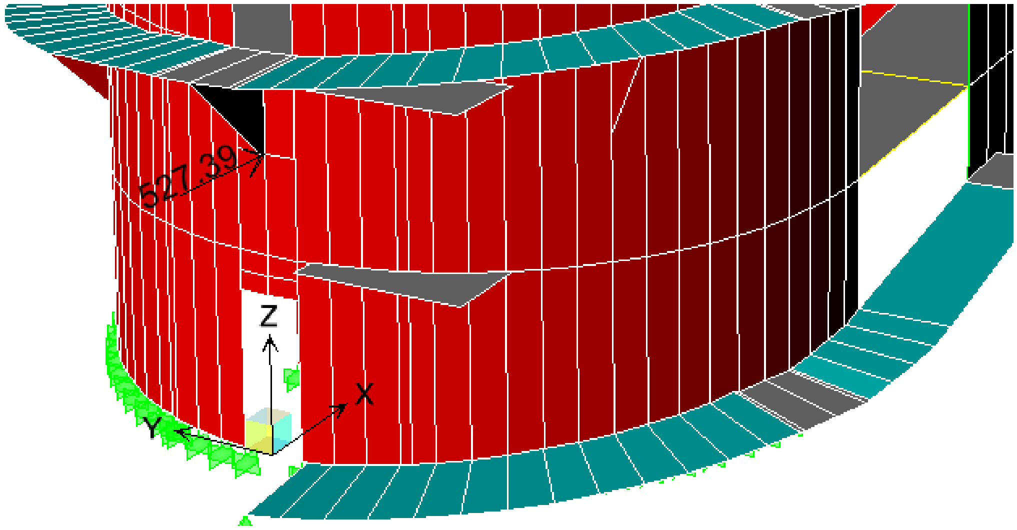

Figure 6.7: Debris impact point load located at the middle of first and second story

6.6.6 Damming of Accumulated Waterborne Debris

According to FEMA P-646, the debris dam width should be the largest of 40 feet (which represents a shipping container) and a full structural bay width. Based on the proposed structural layout, the most critical location in terms of the effects of this particular load are the open bays between the ends of the curved walls and the plane walls, L_{bay} = 20 ft (see Figure 6.8). Therefore, a width of 40 ft was used to represent the damming breath.

$$F_{dm} = \frac{1}{2}\rho_s C_d B_d (hu^2)_{max} = \frac{1}{2} * \ 2.13 \frac{slugs}{ft^3} * 2.0 * 40 ft * 1200.70 \frac{ft^3}{s^2} = 100.88\, Kip$$

The resulting force if then distributed along the total inundation depth and acting in two columns as the most detrimental case (see Figure 6.8).

$$\frac{F_{dm}}{h_{max}} = \frac{100.88\, Kip}{21.92\, ft * (2\ columns)} = 2.30\ \frac{Kips}{ft}$$

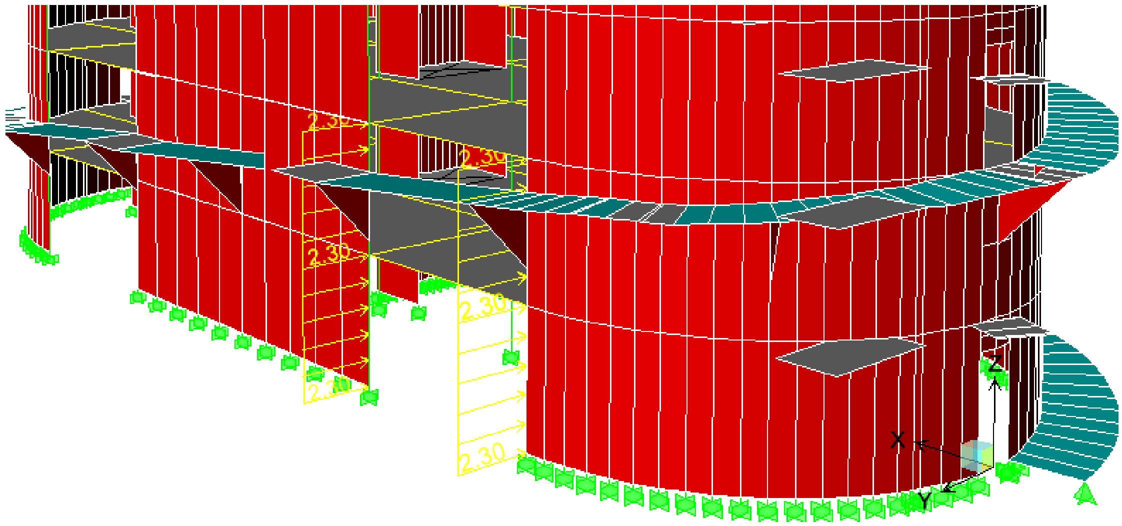

Figure 6.8: Debris damming force distribution at the most detrimental location.

6.6.7 Additional Retained Water Loading on Elevated Floors

Full height windows with negligible resistance to hydrostatic effects are proposed for the open structural bays. Therefore, during the rapid drawdown the inundated floors might have the ability to drain off quickly to avoid any additional retain water loading.

Table 6.10 presents a summary of the tsunami loads calculated.

Table 6.10: Summary of tsunami loads results.

Type of Force	Acting on	Result
Hydrostatic	-	Not Considered
Buoyant	Floor System	0.14 Ksf
	Exterior Ramp	0.034 Ksf
Hydrodynamic Uplift	Floor System	$2.1\text{x}10^{-5}$ Ksf
	Exterior Ramp	$3.4\text{x}10^{-3}$ Ksf
Total Uplift	Floor System	0.14 Ksf
	Exterior Ramp	0.04 Ksf
Hydrodynamic	Columns	0.16 Kip/ft
	Curve Wall 1 (facing offshore)	0.12 Ksf
Impulsive	Curve Wall 2 (facing inland)	0.18 Ksf
Debris Impact	Curved Wall 1	527.4 Kip
Waterborne Debris Damming	Exterior Columns	2.30 Kip/ft
Retained Water	-	Not Considered
Total Base Shear, V_{base} (X-direction)		**1,239.6 Kip**
Total Base Shear, V_{base} (Y-direction)		**100.9 Kip**

CHAPTER 7 - STRUCTURAL ANALYSIS AND DESIGN OF THE VERTICAL EVACUATION STRUCTURE

7.1 Introduction

The structural design for this project consisted in the determination and selection of the highest internal forces in a structural member (slab, beam, column, and wall) computed by the structural analysis software, and design all the other similar members with the same requirements of the controlling element. By using this assumption intended to simplify the design, a conservative structural design will result. The design is based in the *ACI 318-11* considerations. As specified in Section 6.5, the structural system selected to resist the lateral loads was a special reinforced shear wall. For this reason it is imperative to ensure that the seismic lateral forces must be resisted by the shear walls only. Therefore, the combinations used to analyze and design the other members such as, slabs, beams and columns do not include earthquake loads. Table 7.1 displays the combination used for these elements.

Table 7.1: Load combinations used for slabs, beams, and columns.

Type of Combination	Combination
Gravity load	1.4 D
	1.2 D + 1.6 L
Tsunami Loads	1.2 D + 1.0 T_s + 1.0 L_{Ref} + 0.25 L
	0.9 D + 1.0 T_s

7.2 Slab Design

The slab was designed for gravity loads and tsunami effects using the structural analysis software *SAFE*. Deflections due to service loads were verified according the *ACI 318-11*. To perform the design of the slab system, an envelope combination composed of all the four combinations shown in Table 7.1 was created. The mesh size used to analyze the slab system was set to 2' x 2'. To simplify the design, similar slab panels were design using the highest internal forces among them.

Table 7.2: Maximum permissible computed deflections compliance check.

Story	L_{min} (ft)	$(\Delta)_L < L_{min}/360$ (in)	$(\Delta)_L$ from SAFE (in)	Check	$(\Delta)_{D+L} < L_{min}/240$ (in)	$(\Delta)_{D+L}$ from SAFE (in)	Check
1	16.67	0.556	0.064	OK	0.833	0.140	OK
2	16.67	0.556	0.064	OK	0.833	0.140	OK
3	16.67	0.556	0.064	OK	0.833	0.140	OK
4	16.67	0.556	0.064	OK	0.833	0.140	OK
5	16.67	0.556	0.066	OK	0.833	0.140	OK

Table 7.3: Moments results (M_{11}) from *SAFE* and supplied reinforcement configuration.

Story	M_{11} (Along X - Around Y)	M_u (Kip-ft)	b (in)	d (in)	R_n (Ksi)	ρ	A_s (in^2/ft)	Configuration
1	**(+) Moment**	2.66	12.00	5.00	0.12	0.00201	0.12	#4@15" (B)
	(-) Moment	5.15	12.00	5.00	0.23	0.00395	0.24	#4@10" (T)
2	**(+) Moment**	2.66	12.00	5.00	0.13	0.00201	0.12	#4@15" (B)
	(-) Moment	5.15	12.00	5.00	0.22	0.00395	0.24	#4@10" (T)
3	**(+) Moment**	2.66	12.00	5.00	0.11	0.00201	0.12	#4@15" (B)
	(-) Moment	5.15	12.00	5.00	0.18	0.00395	0.24	#4@10" (T)
4	**(+) Moment**	2.66	12.00	5.00	0.11	0.00201	0.12	#4@15" (B)
	(-) Moment	5.15	12.00	5.00	0.22	0.00395	0.24	#4@10" (T)
5	**(+) Moment**	2.76	12.00	5.00	0.12	0.00208	0.12	#4@15" (B)
	(-) Moment	5.02	12.00	5.00	0.22	0.00385	0.23	#4@10" (T)

Table 7.4: Moments results (*M_{22}*) from *SAFE* and supplied reinforcement configuration.

Story	M_{22} (Along Y - Around X)	M_u (Kip-ft)	b (in)	d (in)	R_n (Ksi)	ρ	A_s (in^2/ft)	Configuration
1	(+) Moment	3.20	12.00	4.50	0.18	0.00301	0.16	#4@15” (B)
	(-) Moment	4.16	12.00	4.50	0.23	0.00394	0.21	#4@10” (T)
2	(+) Moment	3.20	12.00	4.50	0.18	0.00301	0.16	#4@15” (B)
	(-) Moment	4.16	12.00	4.50	0.24	0.00394	0.21	#4@10” (T)
3	(+) Moment	3.20	12.00	4.50	0.17	0.00301	0.16	#4@15” (B)
	(-) Moment	4.16	12.00	4.50	0.24	0.00394	0.21	#4@10” (T)
4	(+) Moment	3.20	12.00	4.50	0.17	0.00301	0.16	#4@15” (B)
	(-) Moment	4.16	12.00	4.50	0.24	0.00394	0.21	#4@10” (T)
5	(+) Moment	3.20	12.00	4.50	0.18	0.00301	0.16	#4@15” (B)
	(-) Moment	4.30	12.00	4.50	0.24	0.00408	0.22	#4@10” (T)

It can be noticed that for positive moments of M_{11} direction (Table 7.3), a steel area, A_s = 0.12 in^2/ft is required. This area could be supplied with #4@18" (B) configuration, but for practical purposes, and to provide the same configuration as for positive moments in M_{22} direction, #4@15" (B) was selected.

To determine the cutoff points of the negative moments reinforcement, the ACI SP66 (04) (ACI Detailing Manual) was used as a guide. This manual establish that for end spans $L_{clear} / 4$ is the distance to be longitudinally reinforced, while for interior spans at least, $L_{clear} / 3$, is required.

The tsunami effects in the slabs system of the first two stories were not as severe as the gravity effects. The maximum negative moment in the center of all the panels was about 1.1 Kip-ft/ft, while positive moments near the beam supports were about 1.5 Kip-ft/ft. It is noticeable that to resist the positive moments, the proposed configuration of #4@15"(B) is enough. Nevertheless, to mitigate the negative moments due to tsunami effects, and for practical purposes, the configuration of #4@10"(T) was assigned for both directions, avoiding the cutoff points of the negative moment reinforcement determined in Table 7.3 and Table 7.4. The drawings and details are provided in Appendix C.

7.3 Beams Design

Although beam members were not subjected to earthquake forces during the analysis, but rather they were designed for gravity loads, the ductility details for seismic design were verified. For the beam and column design *Chapter 29: Earthquake Resistant Structures (ACI 318-11 & PCA Notes on 318-11)* was used to provide ductility through the seismic detailing. In the same fashion as for the slab design, to perform the design of beams, an envelope of all the four combinations shown in Table 7.1 was created.

Step 1: Check satisfaction of limitations on section dimensions

A. Check that $P_u < (A_g*f'_c)/10$

Since all the beams cross sections were pre dimensioned with the same depth and width, the beam element with the resultant highest axial force was used.

Beam ID	h (in)	b (in)	A_g (in^2)	P_u (Kips) (Value from *ETABS*)	$(A_g*f'_c)/10$	Check
B-12, Story 5	24	14	336	29.99	134.40	OK

B. Check that the element clear length is greater than four times its effective depth, $l_c > 4*d$

Beam ID	h (in)	d = h – 2.5 (in)	l_c (in)	4*d	Check
1-12	24	21.5	224.0	86.00	OK
13-24	24	21.5	184.4	86.00	OK
25-28	24	21.5	267.2	86.00	OK

C. Check that the width of the beam is larger than 0.3h and 10 in.

Beam ID	h (in)	b_w (in)	0.3h	Check
1-12	24	14	7.20	OK
13-24	24	14	7.20	OK
25-28	24	14	7.20	OK

D. Check that the width of the beam does not exceed the width of the support element *(c_1)*, nor it is the smaller of *(c_2+2c_2)*, and *($c_2+1.5c_1$)*, where c_1 and c_2 are the column dimension.

Beam ID	b_w (in)	$c_2 = c_1$ (in)	Condition 1	$c_2 + 2*c_2$	$c_2 + 1.5*c_1$	Condition 2	
1-12	14	16	OK	48	40	$b_w < c_2 + 1.5*c_1$	OK
13-24	14	16	OK	48	40	$b_w < c_2 + 1.5*c_2$	OK
25-28	14	16	OK	48	40	$b_w < c_2 + 1.5*c_3$	OK

Step 2: Determination of the required flexural reinforcement.

General data to compute the flexural reinforcement is shown in the table below. (Note that steel reinforcement has to be determined within the ranges of ρ_{min} and ρ_{max} as specified by *ACI 318-11*, to ensure a ductile failure.

General Data	
f'_c (Ksi) =	4
f_y (Ksi) =	60
E_s (Ksi) =	29000
β_1 =	0.85
ρ_{min} =	0.00333
ρ_{bal} =	0.02851
ρ_{max} =	0.02064
$\varphi_{flexure}$ =	0.9

A. Mid-Span reinforcement

Note: To simplify the design, the maximum ultimate moments at the mid span locations of all beams were extracted from the model results, and used for the beam.

Beam ID	h (in)	b_w (in)	d = h - 2.5 (in)	Location	M_u (Kips-ft) from *ETABS*	R_n (Ksi)	ρ required	$A_{s\text{-Required}}$ (in^2)
All	24	14	21.5	**Mid-span, (+)**	95.84	0.197	0.00339	1.02
				Mid-span, (-)	-72.72	0.150	0.00333	1.00
				$A_{s\text{-Required}}$ (in^2)	**Configuration**	**$A_{s\text{-Supplied}}$ (in^2)**	**ρ supplied**	**φM_n (Kip-ft)**
				1.02	4#5	1.24	0.00412	115.61
				1.00	4#5	1.24	0.00412	115.61

B. Edges reinforcement

Note: To simplify the design, the maximum ultimate moment values for edges locations were extracted from the model results, and used for both edges of the beam. See drawings and details in Appendix C.

Beam ID	**h (in)**	**b_w (in)**	**d = h - 2.5 (in)**	**Location**	**M_u (Kips-ft) from *ETABS***	**R_n (Ksi)**	**$\rho_{required}$**	**$A_{s\text{-Required}}$ (in^2)**
All	24	14	21.5	**Left, (+)**	81.66	0.168	0.00333	1.00
				Left, (-)	-111.33	0.229	0.00396	1.19
				Right, (+)	81.66	0.168	0.00333	1.00
				Right, (-)	-111.33	0.229	0.00396	1.19
				$A_{s\text{-Required}}$ (in^2)	**Configuration**	**$A_{s\text{-Supplied}}$ (in^2)**	**$\rho_{supplied}$**	**φMn (Kip-ft)**
				1.00	4#5	1.24	0.00412	115.61
				1.19	4#5	1.24	0.00412	115.61
				1.00	4#5	1.24	0.00412	115.61
				1.19	4#5	1.24	0.00412	115.61

Step 3: Standard hook anchorage length determination.

The minimum development length, l_{dh}, for a bar with a 90-degress hook in seismic high risk zones and using normal weight concrete is given by:

$$l_{dh} = \frac{f_y * d_b}{65 * \sqrt{f'_c}} \tag{7.1}$$

But should be the greater of the following conditions;

Condition	**(in)**
$l_{dh} = \frac{60\ Ksi * \left(\frac{5}{8}\right) in}{65 * \frac{\sqrt{4000\ psi}}{1000}} =$	9.12
$\geq 8 * d_b =$	5
$\geq 6\ in$	6

Condition	**(in)**
*Length of the 90-degrees extension = 12 * d_b*	7.5
*Bend diameter = 6 * d_b*	3.75

Step 4: Shear reinforcement requirements.

The probable moment were computed with Equations 7.2 and 7.3. As specified in the *ACI 318-11*, the stress in the tensile flexural reinforcement is equal to $1.25f_y$, and the strength reduction factor is $\varphi = 1.0$.

$$M_{pr} = A_s * (1.25 * f_y) * \left(d - \frac{a}{2}\right) \tag{7.2}$$

$$a = \frac{A_s * (1.25 * f_y)}{0.85 * f'_c * b} \tag{7.3}$$

The table shown below presents the probable moments computed. Since the supplied steel reinforcement area for positive and negative moments is equal, thus the probable flexural strength is the same.

Beam ID	Moment Sign	a (in)	M_{pr} (Kip-ft)
All	(+) Moment	1.95	159.05
	(-) Moment	1.95	159.05

To determine the probable shear forces using Equation 7.4 for both the left and right sides, the beam clear length used was the smallest of the three different beam spans. In addition, the factored shear extracted from *ETABS* was from the combination $(1.2 + 0.2S_{DS})*w_D + 0.5*w_L$, which for this case is, $1.365*w_D + 0.5*w_L$.

$$V_{pr} = \frac{M_{pr} + M_{pr}}{l_c} \tag{7.4}$$

Beam ID	l_c (ft)						
		Shear Forces @ Left					
		V_{pr} [SR] (Kips)	V_{pr} [SL] (Kips)	V_u from *ETABS* (Kips)	$V_{L-SR}=V_{pr}[SR]+V_u$ (Kips)	$V_{L-SL}=V_{pr}[SL]+V_u$ (Kips)	Max{V_{L-SR},V_{L-SL}} V_L (Kips)
All	15.33	-20.75	20.75	21.59	0.84	42.34	42.34
		Shear Forces @ Right					
		V_{pr} [SR] (Kips)	V_{pr} [SL] (Kips)	V_u from *ETABS* (Kips)	$V_{R-SR}=V_{pr}[SR]+V_u$ (Kips)	$V_{R-SL}=V_{pr}[SL]+V_u$ (Kips)	Max{V_{R-SR},V_{R-SL}} V_R (Kips)
		20.75	-20.75	21.59	42.34	0.84	42.34

SR - Sideways Right, SL - Sideways Left.

Before computing the shear strength of steel, V_s, it is necessary to verify if the shear strength supplied by the concrete, V_c, is negligible or not. V_c, which is computed using Equation 7.5, is zero if the probable shear forces are greater than or equal to 50% of the total shear. In the next table is checked this criterium

$$V_c = 2\sqrt{f'_c} b_w d \tag{7.5}$$

Beam ID	V_u=Max{V_L,V_R} (Kips)	50% of V_u	V_{pr} [max]	Comment	V_c (Kips)
All	42.34	21.59	20.75	Vpr < Vu/2	38.07

Hence, the shear strength of the concrete is considered. To compute the required shear strength provided by the steel reinforcement, Equation 7.6 with $\varphi = 0.75$ is used.

$$\varphi V_s = V_u - \varphi V_c \tag{7.6}$$

Substituting:

$$V_s = \frac{42.34\ Kips}{0.75} - 38.07\ Kips = 18.37\ Kips$$

The steel shear strength has to be smaller than the maximum shear, V_{max}, which is computed below. In addition, if $Vs > 4\sqrt{f'c} b_w d$, the maximum stirrups spacing, $d/2$, should be reduced by half, $d/4$.

$$V_{max} = 8\sqrt{f'_c} b_w d = 8 * \sqrt{4000\ psi} * 14\ in * 21.5\ in = 152.30\ Kips$$

$$4\sqrt{f'_c} b_w d = 4 * \sqrt{4000\ psi} * 14\ in * 21.5\ in = 76.15\ Kips$$

Since the shear strength that must be provided by the stirrups Vs *is* < 76.15 *Kips*, $s = d/2$ remain as a condition. For the shear design, stirrups #4 will be used at a spacing of the smaller of the following:

Condition
$s = (A_v * f_y * d) / V_s$
$s = d/2$
$s = 8*d_{b\text{-}smaller}$
$s = 24*dt$
$s = 6\ in$

This conditions are evaluated along the critical section of 2*h_{beam} from the face of the column. The result are displayed in the next table.

Critical Section, 2*h								
Beam ID	**b_w (in)**	**d = h - 2.5 (in)**	**V_s (Kips)**	**$V_{s\text{-}max}$ (Kips)**	**$d_{b\text{-}menor}$ (in)**	**s (in)**	**Configuration**	**# stirrups**
All	14	21.5	18.37	152.30	0.625	5	#4 @ 5"	11

The same procedure was performed outside the critical section resulting in a configuration of #4 @10". See drawings and details in Appendix C.

Step 5: Development length and splices of longitudinal reinforcement.

The development length and splices are determined using Equation 7.7. The next table presents the corresponding values to compute the lengths and their respective descriptions

$$l_d = \eta\left(\frac{3}{40}\,\frac{f_y}{\lambda\sqrt{f'_c}}\,\frac{\psi_t\psi_e\psi_s}{\left(\frac{c_b + K_{tr}}{d_b}\right)}\right)d_b \tag{7.7}$$

Factors	Values	Description
η	1.375	For high seismic risk zones
λ	1	Normal Weight Concrete
Ψt	1.3	Top Bars
	1	Bottom Bars
Ψe	1	Bars without Epoxy
Ψs	0.8	Bars #6 or smaller
	1	Bars #7 or larger
$(C_b + K_{tr}) / d_b$	2.5	Minimum value

The results for the development length and splice length are shown below.

Bar Properties		Development Length		Splice Length, l_e = 1.3*l_d	
Bar #	**d_b (in)**	**l_d (Top) (in)**	**l_d (Bottom) (in)**	**l_e (Top) (in)**	**l_e (Bottom) (in)**
5	0.625	26.00	20.00	34.00	26.00

7.4 Columns Design

The columns were designed for gravity loads and the ductility details for seismic design was verified. To perform the design of columns the four combinations shown in Table 7.1 were used. According to the proposed structural layout and pre-dimensioning parameters, the following column sections were obtained.

Column ID	**h (in)**	**b (in)**	**Diameter (in)**	**A_g (in^2)**
Circular	-	-	16.00	201.06
Rectangular	16.00	16.00	-	256.00

Step 1: Axial load check

A. Check that $P_u > (Ag*f'_c)/10$, to determine if strong column - weak beam design should be performed.

According to the results of the analysis the factored axial loads for circular columns range from 2.74 Kips to 496.13 Kips, while for rectangular columns range from 5.07 Kips to 72.74 Kips. Since for this study only one circular and rectangular column are to be designed, the larger of the factored axial loads was selected to perform the check. Although the maximum factored axial load resulted in a value smaller than $(A_g*f'_c)/10$, the strong column - weak beam design will be implemented for conservatism.

Beam ID	**P_u (Kips) (Value from *ETABS*)**	***$(Ag*f'_c)/10$***	**Check**
Circular	496.13	80.4	OK
Rectangular	72.74	102.4	NOT REQUIRED

Step 2: Check satisfaction of limits on section dimensions

A. Shortest cross-sectional dimension should be at least 12"

Column ID	**h (in)**	**b (in)**	**Diameter (in)**	Comment	Check
Circular	-	-	16	> 12"	OK
Rectangular	16	16	-	> 12"	OK

B. Ratio of shortest cross-sectional dimension to perpendicular dimension > 0.4. This ratio is equal to 1, since it is a square section, hence, it is satisfied.

Both columns were designed using an initial guess of reinforcement area suggested by the model to satisfy the factored moments produced by the combinations shown in Table 7.1. The supplied reinforcement has to be in ranges of $1\% < \rho \leq 6\%$.

Column ID	**$A_{s\text{-required}}$ (in^2)**	**Configuration**	**$A_{s\text{-supplied}}$ (in^2)**	**ρ**	**Comment**
Circular	3.076	10#5	3.1	1.54%	OK
Rectangular	2.56	6#6	2.6	1.03%	OK

Step 3: Nominal flexural strength of columns relative to beams.

To guarantee a strong column - weak beam behavior it is imperative to verify that the sum of the nominal flexure capacities of the columns should be greater than 6/5 times the sum of the nominal flexure capacities of the beams in the same joint (See Equation 7.8).

$$\sum M_{nc} \geq \frac{6}{5} \sum M_{nb} \qquad (7.8)$$

To calculate the nominal moment of beams, when analyzing the positive moment it is important to include the contribution of the steel provided by an effective width of the slab system. The computer software *CSI Column* was used to determine the nominal flexure strength of both cases: for the T-beam (compression at the top, tension at bottom of the section) and for the rectangular section for negative moments. Moment-curvature plots are presented in Figure 7.2 and Figure 7.4 for positive and negative moments respectively.

Moment Direction	**Section Type Analysis**	**(Kip-ft)**
M_{nb} (+)	T-beam	140.17
M_{nb} (-)	Rectangular beam	133.69

A. Circular column:

By means of an iterative procedure based on checking the compliance with the requirement in Equation 7.6, the longitudinal steel reinforcement of the column was increased up to a maximum of 6%. Nevertheless this maximum value allowed by the code was not enough to meet the condition. Hence, the column diameter was increased to 18 inches, where with ρ = 3.1%

provided by 10#8, it was sufficient to meet the requirements. The ultimate axial load used was the value of the combination specified by the *ASCE7-10* to comply with the seismic design for strong column - weak beam check. The suggested combination is $(1.2 + 0.20S_{DS})D + 1E + 0.5L$, resulting in 1.365D + 1E + 0.5L for this particular case. Since neither the columns nor the beams would be designed for seismic loads, the corresponding term was eliminated from the combination, finally resulting in 1.365D + 0.5L, which produced higher values than any of the tsunami loads combination. With the use of the interaction diagram shown in Figure 7.6, it was verified that for this particular ultimate axial load the factored flexure capacity was enough to comply with the strong column - weak beam check. The values of the nominal moments of columns and beams are presented in the next table.

Column ID	P_u (Kips) (1.365D + 0.5L)	Moment Location	M_{nc} (Kip-ft) From I.D.	ΣM_{nc} (Kip-ft)	$\frac{6}{5}\Sigma M_{nb}$ (Kip-ft)	Check
Circular	**380.06**	**M_{nc} (Top)**	177.50	355.00	328.63	OK
		M_{nc} (Bottom)	177.50			

B. Rectangular column:

The same procedure was followed for the rectangular column. In this case the dimensions and required steel reinforcement proposed as initial guess were sufficient to comply with the condition of the Equation 7.8. Since the rectangular columns are edge columns, only one beam is considered to act in the joint, therefore, the criterium was easier to satisfy as shown in table below.

Column ID	P_u (Kips) (1.365D + 0.5L)	Moment Location	M_{nc} (Kip-ft) From I.D.	ΣM_{nc} (Kip-ft)	$\frac{6}{5}\Sigma M_{nb}$ (Kip-ft)	Check
Rectangular	**60.21**	**M_{nc} (Top)**	105.50	211	168.20	OK
		M_{nc} (Bottom)	105.50			

A summary of the columns dimensions for flexure design is shown in the next table. The drawings and details are provided in Appendix C.

Final Column Flexure Design						
Element ID	**h (in)**	**b (in)**	**Diameter (in)**	**Configuration**	**ρ**	**Check**
Circular Column	**-**	-	18	10#8	3.10%	OK
Rectangular Column	**16**	16	-	6#6	1.02%	OK

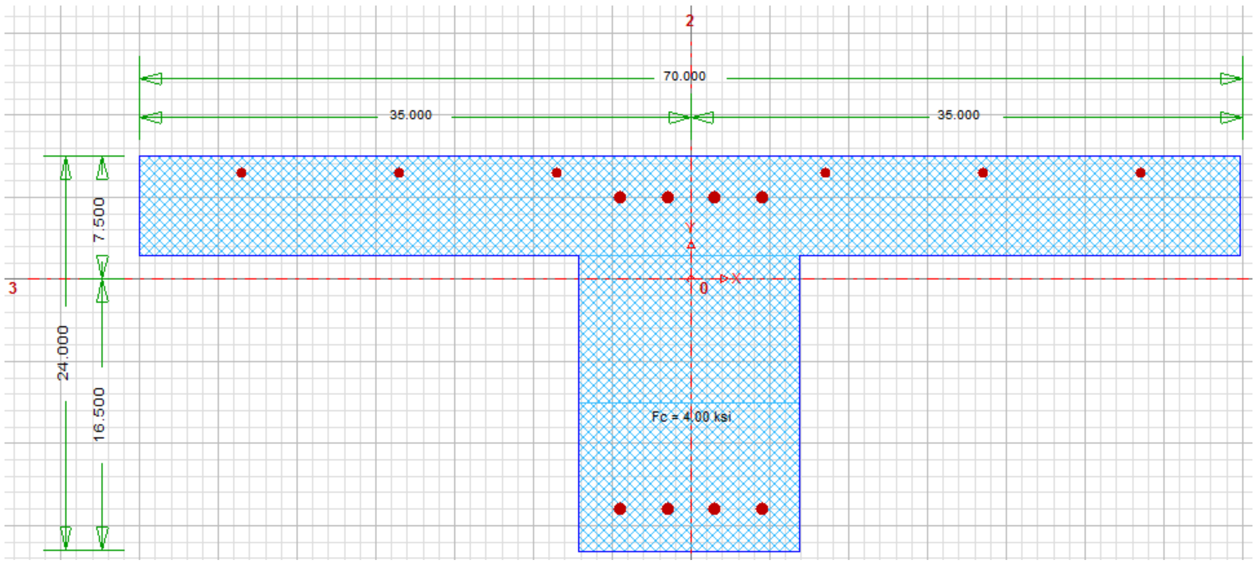

Figure 7.1: T-beam section dimensions [in] and steel reinforcement A_s = *8#5* in rectangular section and *#4@10”* in flanges.

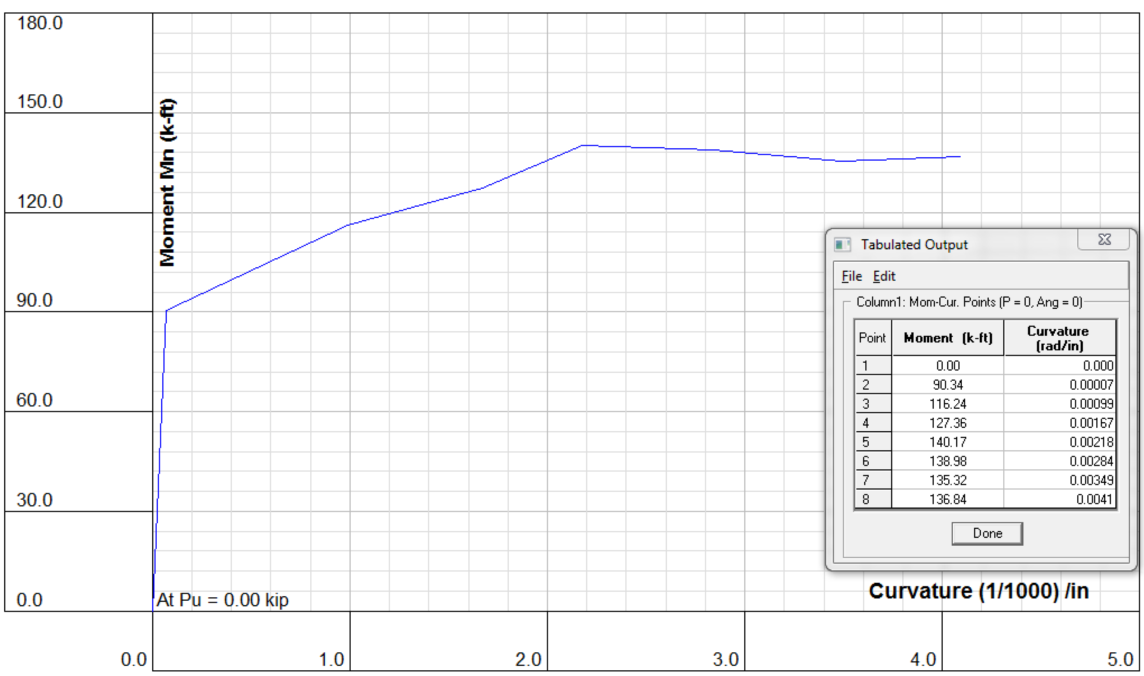

Figure 7.2: Moment-curvature plot for the T-beam section

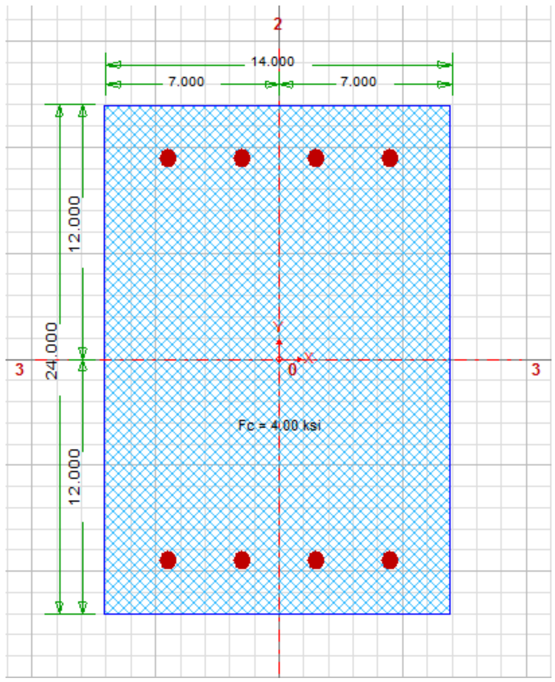

Figure 7.3: Rectangular beam cross section dimensions [in] and steel reinforcement. A_s = *8#5*.

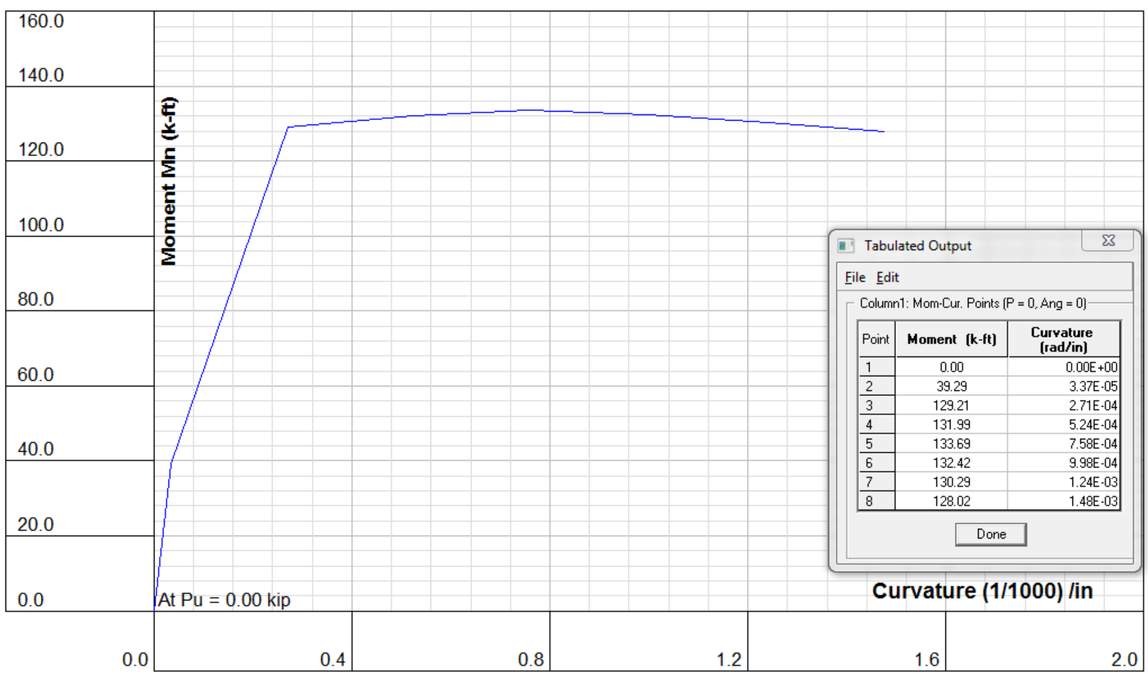

Point	Moment (k-ft)	Curvature (rad/in)
1	0.00	0.00E+00
2	39.29	3.37E-05
3	129.21	2.71E-04
4	131.99	5.24E-04
5	133.69	7.58E-04
6	132.42	9.98E-04
7	130.29	1.24E-03
8	128.02	1.48E-03

Figure 7.4: Moment-curvature plot for the rectangular beam section

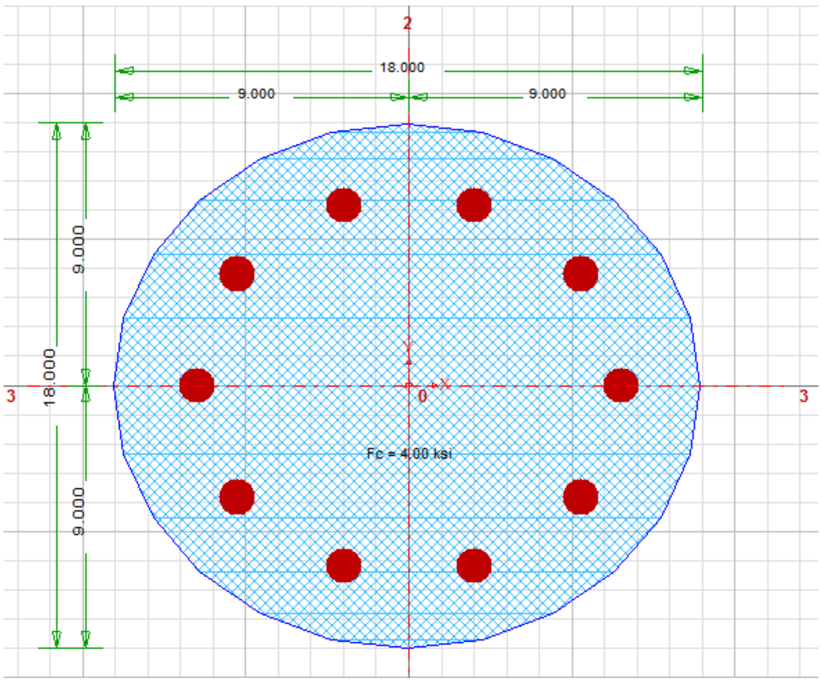

Figure 7.5: Rectangular column cross section dimensions and steel reinforcement, *d = 18in, A_s = 10#8*

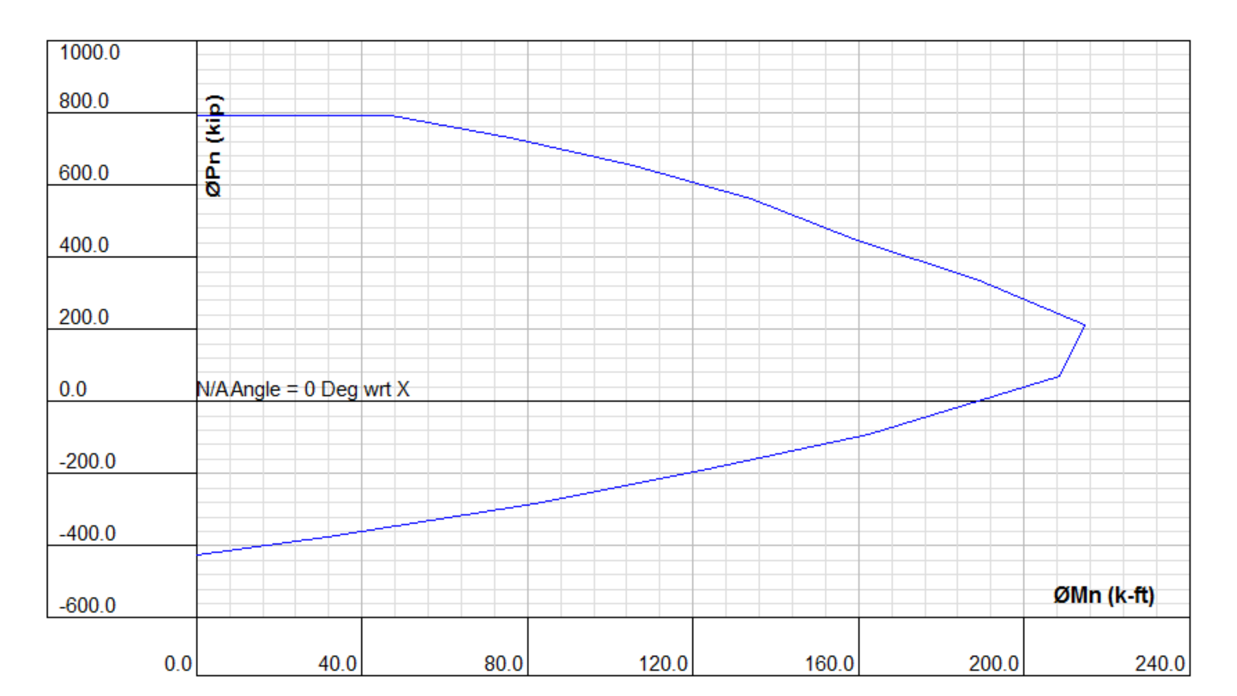

Figure 7.6: Interaction diagram for the circular column, *d = 18in, A_s = 10#8*

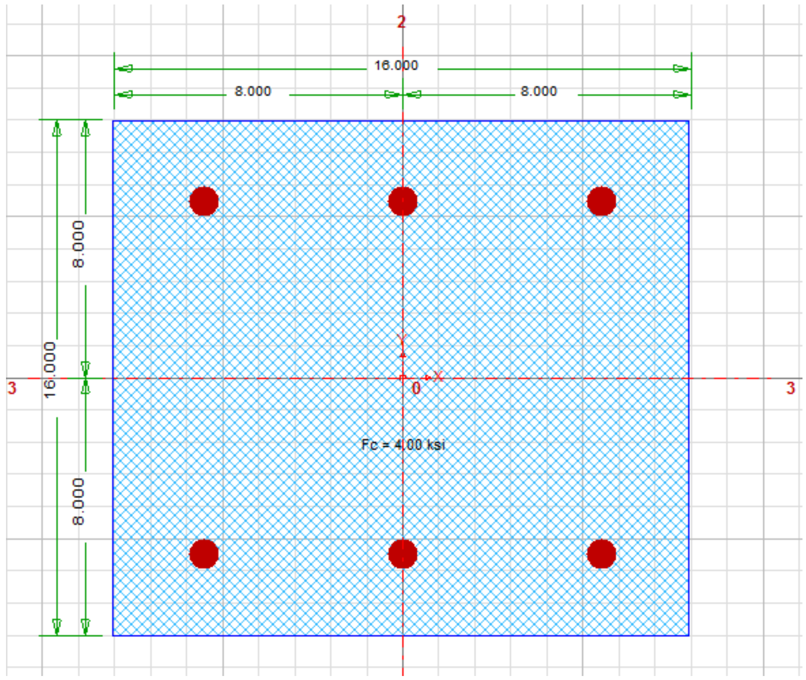

Figure 7.7: Rectangular column cross section dimensions [in]and steel reinforcement, *h* = *b* = *16in*, A_s = *6#6*

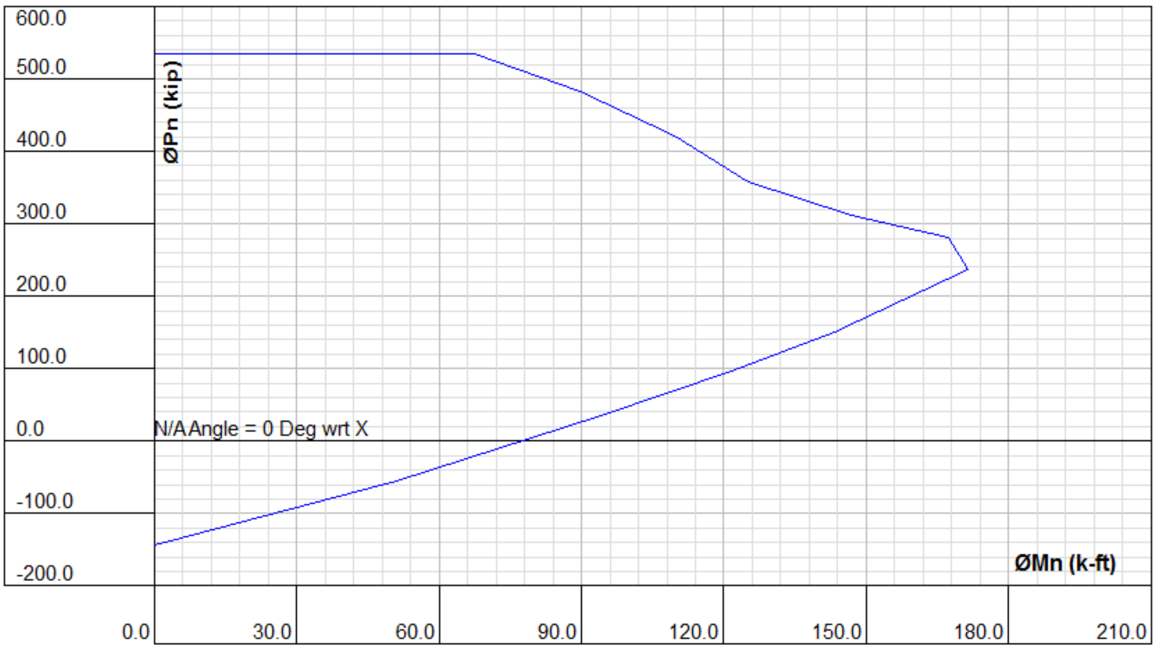

Figure 7.8: Interaction diagram of the rectangular column, *h* = *b* = *16in*, A_s = *6#6*

Step4: Development length and splices of longitudinal reinforcement.

A. Circular column

In the same fashion as for the beam, the development length and splices are determined using Equation 7.7. The next table presents the corresponding values to compute the lengths and their respective descriptions

Factors	Values	Description
η	1.375	For high seismic risk zones
λ	1	Normal Weight Concrete
Ψt	1.3	Top Bars
	1	Bottom Bars
Ψe	1	Bars without Epoxy
Ψs	0.8	Bars #6 or smaller
	1	Bars #7 or larger
$(C_b + K_{tr}) / d_b$	2.5	Minimum value

The results for the development length and splice length are shown below.

Bar Properties		**Development Length**		**Splice Length = 1.3*l_d**	
Bar #	**d_b (in)**	**l_d (Top) (in)**	**l_d (Bottom) (in)**	**l_e(Top) (in)**	**l_e (Bottom) (in)**
8	1.0	51.00	40.00	67.00	52.00

B. Rectangular column

The results for the development length and splice length are shown below.

Bar Properties		**Development Length**		**Splice Length = 1.3*l_d**	
Bar #	**d_b (in)**	**l_d (Top) (in)**	**l_d (Bottom) (in)**	**l_e(Top) (in)**	**l_e (Bottom) (in)**
6	0.75	31.00	24.00	41.00	32.00

Step 4: Determination of transverse reinforcement requirements

A. Circular column

Firstly, the critical distance, l_o, is to be determined using the following conditions: where l_c is the clear length of the column member. As shown in the table, the l_o length is 19 in.

$l_o \geq$ Following Condition	(in)
h_{col} (in)	18.00
1/6 * (clear length of column)	19.00
18in	18.00

To compute the maximum allowed pitch of the spirals which are proposed for circular column, were used the following conditions, as specified in the *ACI 318-11* code

- Where, h_x, is the distance from center to center of the spiral transverse reinforcement
- Assuming a #4 spiral

$s_{max} \leq$ Following Condition	(in)
0.25 * (shortest dimension)	4.00
6 * (longitudinal bar diameter)	6.00
$s_0 = 4 + ((14 - h_x) / 3)$	3.83

Since 3.83 inches is not practical, a maximum pitch of 3.5 inches will be used. Once the pitch is determined, might be check the concrete to steel volumetric ratio condition of Equation 7.9.

$$\rho_v \geq 0.45\left(\frac{A_{gr}}{A_{ch}} - 1\right)\frac{f'_c}{f_{yt}} \geq \frac{0.12f'_c}{f_{yt}} \tag{7.9}$$

$$\rho_v = \frac{A_{st-\#4} * (\pi * h_x)}{A_{ch} * s} = \frac{0.2\ in^2 * (\pi * 14.5\ in)}{\frac{\pi}{4}(18\ in - 2 * 1.5\ in)^2 * 3.5\ in} = 0.0147$$

$$0.45\left(\frac{A_{gr}}{A_{ch}} - 1\right)\frac{f'_c}{f_{yt}} = 0.45\left(\frac{254.47\ in^2}{\frac{\pi}{4}(18\ in - 2 * 1.5\ in)^2} - 1\right)\frac{4Ksi}{60Ksi} = 0.0132$$

$$\frac{0.12f'_c}{f_{yt}} = \frac{0.12 * 4\ Ksi}{60\ Ksi} = 0.0080$$

Hence, the condition is accomplished.

B. Rectangular column

In a similar fashion to circular columns, l_o, is to be determined using the following conditions: where l_c is the clear length of the column member. As shown in the Table, the l_o length is 19 in.

$l_o \geq$ Following Condition	(in)
h_{col} (in)	16.00
1/6 * (clear length of column)	19.00
18in	18.00

To compute the maximum allowed spacing of the stirrups for rectangular column, were used the following conditions, as specified in the *ACI 318-11* code.

- Where h_x is the distance maximum distance from center to center of the stirrups.
- Assuming a #4 stirrup.

$s_{max} \leq$ Following Condition	(in)
0.25 * (shortest dimension)	4.00
6 * (longitudinal bar diameter)	4.00
$s_0 = 4 + ((14 - h_x) / 3)$	4.00

A maximum spacing of 4 inches will be used. Once the spacing is determined, the minimum transverse steel area provided by the proposed stirrup configuration can be determined

Ash $\geq$ Following Conditions	(in^2)
$0.3 * s * b_c * [(A_g/A_{ch})-1] * (f'_c/f_{yt})$	0.40
$0.09 * s * b_c * (f'_c/f_{yt})$	0.23

$$0.03 * s * b_c * \left(\frac{A_g}{A_{ch}} - 1\right) * \left(\frac{f'_c}{f_{yt}}\right)$$
$$= 0.3 * 4\ in * 16\ in * \left(\frac{(16\ in * 16\ in}{(16\ in - (2 * 1.5\ in))^2} - 1\right) * \left(\frac{4Ksi}{60Ksi}\right) = 0.40\ in^2$$

$$0.09 * s * b_c * \left(\frac{f'_c}{f_{yt}}\right) = 0.09 * 4\ in * 16\ in * \left(\frac{4Ksi}{60Ksi}\right) = 0.234\ in^2$$

$$A_{sh\ (supplied)} = 2 * A_{st-\#4} = 2 * 0.20\ \ in^2 = 0.40\ in^2$$

Hence, the condition is accomplished.

Step 5: Checking capacity of the proposed reinforcement for shear.

A. Circular column

Similar as the shear reinforcement design for beams, shear design for columns is not based in the ultimate shear capacity obtained from the analysis, else is based in the nominal flexure capacity of columns. Supported in this criteria, the maximum ultimate probable flexure capacity, could be the factored balanced moment of the column. Values are presented in next Table, where $V_u = (2 * M_{pr} / l_c)$.

$M_{pr} = M_{bal}$ (Kips)	l_c (ft)	V_u (Kips)
214.62	9.50	45.18

Since the same circular column is to be assigned for all similar section column, $V_c = 0$, since P_u is not greater than $A_g * f'_c / 20$ for all the column members.

$$V_s = \frac{A_v f_y d}{s} = \frac{(2 * 0.2\ in^2) * 60\ Ksi * \left(18\ in - 1.5\ in - 0.5\ in - \frac{1\ in}{2}\right)}{3.5\ in} = 106.29\ Kips$$

$$\varphi V_s = 0.75 * 106.29\ Kips = 79.71\ Kips\ \ >\ \ \ 45.18\ Kips\ \ \ \therefore OK$$

For outside the critical section length, l_o, the pitch should be determined as follow:

s ≤ Following Condition	(in)
6"	6.00
$6 * d_l$	6.00

Therefore as summary of the spiral shear reinforcement design is #4 with a pitch of 3.5 inches for distance l_o, and #4 with a pitch of 6 inches outside the critical section length. The drawings and details are provided in Appendix C.

B. Rectangular column

Similar as the shear reinforcement design for beams, shear design for columns is not based in the ultimate shear capacity obtained from the analysis, else is based in the nominal flexure capacity of columns. Supported in this criteria, the maximum ultimate probable flexure capacity, could be the factored balanced moment of the column. Values are presented in next Table, where $V_u = (2* M_{pr} / l_c)$.

$M_{pr} = M_{bal}$ (Kips)	l_c (ft)	V_u (Kips)
171.48	9.50	36.10

Since the same rectangular column is to be assigned for all similar section column, $V_c = 0$, since P_u is not greater than $A_g*f'_c / 20$ for all the column members.

$$V_s = \frac{A_v f_y d}{s} = \frac{(2 * 0.2\ in^2) * 60\ Ksi * \left(16\ in - 1.5\ in - 0.5\ in - \frac{6/8\ in}{2}\right)}{4\ in} = 109.0\ Kips$$

$$\varphi V_s = 0.75 * 109.00\ Kips = 81.75\ Kips \quad > \quad 36.10\ Kips \quad \therefore OK$$

Similar to circular column, for outside the critical section length, l_o, the spacing should be determined as follow:

s ≤ Following Condition	(in)
$6'' =$	6.00
$6 * d_l =$	4.50

Therefore as summary of the stirrup shear reinforcement design is #4 @ 4 inches for distance l_o, and #4 @ 4.5 inches outside the critical section length. See drawings and details in Appendix C.

7.5 Structural Walls Design

As mentioned previously, the proposed building is a special shear wall system designed to resist all the seismic loads by means of the structural walls. Since earthquake loads are distributed proportionally by the stiffness of the structure, a horizontal distribution of forces to each shear walls was performed. As a result of this analysis, the actual load in terms of shears and moments that a wall member will be subjected to according to its rigidities will be determined. Figure 7.9 shows and identifies the structural wall layout to be considered.

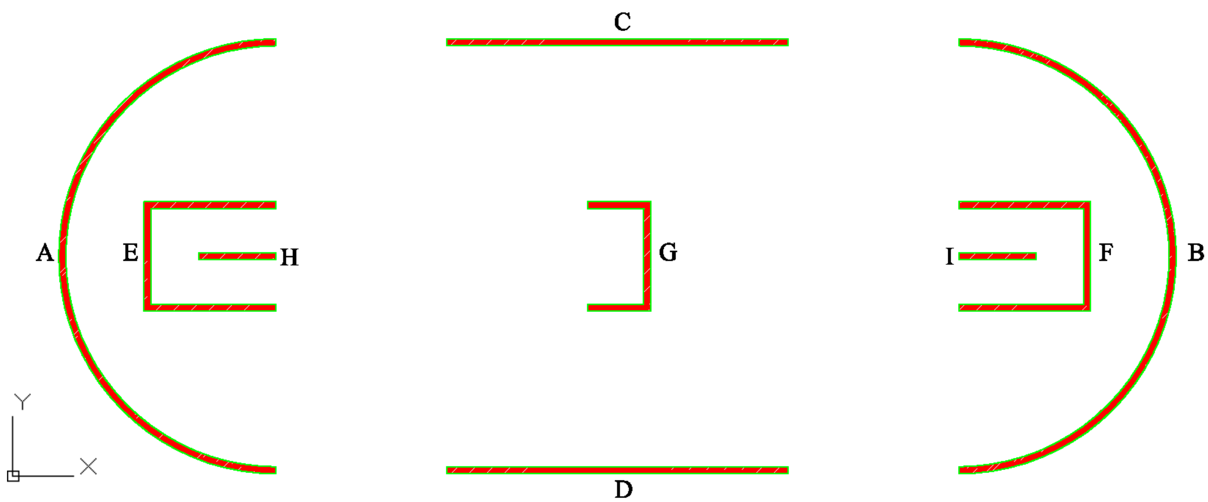

Figure 7.9: Layout of the individual shear walls

For the horizontal distribution of forces analysis, Equations 7.10 to 7.15 are part of the procedure to determine the percentage of base shear in each wall.

The total external loads to be resisted by a particular wall *w* in the x and y directions are given by:

$$F_{wx} = F'_{wx} + F''_{wx} \tag{7.10}$$

$$F_{wy} = F'_{wy} + F''_{wy} \tag{7.11}$$

where subscript *w* represents a particular wall in analysis (*w* goes from A to I).

The loads induced in a wall by inter-story translation only in x and y directions are given by:

$$F'_{wx} = \frac{F_x \, I_{wy}}{\sum I_{wy}} \tag{7.12}$$

$$F'_{wy} = \frac{F_y\, I_{wx}}{\sum I_{wx}} \tag{7.13}$$

Loads induced in a wall by inter-story torsion only in x and y directions are given by:

$$F''_{wx} = \frac{(F_x * e_y) * y_w * I_{wy}}{\sum({x_w}^2 I_{wx} + {y_w}^2 I_{wy})} \tag{7.14}$$

$$F''_{wy} = \frac{(F_y * e_x) * x_w * I_{wx}}{\sum({x_w}^2 I_{wx} + {y_w}^2 I_{wy})} \tag{7.15}$$

where:

F_x = total external load to be resisted by all walls, in x-direction (base shear),

F_y = total external load to be resisted by all walls, in y-direction (base shear),

I_{wx} = second moment of area of a wall section about the x axis,

I_{wy} = second moment of areas of a wall section about the y axis,

$\sum I_{wx}$ = total second moment of areas of all walls in the x-direction,

$\sum I_{wy}$ = total second moment of area of all walls in the y-direction,

x_w = x-coordinate of a wall with respect to the center of rigidity (CR) of the lateral load resisting system,

y_w = y-coordinate of a wall with respect to the center of rigidity (CR) of the lateral load resisting system,

e_x = eccentricity resulting from non-coincidence of the center of gravity (CG) and the center of rigidity (CR), in the x-direction, and

e_y = eccentricity resulting from non-coincidence of the center of gravity (CG) and the center of rigidity (CR), in the y-direction

Since the proposed building has a regular and symmetric layout, the center of mass and center of rigidity coincide, and therefore the torsion caused by the eccentricity is null. Nevertheless, a torsional effect by a 5% accidental eccentricity was considered in the analysis. The results of the seismic horizontal distribution of forces are presented in Table 7.5

Table 7.5: Base shear distribution to individual shear walls

	A	B	C	D
% F'_{ix} (kip)	20.8%	20.8%	23.9%	23.9%
% F'_{iy} (kip)	47.0%	47.0%	0.0%	0.0%
E	**F**	**G**	**H**	**I**
4.7%	4.7%	0.6%	0.3%	0.3%
2.4%	2.4%	1.2%	0.0%	0.0%
	A	**B**	**C**	**D**
% F''_{ix} (kip)	0.0%	0.0%	-0.3%	0.3%
% F''_{iy} (kip)	-6.0%	6.0%	0.0%	0.0%
E	**F**	**G**	**H**	**I**
0.0%	0.0%	0.0%	0.0%	0.0%
-0.3%	0.3%	0.0%	0.0%	0.0%
	A	**B**	**C**	**D**
% F_x (kip)	20.8%	20.8%	23.6%	24.1%
% F_y (kip)	41.0%	53.0%	0.0%	0.0%
E	**F**	**G**	**H**	**I**
4.7%	4.7%	0.6%	0.3%	0.3%
2.0%	2.7%	1.3%	0.0%	0.0%
	A	**B**	**C**	**D**
F_x (kip)	823.75	823.75	934.25	954.36
F_y (kip)	1,622.40	2,095.03	0.00	0.00
E	**F**	**G**	**H**	**I**
185.41	185.41	24.38	10.76	10.76
81.00	104.91	49.49	0.00	0.00

For wall design, the contribution of the earthquake was included from the values presented in Table 7.5, and by using the load combinations shown in Table 7.10. The output from the structural analysis included the ultimate values of the gravity and tsunami loads combinations. In addition, the corresponding to ultimate values of the gravity terms (dead load and live load) inside the earthquake loads combinations were extracted from ETABS and algebraically added to the seismic contribution to get the ultimate values of the whole earthquake load combination.

For simplification purposes, only wall B (curved wall) and wall D (plane wall), which resulted with the higher shear forces will be designed. Recalling the the increase in the circular columns diameter to 18 inches, in turn increased the total weight of the structure. Similarly, the base shear and the seismic loads distribution per story previously mentioned in Table B.14 changed. For this reason Table 7.6 presents the updated values.

Table 7.6: Modified lateral seismic loads distribution per story.

Story	W_i (kip)	h_i (ft)	$W_i * h_i^k$ (kip*ft)	F_i (kip)
6	139.18	69.00	9,181.87	152.60
5	1263.80	57.50	69,615.52	1,157.01
4	1434.64	46.00	63,370.42	1,053.22
3	1434.64	34.50	47,672.87	792.32
2	1434.64	23.00	31,918.71	530.49
1	1434.64	11.50	16,076.97	267.20
Total	**7,141.5**		**237,836.4**	**V_{base} = 3,952.84**

In Table 7.7 and Table 7.8 are shown the results of the distribution by stories of shears and moments due to seismic loads in walls D and B respectively, for both X and Y load direction.

Table 7.7: Shear and moment forces distribution along Wall D

Wall D	**F_x (Kips) =**	954.36				
	F_y (Kips) =	0.00				
Story	**%V_D /Story**	**F_x (K-ft)**	**F_y (K-ft)**	**h_i (ft)**	**M_x (K-ft)**	**M_y (K-ft)**
6	0.0%	0.00	0.00	69.00	0.00	0.00
5	30.4%	290.56	0.00	57.50	16707.37	0.00
4	27.7%	264.50	0.00	46.00	12166.86	0.00
3	20.8%	198.98	0.00	34.50	6864.75	0.00
2	14.0%	133.22	0.00	23.00	3064.13	0.00
1	7.0%	67.10	0.00	11.50	771.68	0.00
Total	100.0%	954.36	0.00		39,574.78	0.00

Table 7.8: Shear and moment forces distribution along Wall B

Wall B	F_x (Kips) =	823.75				
	F_y (Kips) =	2095.03				
Story	**%V_B /Story**	**F_x (K-ft)**	**F_y (K-ft)**	**h_i (ft)**	**M_x (K-ft)**	**M_y (K-ft)**
6	0.00	0.00	0.00	69.00	0.00	0.00
5	0.30	250.80	637.85	57.50	14,420.86	36,676.23
4	0.28	228.30	580.63	46.00	10,501.75	26,708.85
3	0.21	171.75	436.80	34.50	5,925.26	15,069.58
2	0.14	114.99	292.45	23.00	2,644.79	6,726.42
1	0.07	57.92	147.30	11.50	666.07	1,694.00
Total	1.00	823.75	2,095.03		34,158.72	86,875.08

Step 1: Check wall preliminary design for ultimate axial loads and moments.

After obtaining the seismic demands on the walls to be designed, the magnitudes were added to the *ETABS* output values of gravity effects with the proper combination factors to form the earthquake load combinations. By generating interaction diagrams of the two walls D and B using the data specified in Table 7.9, both were checked to comply with the axial and moment forces of all the combinations in Table 7.10. Figure 7.10 to Figure 7.15 display the wall sections built in *CSI Column* software and their respective interaction diagrams for both X and Y earthquake direction. Each diagram shows the values of ultimate axial and moments forces bounded by the factored capacity of each wall member. This shows that the design meet the requirements established by the ultimate loads.

Table 7.9: Proposed wall dimensions and steel reinforcement

Wall ID	t_w (in)	ρ_{min}	Configuration
D	10	0.0025	2 curtains of #4@16"
B	10	0.0025	2 curtains of #4@16"

Table 7.10: Load combinations used for wall design.

Type of Combination	Combination	
Gravity load	1.4 D	1.4 D
	1.2 D + 1.6 L	1.2 D + 1.6 L
Tsunami Loads	1.2 D + 1.0 T_s +1.0 L_{Ref} +0.25 L	1.2 D + 1.0 T_s +1.0 L_{Ref} +0.25 L
	0.9 D + 1.0 T_s	0.9 D + 1.0 T_s
Earthquake Loads	(1.2 + 0.2S_{DS}) D + 1.0 E + 0.5 L	1.348 D + 1.0 E + 0.5 L
	(1.2 - 0.2S_{DS}) D - 1.0 E + 0.5 L	1.052 D - 1.0 E + 0.5 L
	(0.9 - 0.2S_{DS}) D +1.0 E	0.752D +1.0 E
	(0.9 + 0.2S_{DS}) D - 1.0 E	1.048D - 1.0 E

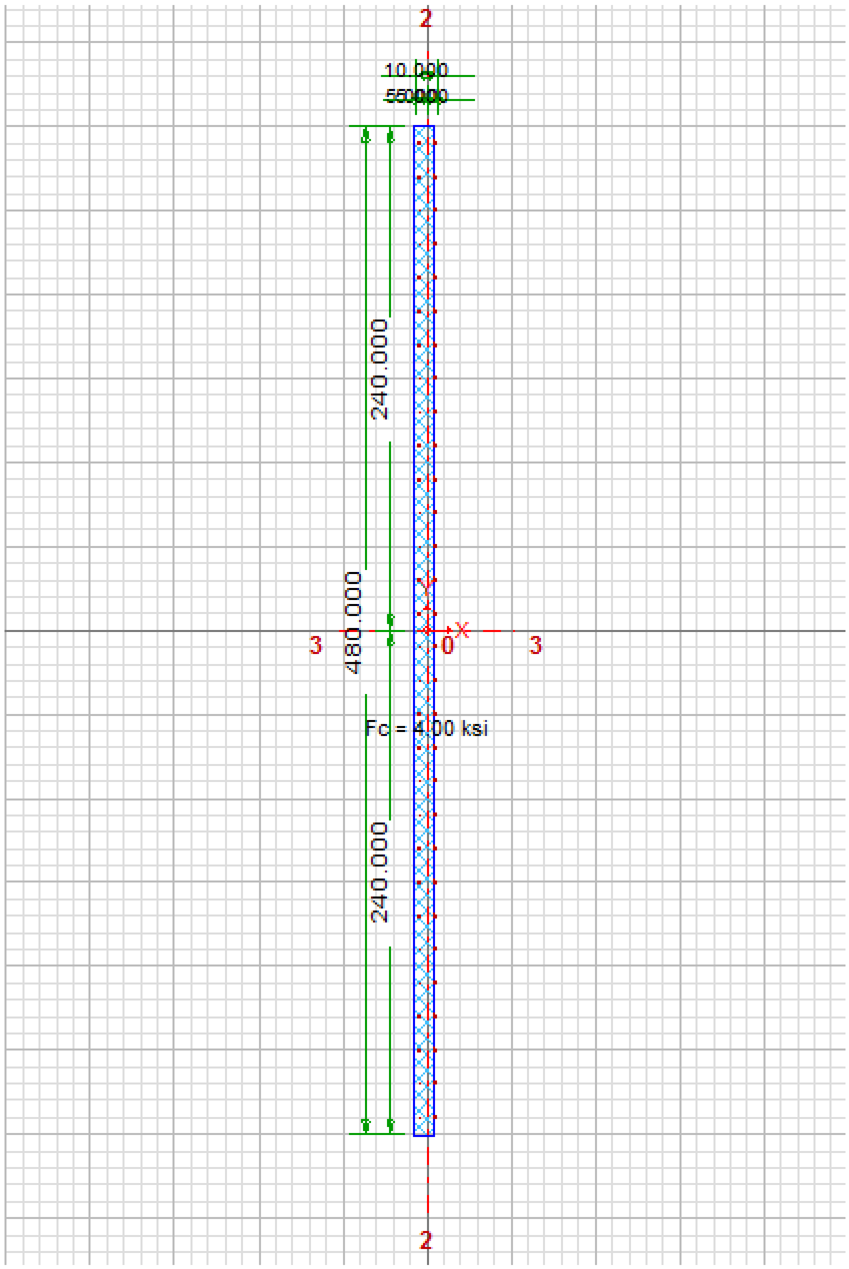

Figure 7.10: Wall D cross section dimensions and steel reinforcement, *L= 480 in, t_w = 10 in, A_s = 2 curtains of # 4@ 16".*

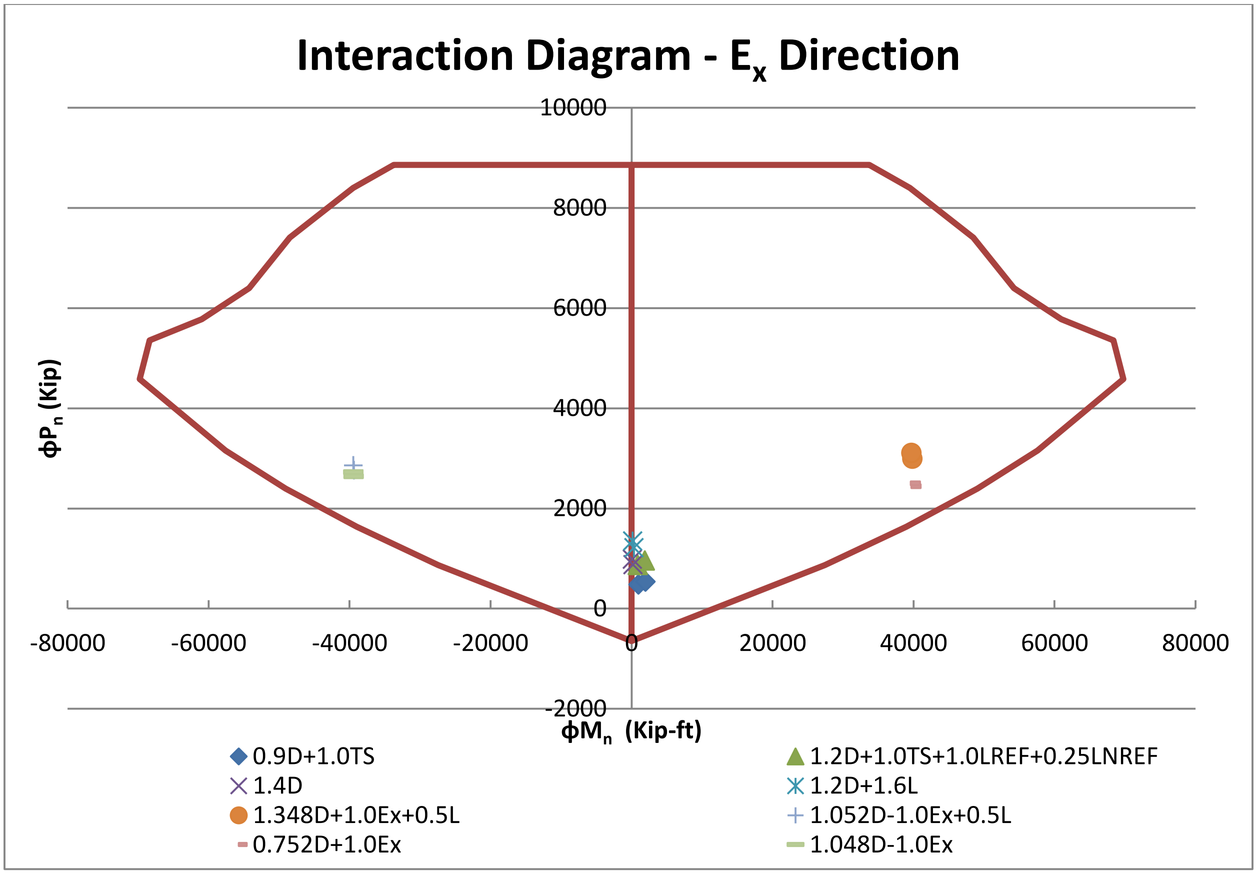

Figure 7.11: Interaction diagram of Wall D, considering earthquake in X- direction.

From Figure 7.11, is observed that the earthquake combination 0.752D + 1.0E_x, governs the design of wall D for the E_x direction, with an ultimate axial load of 2,501.2 Kips, and a flexure moment of 39,631 Kip-ft.

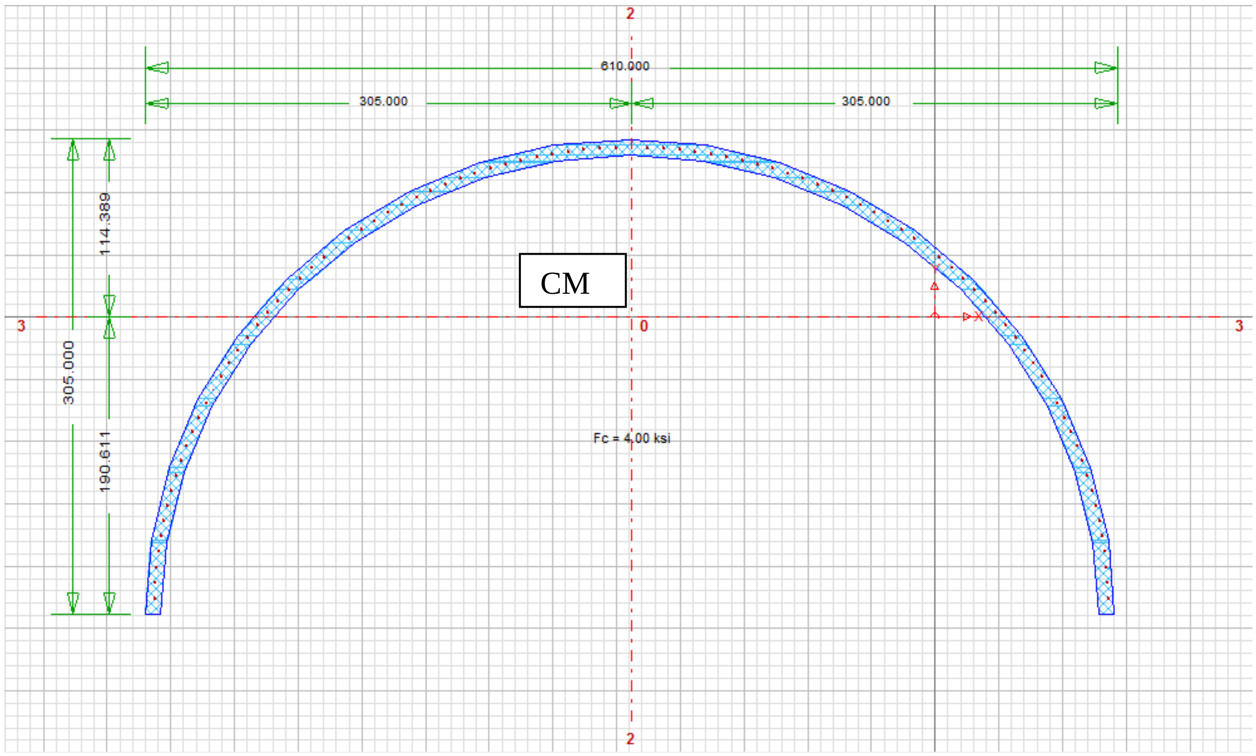

Figure 7.12: Wall B cross section and dimensions (E_x analysis) , *t_w = 10 in, A_s =2 curtains, # 4 @ 16"*.

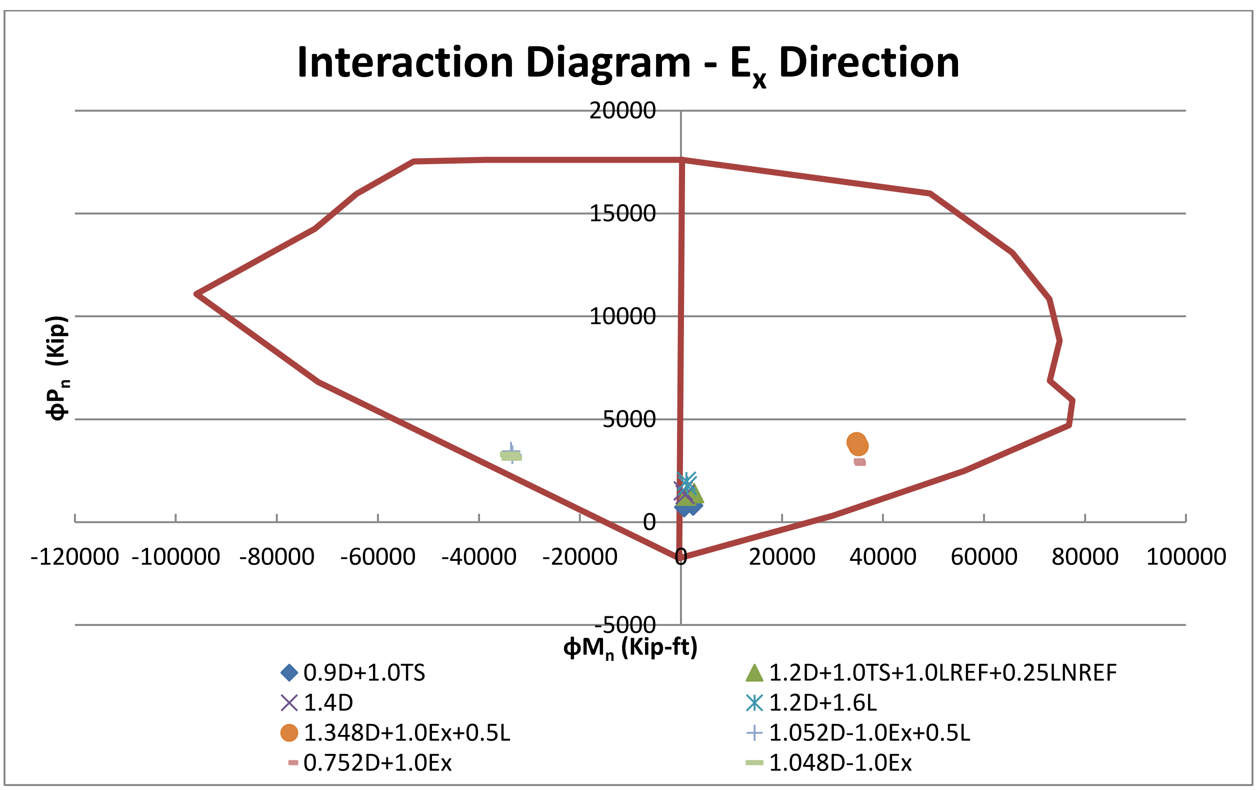

Figure 7.13: Interaction diagram of Wall B, considering earthquake in X- direction.

By observing the interaction diagram in Figure 7.13, it is noticed the asymmetry of the curves meaning that this wall shape has different strengths depending on the direction of the load. The section modulus of the wall for a load coming from the convex side to the concave side of the wall resulted in 241.54 ft^3, while in the opposite direction the value is 407.27ft^3. From the same figure, it can be observed that the earthquake combination 1.048D - 1.0E_x governs the design of wall B for the E_x direction, with an ultimate axial load of 3,295.0 Kips, and a flexure moment of 33,338 Kip-ft.

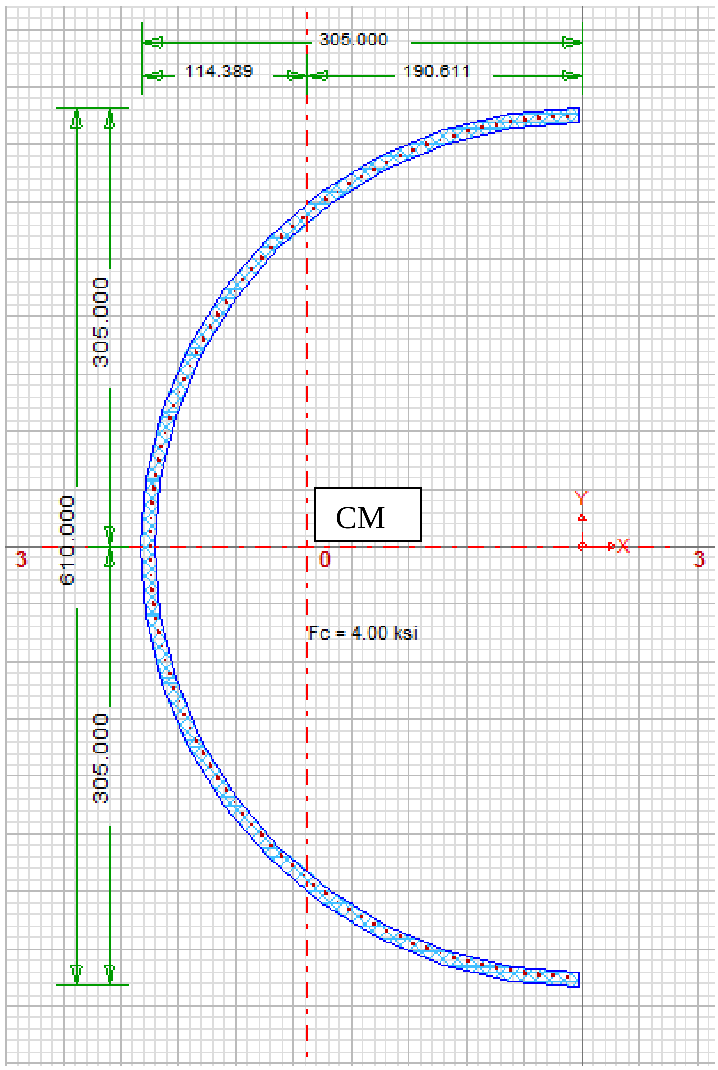

Figure 7.14: Wall B cross section and dimensions (E_y analysis) , *t_w = 10 in, A_s =2 curtains, # 4 @ 16".*

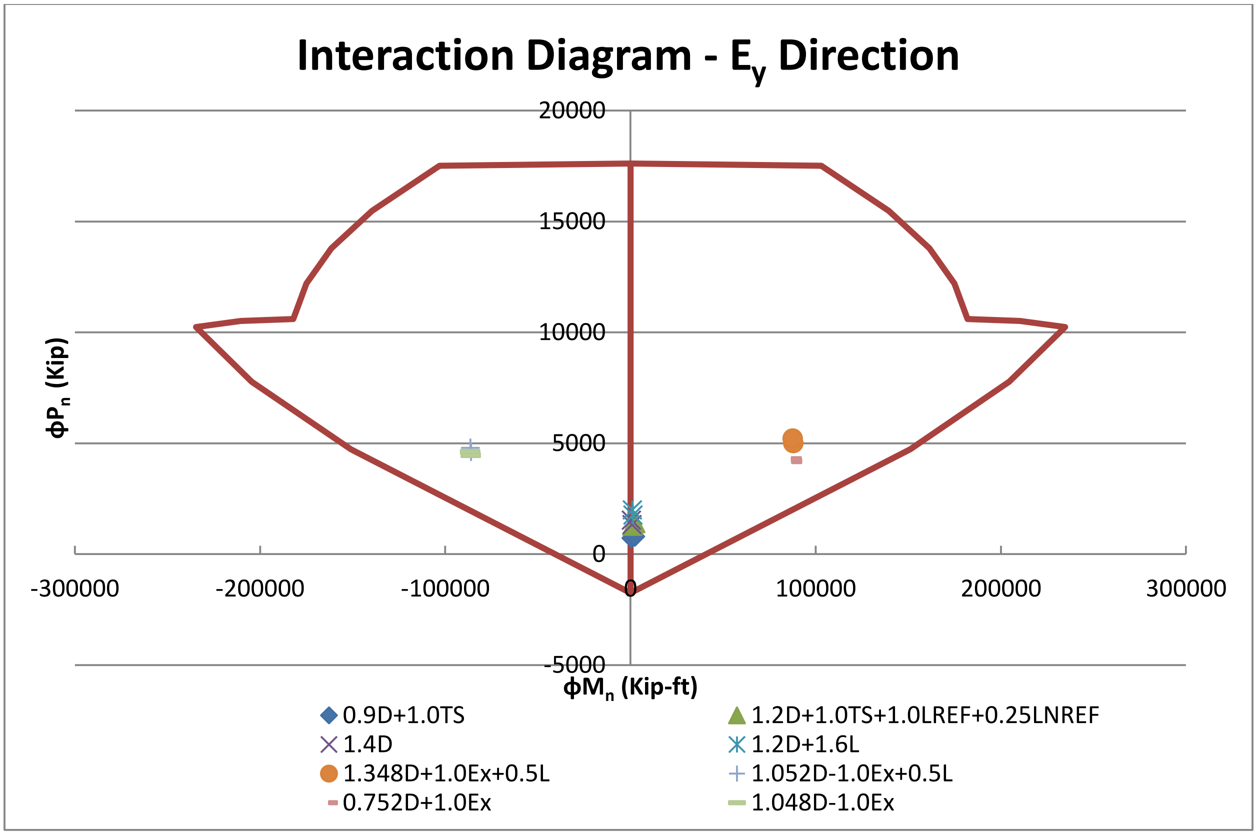

Figure 7.15: Interaction diagram of Wall B, considering earthquake in Y- direction.

Observing Figure 7.15, it is concluded that the earthquake combination 1.048D - 1.0E_y governs the design of wall B for the E_y direction, with an ultimate axial load of 4,629.2 Kips, and a flexure moment of 86,547 Kip-ft.

Step 2: Minimum longitudinal and transverse reinforcement requirements in the wall.

A. Plane Wall D

Earthquake in X - direction

a. Check if two curtains of reinforcement are required. For normal weight concrete, λ = 1.

$$2 * A_{cv} * \lambda * \sqrt{f'_c} = 2 * 4{,}800\ in^2 * 1 * \frac{\sqrt{4{,}000\ psi}}{1{,}000} = 607.2\ Kips < V_u = 958.95\ Kips$$

Condition	Number of curtains to be used if condition accomplished
If $V_u < 2*A_{cv}*\lambda*\sqrt{f'_c}$	1
If $t_w = 10\ in$	2

Hence, two curtains are required.

b. Required longitudinal and transverse reinforcement in wall.

For wall members the minimum distributed reinforcement ratios are $\rho_{min} = \rho_H = \rho_V = 0.0025$ and a spacing, $s = 18\ in.$

$$\frac{A_{cv}}{L} = 12 * t_w = 12\frac{in}{1ft} * 10\ in = \frac{120\ in^2}{foot\ of\ wall}$$

$$\frac{A_s}{L} = \rho_{min} * \frac{A_{cv}}{L} = 0.0025 * \frac{120\ in^2}{foot\ of\ wall} = \frac{0.30\ in^2}{foot\ of\ wall}$$

$$\frac{A_s}{L} = \frac{0.15\ in^2}{ft/curtain}$$

Assuming #4 bars, the required spacing is;

$$s = \frac{A_{s(\#4)} * 12}{A_{s-supplied}} = \frac{2\ curtains * 0.2\ in^2 * \frac{12\ in}{1\ ft}}{\frac{0.30\ in^2}{ft}} = 16\ in < 18\ in\ \therefore OK$$

B. Curved Wall B

Earthquake in X - direction

a. Check if two curtains of reinforcement are required. For normal weight concrete, λ = 1.

$$2 * A_{cv} * \lambda * \sqrt{f'_c} = 2 * 9{,}424.78\ in^2 * 1 * \frac{\sqrt{4{,}000\ psi}}{1{,}000} = 1{,}192.2\ Kips > V_u = 868.26\ Kips$$

Earthquake in Y - direction

$$2 * A_{cv} * \lambda * \sqrt{f'_c} = 2 * 9{,}424.78\ in^2 * 1 * \frac{\sqrt{4{,}000\ psi}}{1{,}000} = 1{,}192.2\ Kips < V_u = 2{,}139.54\ Kips$$

Condition	Number of curtains to be used if condition accomplished
If $V_u < 2*A_{cv}*\lambda*\sqrt{f'_c}$	1
If $t_w = 10\ in$	2

Since, t_w = 10” for all the walls, two curtains with a steel reinforcement configuration of #4 @

16" are required to comply with the minimum distributed reinforcement ratios.

Step 3: Reinforcement requirements for shear using Equation 7.16. For normal weight concrete, $\lambda = 1$.

A. Plane Wall D

$$\phi V_n = \phi A_{cv} * \left(\alpha_c \lambda \sqrt{f'_c} + \rho_t * f_y\right) \tag{7.16}$$

where: $\alpha_c = 2\left(3 - \frac{h_w}{l_w}\right) = 2 * \left(3 - \frac{57.5\,ft}{40.0\,ft}\right) = 3.13$

$$\phi V_n = \frac{0.75 * 4{,}800\ in^2 * \left(3.13 * 1 * \sqrt{4{,}000\ psi} + 0.00333 * 60{,}000\ psi\right)}{1{,}000} = 1{,}431.5\ Kips$$
$$> 958.95\ \therefore OK$$

Earthquake in Y - direction

Since stiffness for a plane wall in its weak axis is negligible, earthquake in Y-direction was not analyzed.

B. Curve Wall B

Earthquake in X - direction

$$\begin{aligned}\phi V_n &= \phi A_{cv} * \left(\alpha_c \lambda \sqrt{f'_c} + \rho_t * f_y\right) \\ &= \frac{0.75 * 9{,}424.78\ in^2 * \left(4.54 * 1 * \sqrt{4{,}000\ psi} + 0.00333 * 60{,}000\ psi\right)}{1{,}000} \\ &= 3{,}441.5\ Kips > 868.26 \therefore OK\end{aligned}$$

Earthquake in Y - direction

$$\begin{aligned}\phi V_n &= \phi A_{cv} * \left(\alpha_c \lambda \sqrt{f'_c} + \rho_t * f_y\right) \\ &= \frac{0.75 * 9{,}424.78\ in^2 * \left(4.54 * 1 * \sqrt{4{,}000\ psi} + 0.00333 * 60{,}000\ psi\right)}{1{,}000} \\ &= 3{,}441.5\ Kips > 2{,}139.54 \therefore OK\end{aligned}$$

Hence, the final wall reinforcement configuration is as follows:

Wall ID	Horizontal Configuration	Vertical Configuration
Plane wall D	#4 @ 16 "	#4 @ 16 "
Curve wall B	#4 @ 16 "	#4 @ 16 "

Step 4: Check if boundary elements (B.E.) are required using Equation 7.17.

A. Plane Wall D

$$\frac{P_u}{A_{cv}} + \frac{M_u * \frac{l_w}{2}}{I_g} < 0.2f'_c \tag{7.17}$$

$$0.2f'_c = 0.2 * 4\ Ksi = 0.8\ Ksi$$

$$\frac{P_u}{A_{cv}} + \frac{M_u * \frac{l_w}{2}}{I_g} = \frac{1{,}497.4\ Kips}{4{,}800.0\ in^2} + \frac{19{,}914\ Kip - ft * \left(\frac{12\ in}{1\ ft}\right) * \frac{480\ in}{2}}{92.16\ x\ 10^6\ in^4} = 0.84\ Ksi > 0.80\ Ksi$$

$$\therefore\ B.E. required$$

Note: The boundary elements were checked for the designed walls thickness of t_w = 10” where for the case of the plane wall D the resulting stress computed with the Equation 7.17 exceeded the 0.2*f'_c, thus requiring a (B.E.) for this case. Since it was not intended to affect the proposed structural layout with the addition of a (B.E.), the check was accomplished increasing the wall thickness to t_w = 12”. The modification was performed for all the structural walls to maintain a similar lateral force distribution which is affected by the thickness (rigidities) of the walls. It is important to highlight that for the walls design were not considered the circular columns at the ends of each wall nor the rectangular column inside the wall members which certainly would increase the capacity of each wall.

$$\frac{P_u}{A_{cv}} + \frac{M_u * \frac{l_w}{2}}{I_g} = \frac{1{,}497.4\ Kips}{5{,}760.0\ in^2} + \frac{19{,}914\ Kip - ft * \left(\frac{12\ in}{1\ ft}\right) * \frac{480\ in}{2}}{11.06\ x\ 10^7\ in^4} = 0.69\ Ksi < 0.80\ Ksi$$

$$\therefore No\ B.E. required$$

B. Curve Wall B

Earthquake in X - direction

a. Load from convex to concave side of the curve wall

$$\frac{P_u}{A_{cv}} + \frac{M_u}{S} < 0.2f'_c$$

$$\frac{P_u}{A_{cv}} + \frac{M_u}{S} = \frac{1{,}948.2\ Kips}{11{,}309.7\ in^2} + \frac{17{,}398\ Kip - ft * \left(\frac{12\ in}{1\ ft}\right)}{501{,}048{,}98\ in^3} = 0.59\ Ksi < 0.80\ Ksi$$
$$\therefore No\ B.E.required$$

b. Load from concave to convex side of the curve wall

$$\frac{P_u}{A_{cv}} + \frac{M_u}{S} < 0.2f'_c$$

$$\frac{P_u}{A_{cv}} + \frac{M_u}{S} = \frac{1{,}647.5\ Kips}{11{,}309.7\ in^2} + \frac{16{,}915\ Kip - ft * \left(\frac{12\ in}{1\ ft}\right)}{844{,}730.55\ in^3} = 0.39\ Ksi < 0.80\ Ksi$$
$$\therefore No\ B.E.required$$

Earthquake in Y - direction

Note: For earthquake load in Y-direction, the section modulus is the same for both way, due to symmetry around the axis of rotation.

$$\frac{P_u}{A_{cv}} + \frac{M_u}{S} < 0.2f'_c$$

$$\frac{P_u}{A_{cv}} + \frac{M_u}{S} = \frac{2{,}604.2\ Kips}{11{,}309.7\ in^2} + \frac{43{,}756\ Kip - ft * \left(\frac{12\ in}{1\ ft}\right)}{1{,}663{,}209.16\ in^3} = 0.55\ Ksi < 0.8\ Ksi$$
$$\therefore No\ B.E.required$$

Therefore, no boundary elements are required for any of the designed walls when using a wall thickness of t_w = 12”. For a wall with t_w = 12”, the minimum steel reinforcement became 0.36 in^2 per foot of wall, resulting in a configuration presented in the table below.

Wall ID	Horizontal Configuration	Vertical Configuration
Plane wall D	#4 @ 12 "	#4 @ 12 "
Curve wall B	#4 @ 12 "	#4 @ 12 "

7.5.1 Punching Shear Check on Debris Impacted Wall

Equation 7.18 shows the concrete shear capacity of the wall to be impacted which might be compared to the expected debris impact point load of F_i = 527.4 Kip.

$$V_c = 4\sqrt{f_c'}b_o d \tag{7.18}$$

where:

Considering a point load on the wall, the perimeter of the projected area, $b_o = 4d$ (see Figure 7.16 and Figure 7.17 for details),

Clear Cover, $C.C. = 1\ in$, and

$$d = t_w - C.C. - \frac{d_l}{2} = 10\ in - 1\ in - \frac{0.5}{2} = 8.75\ in.$$

$$V_c = 4\sqrt{f_c'} * 4d * d = 4\sqrt{f_c'} * 4d^2 = \frac{4\sqrt{4{,}000\ psi} * 4 * (8.75\ in^2)}{1{,}000} = 77.48\ Kip < 527.4\ Kip$$

Hence, the debris impact force will cause punching shear on the curved wall. Although it might cause local failure of the wall, it do not produce collapse of the entire structural system.

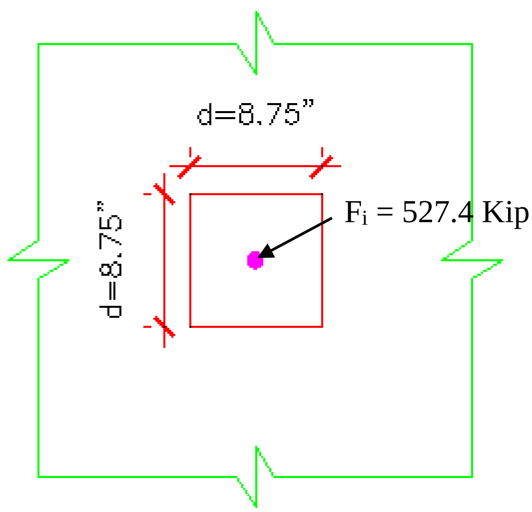

Figure 7.16: Punching shear diagram (plan view)

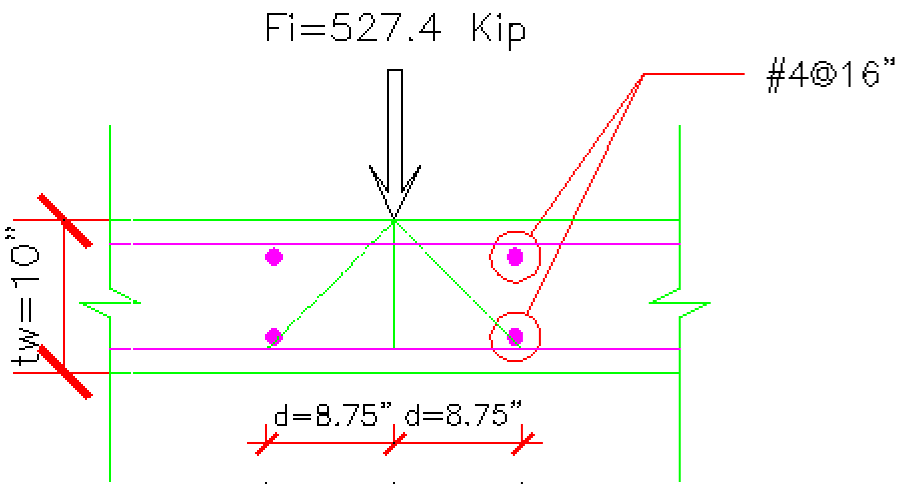

Figure 7.17: Punching shear diagram (section view)

7.6 Exterior Ramp Design

The thickness of the ramp slab is set to be 6 inches. Deflections were computed and met the requirements for service loads as specified by *ACI 318-11*.

A. Wall supported segments

The wall supported ramp segments, are the ramp portion supported by the pier walls in a cantilever mode. Below is presented the design for these segments.

Location	M_u (Kip-ft)	b (in)	d (in)	R_n (Ksi)	ρ	A_s (in^2)	Configuration
Cantilever wall support (Transverse direction)	-3.05	12.00	5.00	0.136	0.00201	0.14	#4@16" (T)
Above ramp supports (Longitudinal direction)	-2.20	12.00	4.50	0.121	0.00205	0.12	#4@16" (T)

B. Free segments (No wall supported)

For the segments which are not supported by pier wall members, edge beams of 18" X 8" are proposed to distribute the load in a one way direction on these two simply supported beams. According to the model results the beams and ramp slab design are presented below.

Beam ID	h (in)	b_w (in)	d = h - 2.5 (in)	Moment Sign	M_u (Kips-ft) from ETABS	R_n (Ksi)	$\rho_{required}$	$A_{s\text{-}Required}$ (in^2)	Config.
Ramp Beams	18	8	15.5	(+)	20.19	0.042	0.00333	0.41	2#5
				(-)	28.29	0.058	0.00333	0.41	2#5

Direction	M_u (Kip-ft)	b (in)	d (in)	R_n (Ksi)	ρ	A_s (in^2)	Configuration
Transverse direction	0.70	12.00	5.00	0.031	0.00180	0.11	#3@12" (B)
Longitudinal direction	0.00	12.00	4.50	0.00	0.00180	0.10	#3@12" (B)

The transverse reinforcement of the simply supported beams resulted in a configuration of #3 @ 6". The drawings and details are provided in Appendix C.

7.7 Displacements and inter-story drifts results

In Figure 7.18 and Figure 7.19 are shown the building displacement curves in X and Y directions for both tsunami load and earthquake load combinations. From these results it is observed how the displacement magnitudes increases as the story level increases for all the lateral load combinations in the X-direction and in the Y-direction. It is noticed that for the earthquake load combinations which contains a negative earthquake term, the lateral displacements resulted with negative values. The maximum displacement in the X-direction for tsunami load combinations was 0.01 inches, while for the earthquake load combinations, were 0.091 inches for the positive direction and 0.093 inches for the negative direction.

The tsunami displacements in the Y-direction resulted in negative values, since the tsunami loads established in the structural model were assigned acting in the negative Y-direction (see Figure 7.19). The maximum displacement for tsunami load combinations was 0.002 inches, while for the earthquake load combinations, were 0.155 inches for the positive direction and 0.157 inches for the negative direction. By comparing the displacement magnitudes produced by tsunami load combinations and earthquake load combinations it is evident that seismic loads governs the design due to low tsunami load effects in the area.

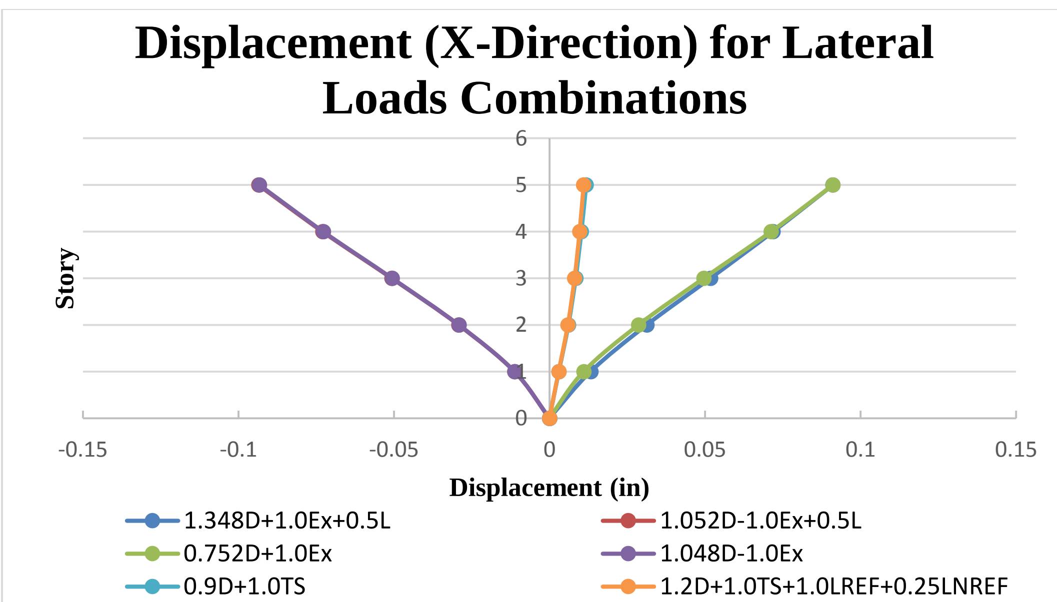

Figure 7.18: Building displacement per story in X-direction for lateral loads combinations

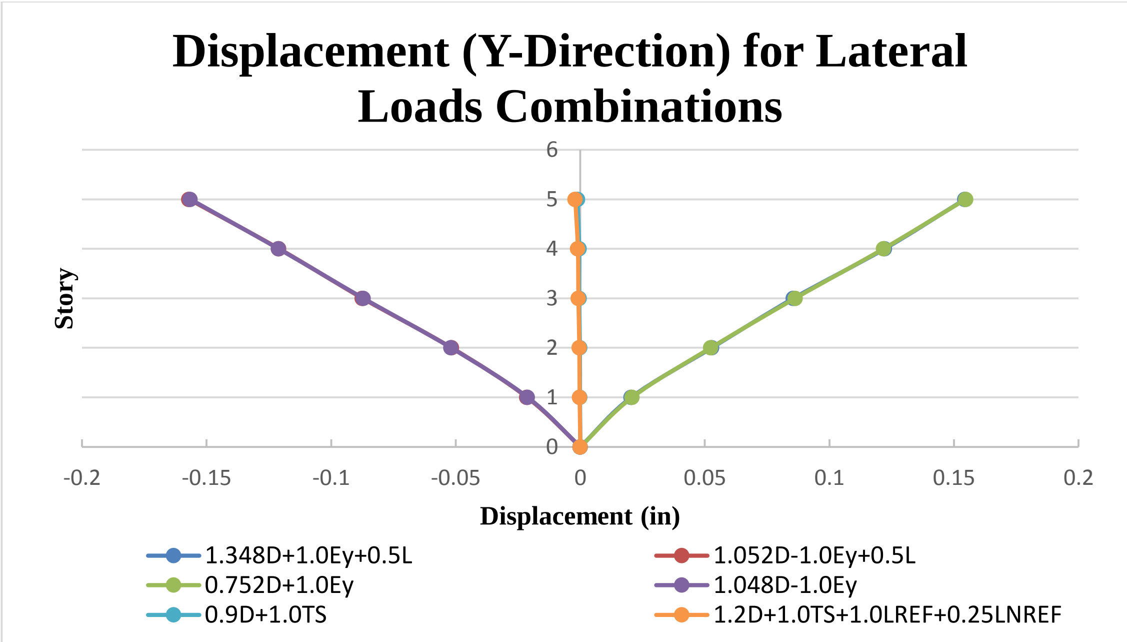

Figure 7.19: Building displacement per story in Y-direction for lateral loads combinations

In Figure 7.20 and Figure 7.21 are shown the inter-story drifts curves in X and Y directions for both tsunami load and earthquake load combinations. From these results it is observed how the lower levels experiences higher drifts for tsunami loads combinations. This was to be expected, since tsunami loads are acting in the first two stories for this particular case. The drifts in the X-direction, range from $1.2x10^{-5}$ to $1.1x10^{-4}$ along the building height, while for the Y-direction, range from $6.0x10^{-6}$ to $3.5x10^{-5}$. This variation of drifts magnitudes amongst both direction is obtained, since most of the tsunami loads defined in the model were acting in X-direction.

On the other hand, the results for the earthquake loads combinations, it is noticed the increase of story drifts while increasing the story level. Drifts magnitudes ranging from $9x10^{-5}$ to $1.9x10^{-4}$ for X-direction while $1.5x10^{-4}$ to $2.6x10^{-4}$ for Y-direction, certainly higher than produced by tsunami loads combinations.

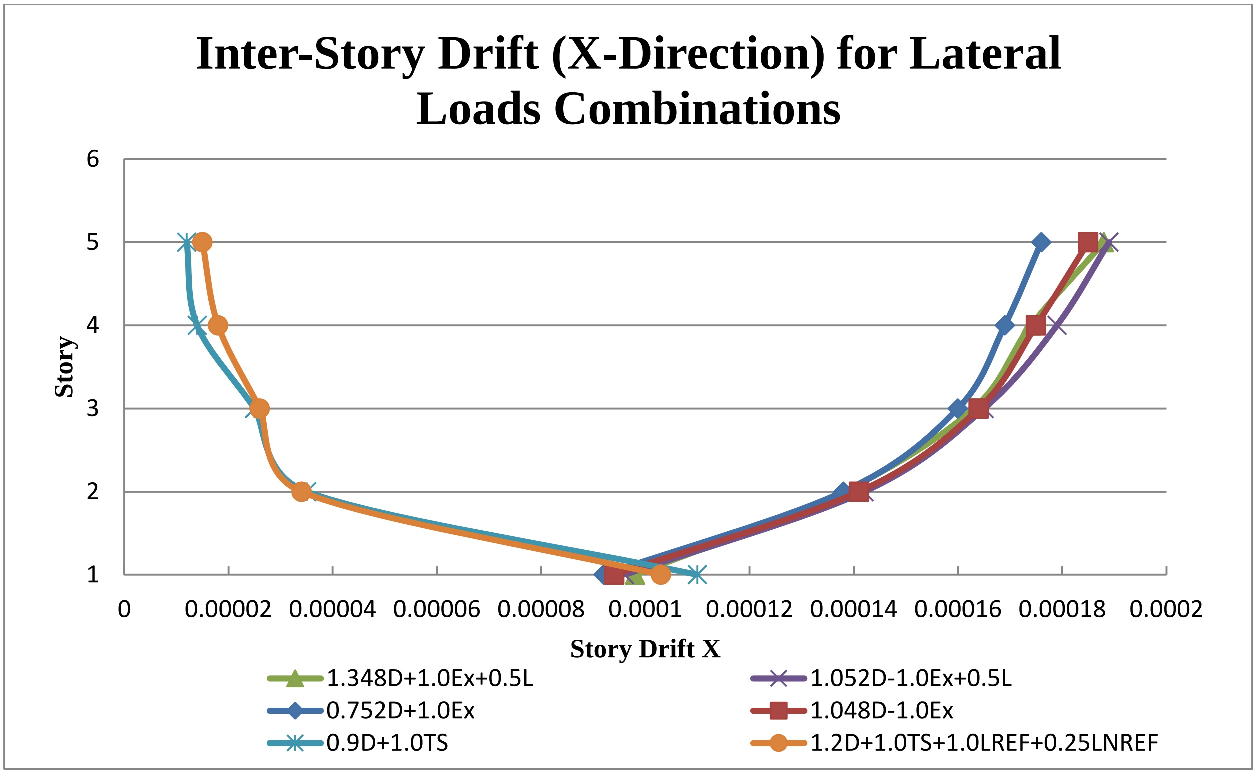

Figure 7.20: Story drift values in X-direction for lateral loads combinations.

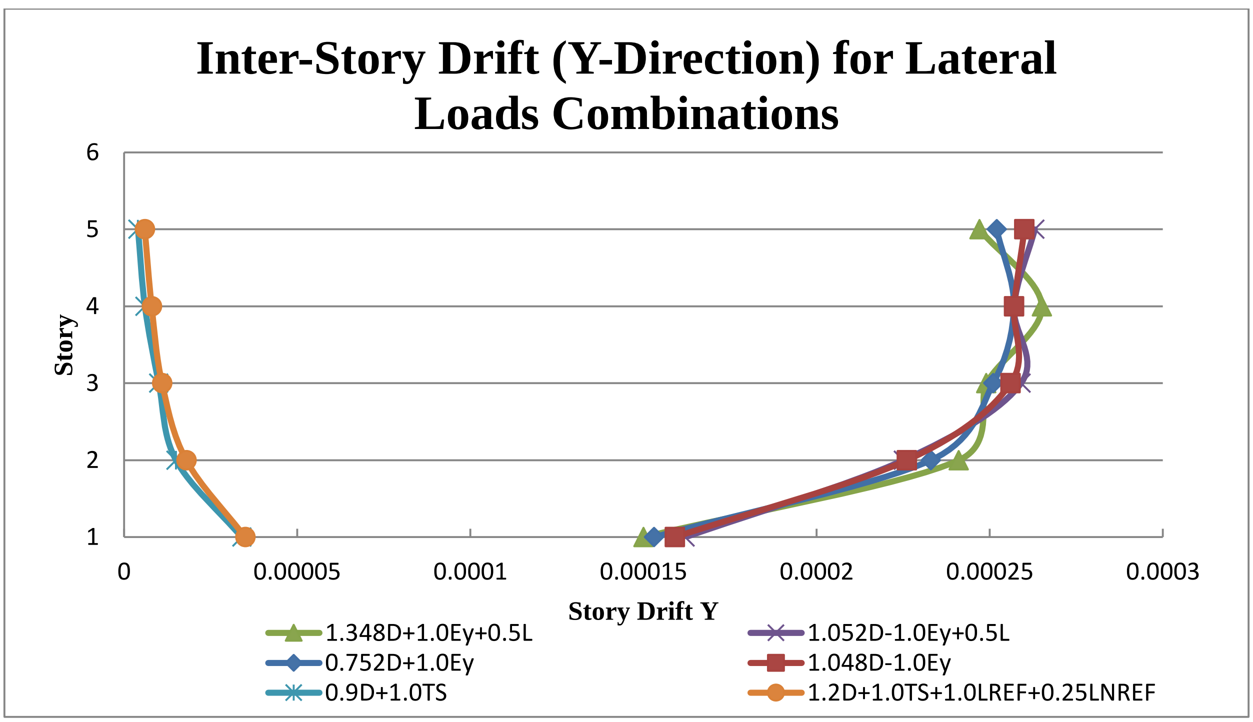

Figure 7.21: Story drift values in Y-direction for lateral loads combinations.

7.8 Foundation Design Recommendations

According to previous observations, scour around shallow foundations can lead to failure of the supported structural elements. Thus, deep foundations with tensile capacity should be the option to found a vertical evacuation structure. Nevertheless, the resulting design must be able to withstand the tsunami effects after scouring has exposed the pile cap and the top of piles.

In Table 7.11, the suggestions from Dames and Moore (1980) that relate scour depth to distance from shoreline and soil type are presented. According the subsurface explorations log in Appendix A, (Advanced Soil Engineering, 2007) near the site of interest, yellowish brown silty clay limestone fragments some sand, extends to depths varying from 0.0 to 18.0.

Recalling that:

$h_{max} = 21.92\ ft$,

$D_h = 2{,}250\ ft$ (Shoreline distance from the site of interest) > 300 ft,

and assuming a soft clay as soil type, scour depths of approximately 15% of the predicted inundation depth at the site could be experienced.

$$Scour_{depth} = 0.15 * 21.92\ ft = 3.30\ ft$$

Table 7.11: Approximate scour depth as a percentage of the maximum flow depth, h_{max} (FEMA P-646, 2012).

Soil Type	Scour depth (% of h_{max}) (Shoreline Distance < 300 feet)	Scour depth (% of h_{max}) (Shoreline Distance > 300 feet)
Loose sand	80	60
Dense sand	50	35
Soft silt	50	25
Stiff silt	25	15
Soft clay	25	15
Stiff clay	10	5

A possible solution to avoid the effects of scour, could be to provide a foundation protection system. This system could consist of a concrete mat around the structure ground surface with the idea of avoiding the erosion and consequent scour of the building foundations. Although in this work foundations were not designed, in Appendix C, a plan and elevation drawings shows the suggested foundation ideas.

7.9 Cost Estimate Analysis

A rough cost estimate based on the square footage quantities was performed. The unit price for a square foot of construction was set to $250.00.

Story	Quantity	Unit	Unit Price	Total Cost
Base	6,971.29	SF	$ 250.00	$ 1,742,821.35
1	6,971.29	SF	$ 250.00	$ 1,742,821.35
2	6,971.29	SF	$ 250.00	$ 1,742,821.35
3	6,971.29	SF	$ 250.00	$ 1,742,821.35
4	6,971.29	SF	$ 250.00	$ 1,742,821.35
5 / Top Roof	6,971.29	SF	$ 250.00	$ 1,742,821.35
Staircase/Elevator Core Roof	444.00	SF	$ 250.00	$ 111,000.00
			Total	$ 10,567,928.11

By doing this simplified cost estimate, is provided an idea of the cost of the vertical evacuation structure without considering the foundations cost.

CHAPTER 8 - SUMMARY, CONCLUSIONS, AND FUTURE WORK

8.1 Summary

After the disasters caused by the Ocean Indian Tsunami (2004) and Tohoku Tsunami (2011), the society is much more aware of the necessity to have available vertical evacuation structures from tsunamis. This situation has highlighted the need to incorporate the tsunami-resistant design in the building codes. For this reason, federal agencies and the academic sector have joined efforts to produce design guidelines such as FEMA P-646, to eventually incorporate them in future building codes. This study focused on the design of a reinforced concrete tsunami-resistant building to serve as a vertical evacuation structure for Bo. Espinal-Aguada, PR, using the guidelines of FEMA P-646. Particular site data including, demographic information, tsunami risk evaluations, tsunami design hydrodynamic parameters, and FEMA P-646 tsunami load calculation provisions were required to perform the vertical evacuation structure design in this research work.

8.2 Conclusions

- Hydrodynamic parameters for tsunami-resistant design such as maximum inundation depth, maximum flow velocity, and maximum momentum flux, were determined for the site of interest in Bo. Epinal-Aguada, with aids of the tsunami numerical simulation performed by Mercado et al. (2011). Tsunami loads were computed using the guidelines in FEMA P-646 provisions.
- Based on the Puerto Rico 2010 Census data, different uses for the designed vertical evacuation structure when not serving as refuge were suggested. For instance, it can also serve as a children club, electronic library, assembly room, and a fitness center.

- A structural layout was proposed taking into consideration several alternatives to quickly move up to the refuge area little more than 85% of the residents.
- Exterior columns were avoided to reduce the possibility of progressive collapse. In lieu of them, reinforced concrete shear walls were supplied at the perimeter of the structure. Other attributes of tsunami-resistant structures defined by FEMA P-646 were adopted.
- Since the computed hydrodynamic parameters of the tsunami were relative low for this particular area, the design was governed by the earthquake load combinations in all the structural members. However, the slab system was designed against the uplift effects from tsunami for the first two stories.
- Building displacement and inter-story drift curves were developed to compare the structure behavior due to tsunami and earthquake loads separately. The seismic loads resulted in higher displacement and higher drift values for this particular case.
- A vertical evacuation building was designed taking into consideration dead loads, live loads, earthquake loads, and tsunami loads according to the current codes criteria and considerations to provide an alternative evacuation solution for the Bo. Espinal-Aguada coastal community. Nevertheless, the present work could be considered as a methodology for the design of vertical evacuation structures in high risk coastal communities around the island of Puerto Rico.
- Suggested ideas to protect deep foundations from scouring were presented and a rough cost estimate of the structural components for the vertical evacuation structure was computed.

8.3 Future Work

The results of this study have some limitations due to some assumptions and simplifications. Further studies should focus on:

- Determination of drag coefficients and hydrodynamic uplift coefficient for specific building layouts.
- Evaluate the effects of aftershocks while the building is subjected to tsunami loads at the same time.
- Perform a time history analysis of the designed building using specific earthquake

records for the site in analysis.

- Perform an in site soil study to determine the type of soil and if it can be liquefied.
- Foundations should be designed according to the accepted practice in the field of soil mechanics and foundation engineering.

8.4 References

ACI Committee 318, 2011, "Building Code Requirements for Structural Concrete and Commentary," ACI 318-11, American Concrete Institute, 503 pages.

ACI, 2004, "ACI Detailing Manual-2004," SP-66(04), American Concrete Institute, 219 pages.

ASCE, 2010, "Minimum Design Loads for Buildings and Other Structures," ASCE/SEI 7-10, American Society of Civil Engineers. May 2010.

CRIM, 2014, "Portal de Catastro Digital," Centro de Recaudación de Ingresos Municipales-Oficina del Catastro Digital de Puerto Rico website: http://www.satasgis.crimpr.net/flexviewers/cdpr_crim/. Retrieved on September 14, 2014.

CSI, 2004, "Analysis and Design of Reinforced Concrete Columns," CSI Column, Version 8.2.2, Computers and Structures, Inc.

CSI, 2010, "Extended Three Dimensional Analysis of Building Systems," ETABS, Nonlinear Version 9.7.2, Computers and Structures, Inc.

CSI, 2010, "Slab Analysis by the Finite Element Method," SAFE, Standard Version 12.3.1, Computers and Structures, Inc.

Dames & Moore, 1980, "Design and Construction Standards for Residential Construction in Tsunami-Prone Areas in Hawaii," prepared for the Federal Emergency Management Agency, Washington D.C.

DA & DAF, 1994, "Planning and Design of Roads, Airfields, and Heliports in the Theater of Operations-Airfield and Heliport Design," FM 5-430-00-2 / AFJPAM 32-8013, Vol II, Headquarters, Department of the Army & Department of the Air Force, Washington, D.C., 539 pages.

Dudley, W.C., and Lee, M., "Tsunami," 2nd ed. Honolulu: University of Hawaii Press, 1998.

FEMA, 2012, "Guidelines for Design of Structures for Vertical Evacuation from Tsunamis," FEMA P-646, Second Edition, Federal Emergency Management Agency, Washington, D.C., 180 pages.

Fraser, S., Leonard, G.S., Matsuo, I., and Murakami, H., 2012, “Tsunami Evacuation: Lessons from the Great East Japan earthquake and tsunami of March 11th 2011,” GNS Science Report 2012/17, Institute of Geological and Nuclear Sciences, Wellington, New Zealand, 89 pages.

Heintz, J.A., and Mahoney, M., 2009, “Guidelines for Design of Structures for Vertical Evacuation from Tsunamis,” Applied Technology Council, Redwood City, California, and Federal Emergency Management Agency, Washington, D.C., 8 pages.

Lander, J.F., and Lockridge, P.A., 1989, "United States Tsunamis (Including United States Possessions) 1690-1988," Boulder: National Geophysical Data Center.

López, A., M., Horrillo, J., Pampell, A., Huérfano, V., and Mercado, A., 2014, " Advanced Tsunami Numerical Simulations and Energy Considerations by use of 3D-2D Coupled Models: The October 11, 1918 Mona Passage Tsunami," Pure and Applied Geophysics, 18 pages.

Martínez, J.A., 2012, "Determinación de las Comunidades con Necesidad de Desalojo Vertical en Aguada, PR; Rutas de Desalojo y Señalización," Workshop on Vertical Evacuation in Tsunami Prone Areas 2012-06, College of Engineers and Land Surveyors of Puerto Rico Headquarter, San Juan, Puerto Rico, 41 slides.

Mercado, A., 2011, “Puerto Rico NTHMP Tsunami Flood Map – Maximum of the Maximums: Local Sources,” NOAA-MOST model, University of Puerto Rico at Mayaguez, Department of Marine Sciences, Puerto Rico Seismic Network website: http://redsismica.uprm.edu/Spanish/desalojovertical/docs/Aurelio_Mercado_Puerto_Rico_NTHMP_mapping.pdf. Retrieved on November 12, 2013.

Mercado, A., 2012, "Tsunami Flood Map Development for Puerto Rico," Workshop on Vertical Evacuation in Tsunami Prone Areas 2012-06, College of Engineers and Land Surveyors of Puerto Rico Headquarter, San Juan, Puerto Rico, 39 slides.

Muñoz, N., 2007, "Preliminary Geotechnical Exploration Performed at the Site of the Proposed Discovery Bay Resort & Marina," File No. 1061, Advanced Soil Engineering, 102 pages.

NOAA & PMEL, 2006, “Method of Splitting Tsunami (MOST) Software Manual,” Software Manual, National Oceanographic and Atmospheric Administration and Pacific Marine Environmental Laboratory, Seattle, Washington, 108 pages.

Pacheco, K.H., and Robertson, I.N., 2005, "Evaluation of Tsunami Loads and their Effect on Reinforced Concrete Building," Research Report UHM/CEE 2005-05, University of Hawaii at Manoa, College of Engineering, Honolulu, Hawaii, 209 pages.

Reid, Fielding, H., and Taber, S., "The Porto Rico Earthquake of 1918--With Descriptions of Earlier Earthquakes," Report of the Earthquake Investigation Commission, United States House of Representatives Document No. 269, Government Printing Office, Washington D.C., 1919b.

Robertson, I.N., 2012, "Current Tsunami Design Guidance in the United States - FEMA P-646," Conference Paper 2012-12, 14th U.S.-Japan Workshop on the Improvement of Structural Design and Construction Practices, Maui, Hawaii, 9 pages.

Segarra, R., 2009, "Hydrology and Hydraulics, Detail Project Report, Environmental Impact Assesment: Levee System along the Caño de Madre Vieja Area for Discovery Bay Resort and Marina Development, Rio Culebrinas at Aguadilla and Aguada, Puerto Rico," 43 pages.

USC, 2005, "Tsunamis from Puerto Rico and the Virgin Islands," 1967 Virgin Islands and 1918 Puerto Rico, University of Southern California, Tsunami Research Center website. https://www.usc.edu/dept/tsunamis/caribbean/webpages/index.html. Retrieved on March 24, 2014.

USCB, 2012, "2010 Census of Population and Housing," Population and Housing Unit Counts, CPH-2-53, Puerto Rico, U.S. Government Printing Office, Washington, D.C., 2012.

Yeh, H., Robertson, I.N., and Preuss, J., 2005, “Development of Design Guidelines for Structures that Serve as Tsunami Vertical Evacuation Sites,” Open File Report 2005-4, Washington Division of Geology and Earth Resources, Olympia, Washington, 40 pages.

APPENDIX - A   SOIL BORING LOG NEAR THE SITE OF INTEREST

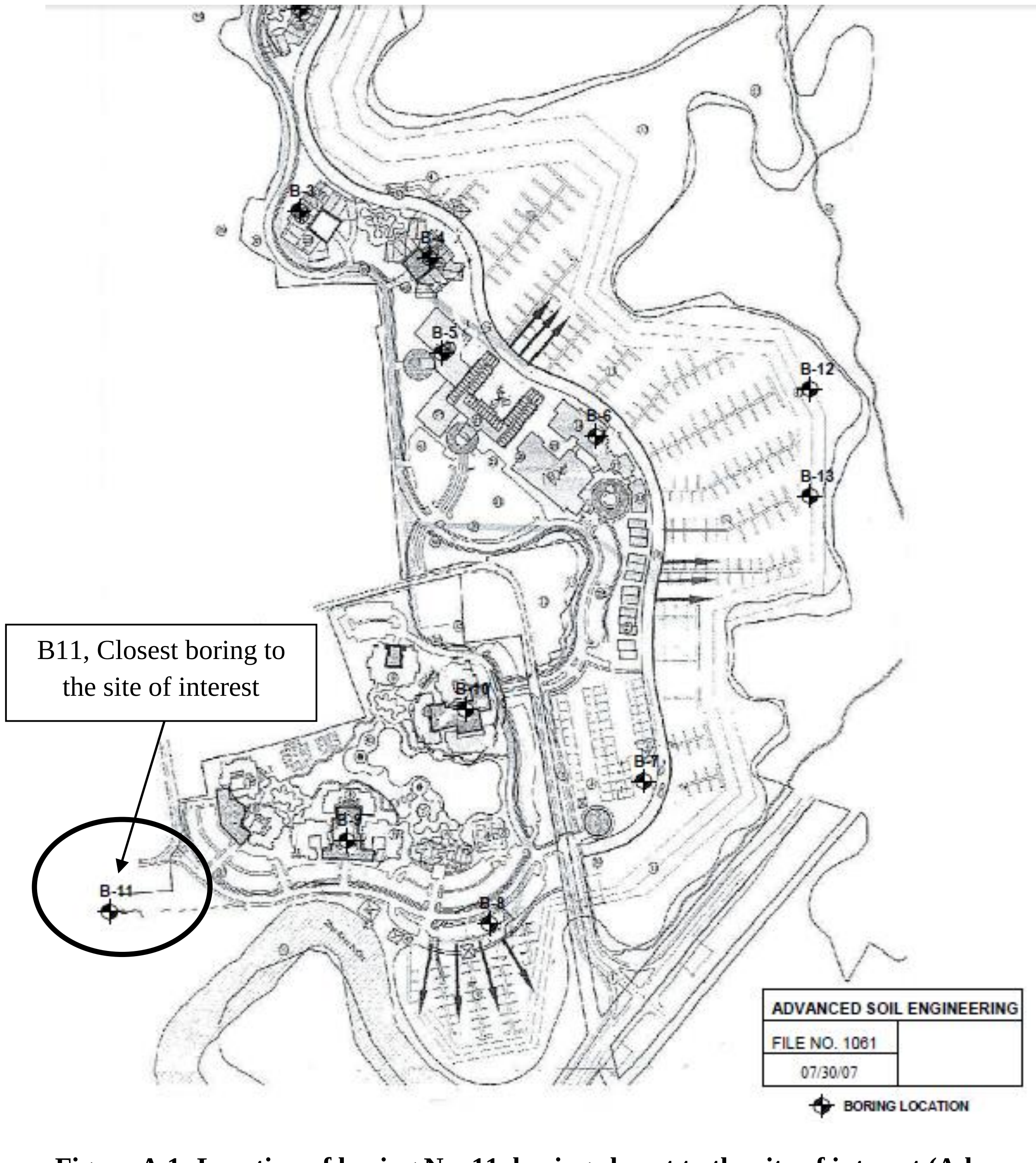

Figure A.1: Location of boring No. 11, boring closest to the site of interest (Advanced Soil Engineering, 2007: *On the Preliminary Geotechnical Exploration Performed at the Site of the Proposed Discovery Bay Resort & Marina, Espinal Ward, Aguada, Puerto Rico*)

Figure A.2: Location of boring No. 11 presented in Figure A.1.

SUBSURFACE EXPLORATION LOG

ASE — ADVANCED SOIL ENGINEERING
P.O. BOX 1206
ISABELA, P.R. 00662
TEL & FAX (787) 830 - 9306

FILE NO. 1061
BORING NO. 11
PAGE 1 OF 2

CLIENT: CORDECO NORTHWEST, CORP.
PROJECT: DISCOVERY BAY RESORT & MARINA
LOCATION: AGUADA, PUERTO RICO
GROUND ELEVATION:
DATE STARTED: 06/19/07
DATE FINISH: 06/19/07
GROUND WATER DEPTH: 12.0 FT.

DRILLER: M. RASUK
LAB. TECH: E. RODRIGUEZ
BORING TYPE: AUGER
BORING DIAMETER: 4"

DEPTH (FT)	SAMPLER	SAMPLE NO	BLOWS / 6"	SPT N VALUE	SYMBOL	VISUAL - MANUAL DESCRIPTION	USCS CLASS	W (%)	Qu	Qp	γ	ϕ	LL	PI
		SS-1	1 - 2 - 3	5		Yellowish brown silty clay some limestone fragments trace sand		13						
		SS-2	10 - 7 - 8	15		As above.		15						
5		SS-3	2 - 6 - 2	8		As above.		20						
		SS-4	1 - 1 - 1	2		As above.		19						
10		SS-6	WH - 1 - 1	2		As above.		27						
15		SS-6	WH - 1 - 2	3		As above. (FILL)		23						
20		SS-7	2 - 1 - 2	3		Light brown sand trace silt		20						
25		SS-8	2 - 3 - 2	5		As above.		21						
30		SS-9	3 - 2 - 2	4		Light brown and gray silty clay trace sand	CH	26					60.5	35.0
35		SS-10	2 - 2 - 3	5		As above.		37						

continue

N = BLOWS DELIVERED PER FOOT BY A 140 LB. HAMMER FALLING 30 INCHES
W = NATURAL MOISTURE CONTENT - %
Qu = UNCONFINED COMPRESSIVE STRENGTH - T.S.F.
Qp = CALIBRATED PENETROMETER READING - T.S.F.
WH = WEIGHT OF HAMMER
SYMBOL (SEE APPENDIX NO. 4 FOR MORE DETAILS)
γ = ESTIMATED UNIT WEIGHT - P.C.F.
ϕ = ANGLE OF INTERNAL FRICTION - DEGREES
LL = LIQUID LIMIT
PI = PLASTICITY INDEX
(*) ELEVATIONS TAKEN FROM PLANS PREPARED BY DESIGNER

Figure A.3: Subsurface exploration log of boring No. 11-1 (Advanced Soil Engineering, 2007: ***On the Preliminary Geotechnical Exploration Performed at the Site of the Proposed Discovery Bay Resort & Marina, Espinal Ward, Aguada, Puerto Rico*****)**

SUBSURFACE EXPLORATION LOG

ADVANCED SOIL ENGINEERING
P.O. BOX 1286
ISABELA, P.R. 00662
TEL & FAX: (787) 830 - 0366

FILE NO. 1061
BORING NO. 11
PAGE 2 OF 2

CLIENT:	CORDECO NORTHWEST, CORP.		
PROJECT:	DISCOVERY BAY RESORT & MARINA		
LOCATION:	AGUADA, PUERTO RICO		
GROUND ELEVATION:		DRILLER:	M. RASUK
DATE STARTED:	06/19/07	LAB. TECH:	E. RODRIGUEZ
DATE FINISH:	06/19/07	BORING TYPE:	AUGER
GROUND WATER DEPTH:	12.0 FT.	BORING DIAMETER:	4"

DEPTH (FT)	SAMPLER	SAMPLE NO	BLOWS / 6"	SPT N VALUE	SYMBOL	VISUAL - MANUAL DESCRIPTION	USCS CLASS	W (%)	Qu	Qp	γ	φ	LL	PI
						Light brown and gray silty clay trace sand								
40		SS-11	3 - 3 - 2	5		As above.		33						
						END OF BORING								
45														
50														
55														
60														
65														
70														

N = BLOWS DELIVERED PER FOOT BY A 140 LB. HAMMER FALLING 30 INCHES
W = NATURAL MOISTURE CONTENT - %
Qu = UNCONFINED COMPRESSIVE STRENGTH - T.S.F.
Qp = CALIBRATED PENETROMETER READING - T.S.F.
WH = WEIGHT OF HAMMER
SYMBOL (SEE APPENDIX NO-I FOR MORE DETAILS)
γ = ESTIMATED UNIT WEIGHT - P.C.F.
φ = ANGLE OF INTERNAL FRICTION - DEGREES
LL = LIQUID LIMIT
PI = PLASTICITY INDEX
(*) ELEVATIONS TAKEN FROM PLANS PREPARED BY DESIGNER

Figure A.4: Subsurface exploration log of boring No. 11-2 (Advanced Soil Engineering, 2007: *On the Preliminary Geotechnical Exploration Performed at the Site of the Proposed Discovery Bay Resort & Marina, Espinal Ward, Aguada, Puerto Rico*)

APPENDIX - B *ASCE7-10* REFERENCE TABLES, FIGURES, AND EQUATIONS

Table B.1: Occupancy category of buildings and other structures for flood, wind, snow, earthquake and ice loads.

Nature of Occupancy	Occupancy Category
Buildings and other structures that represent a low hazard to human life in the event of failure, including, but not limited to: • Agricultural facilities • Certain temporary facilities • Minor storage facilities	I
All buildings and other structures except those listed in Occupancy Categories I, III, and IV	II
Buildings and other structures that represent a substantial hazard to human life in the event of failure, including, but not limited to: • Buildings and other structures where more than 300 people congregate in one area • Buildings and other structures with daycare facilities with a capacity greater than 150 • Buildings and other structures with elementary school or secondary school facilities with a capacity greater than 250 • Buildings and other structures with a capacity greater than 500 for colleges or adult education facilities • Health care facilities with a capacity of 50 or more resident patients, but not having surgery or emergency treatment facilities • Jails and detention facilities Buildings and other structures, not included in Occupancy Category IV, with potential to cause a substantial economic impact and/or mass disruption of day-to-day civilian life in the event of failure, including, but not limited to: • Power generating stations[a] • Water treatment facilities • Sewage treatment facilities • Telecommunication centers Buildings and other structures not included in Occupancy Category IV (including, but not limited to, facilities that manufacture, process, handle, store, use, or dispose of such substances as hazardous fuels, hazardous chemicals, hazardous waste, or explosives) containing sufficient quantities of toxic or explosive substances to be dangerous to the public if released. Buildings and other structures containing toxic or explosive substances shall be eligible for classification as Occupancy Category II structures if it can be demonstrated to the satisfaction of the authority having jurisdiction by a hazard assessment as described in Section 1.5.2 that a release of the toxic or explosive substances does not pose a threat to the public.	III
Buildings and other structures designated as essential facilities, including, but not limited to: • Hospitals and other health care facilities having surgery or emergency treatment facilities • Fire, rescue, ambulance, and police stations and emergency vehicle garages • Designated earthquake, hurricane, or other emergency shelters • Designated emergency preparedness, communication, and operation centers and other facilities required for emergency response • Power generating stations and other public utility facilities required in an emergency • Ancillary structures (including, but not limited to, communication towers, fuel storage tanks, cooling towers, electrical substation structures, fire water storage tanks or other structures housing or supporting water, or other fire-suppression material or equipment) required for operation of Occupancy Category IV structures during an emergency • Aviation control towers, air traffic control centers, and emergency aircraft hangars • Water storage facilities and pump structures required to maintain water pressure for fire suppression • Buildings and other structures having critical national defense functions Buildings and other structures (including, but not limited to, facilities that manufacture, process, handle, store, use, or dispose of such substances as hazardous fuels, hazardous chemicals, or hazardous waste) containing highly toxic substances where the quantity of the material exceeds a threshold quantity established by the authority having jurisdiction. Buildings and other structures containing highly toxic substances shall be eligible for classification as Occupancy Category II structures if it can be demonstrated to the satisfaction of the authority having jurisdiction by a hazard assessment as described in Section 1.5.2 that a release of the highly toxic substances does not pose a threat to the public. This reduced classification shall not be permitted if the buildings or other structures also function as essential facilities.	IV

A. Wind Loads

The procedure used in the determination of the wind loads was the analytical method described in *ASCE7-10*.

The velocity pressure evaluated at height z above ground in lb/ft^2 is given by,

$$q_z = 0.00256 K_z K_{zt} K_d V^2 I \qquad B.1$$

The velocity pressure evaluated at height $z = h$ above ground in lb/ft^2 is given by,

$$q_h = 0.00256 K_h K_{zt} K_d V^2 I \qquad B.2$$

where:

K_z = velocity pressure exposure coefficient evaluated at height z, defined in Table B.2,

K_z = velocity pressure exposure coefficient evaluated at height $z = h$, defined in Table B.2,

K_{zt} = topographic factor, defined in *ASCE7-10: Section 6.5.7*. In sites where no hills, ridges, or escarpments are found, K_{zt} =1,

K_d = wind directionality factor, defined in Table B.3. According to *ASCE7-10: Section 6.5.6.3*, Exposure category C shall apply for this particular case,

V = basic wind speed (mph), defined in Figure B.1, and

I = importance factor, defined in Table B.4.

To compute the velocity pressure Equation B.1 and B.2 were used. Since the earthquake lateral load are expected to be higher than lateral wind loads, the wind loads analysis described in this procedure will take conservative values. For instance the velocity pressure, q_h is assumed to act along the entire building height for the windward wall surface. According to Table B.2, for a height of 69 ft, a K_h = 1.17 shall be used. Since the site of interest do not include hills, ridges nor escarpments, a topographic factor of K_{zt} = 1 was implemented. Since the structure to be analyzed is a building, the wind directionality factor was taken from Table B.3 as K_d = 0.85. According to the ASCE7-10, for occupancy category IV in Puerto Rico, a basic wind speed of 180 mph shall be considered with an importance factor of 1.15 (See Figure B.1 and Table B.4 respectively).

Table B.2: Velocity pressure exposure coefficients, K_h and K_z

Height above ground level, z		Exposure (Note 1)			
		B		C	D
ft	(m)	Case 1	Case 2	Cases 1 & 2	Cases 1 & 2
0-15	(0-4.6)	0.70	0.57	0.85	1.03
20	(6.1)	0.70	0.62	0.90	1.08
25	(7.6)	0.70	0.66	0.94	1.12
30	(9.1)	0.70	0.70	0.98	1.16
40	(12.2)	0.76	0.76	1.04	1.22
50	(15.2)	0.81	0.81	1.09	1.27
60	(18)	0.85	0.85	1.13	1.31
70	(21.3)	0.89	0.89	1.17	1.34

Table B.3: Wind directionality factor, K_d

Structure Type	Directionality Factor K_d*
Buildings	
Main Wind Force Resisting System	0.85
Components and Cladding	0.85
Arched Roofs	0.85
Chimneys, Tanks, and Similar Structures	
Square	0.90
Hexagonal	0.95
Round	0.95
Solid Signs	0.85
Open Signs and Lattice Framework	0.85
Trussed Towers	
Triangular, square, rectangular	0.85
All other cross sections	0.95

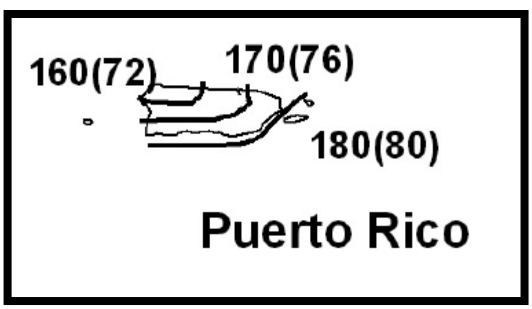

Figure B.1: Basic wind speeds for occupancy category III and IV buildings and other structures.

Table B.4: Importance factor, I for wind loads.

Category	Non-Hurricane Prone Regions and Hurricane Prone Regions with V = 85-100 mph and Alaska	Hurricane Prone Regions with V > 100 mph
I	0.87	0.77
II	1.00	1.00
III	1.15	1.15
IV	1.15	1.15

By using the corresponding values to determine the velocity pressure at a height, h, it resulted in:

$$q = q_h = 0.00256 * 1.17 * 1 * 0.85 * (180\,mph)^2 * 1.15 = 94.86\,psf$$

The design pressure to be used in determination of wind loads for buildings, in lb/ft^2 is given by,

$$p = qGC_p - q_i(GC_{pi}) \qquad B.3$$

where:

$q = q_z$ for windward walls pressures evaluated at height z above the ground ($q = q_h$, to be conservative),

$q = q_h$ for leeward walls, side walls, and roof pressures evaluated at total height of the building, h,

G = gust effect factor (G = 0.85 for rigid structures, T < 1 sec.),

C_p = external pressure coefficient, defined in Table B.5,

$q_i = q_h$, for positive internal pressure conservatively evaluated at height h, and

(GC_{pi}) = product of internal pressure coefficient and gust effect factor to be used in determination of wind loads for buildings, defined in Table B.6.

For rigid structures with a natural period lower than 0.5 s, a gust factor of G = 0.85 could be used. From Table B.5, and external pressure coefficient C_p = 0.8 for windward surface wall. To be conservative, the total wind force will be computed for the worst case where the windward and leeward surfaces are L = 130 ft, and side wall is B = 50 ft. Therefore, for an L/B ratio of 0.38, the external pressure coefficient C_p = -0.5 for the leeward surface wall was taken. As the building is considered to be an enclosed building, the internal pressure coefficient GC_{pi} = ± 18 (See Table B.6).

Table B.5: External pressure coefficients, C_p

Wall Pressure Coefficients, C_p			
Surface	**L/B**	**C_p**	**Use With**
Windward Wall	All values	0.8	q_z
Leeward Wall	0-1	-0.5	q_h
	2	-0.3	
	≥4	-0.2	
Side Wall	All values	-0.7	q_h

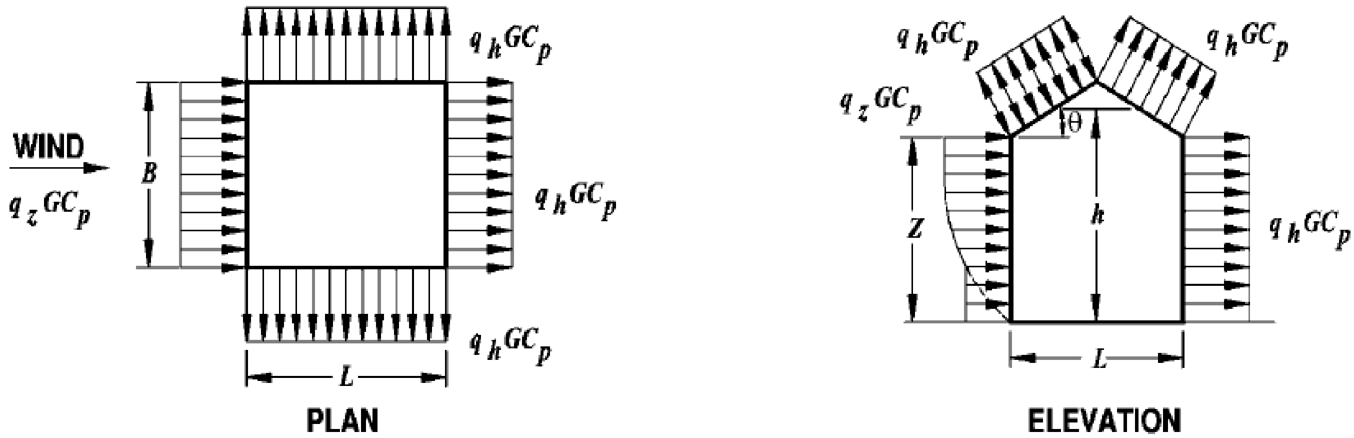

Figure B.2: Wind pressures diagram

Table B.6: Internal pressure coefficient, GC_{pi}

Enclosure Classification	GC_{pi}
Open Buildings	0.00
Partially Enclosed Buildings	+0.55 -0.55
Enclosed Buildings	+0.18 -0.18

The computations for the combination of windward and leeward with positive and negative internal pressures are presented below.

Windward: (positive internal pressure):

$$p = qGC_p - q_i(GC_{pi}) = q_hGC_p - q_h(GC_{pi}) = 94.86\,psf * (0.85 * (+0.8) - (+0.18))$$
$$= 47.43\,psf$$

Leeward: (positive internal pressure):

$$p = qGC_p - q_i(GC_{pi}) = q_hGC_p - q_h(GC_{pi}) = 94.86\,psf * (0.85 * (-0.5) - (+0.18))$$
$$= -57.39\,psf$$

Windward: (negative internal pressure):

$$p = qGC_p - q_i(GC_{pi}) = q_hGC_p - q_h(GC_{pi}) = 94.86\,psf * (0.85 * (+0.8) - (-0.18))$$
$$= 81.58\,psf$$

Leeward: (negative internal pressure):

$$p = qGC_p - q_i(GC_{pi}) = q_hGC_p - q_h(GC_{pi}) = 94.86\,psf * (0.85 * (-0.5) - (-0.18))$$
$$= -23.24\,psf$$

The wind pressure diagrams considering positive and negative internal pressures are shown in Figure B.3 and Figure B.4 respectively.

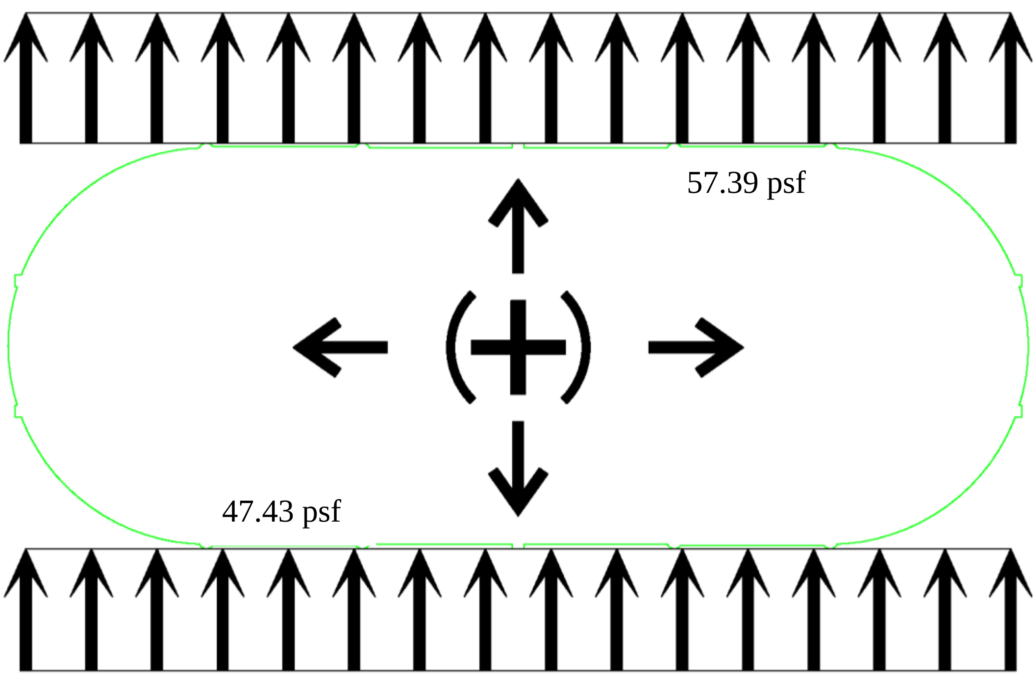

Figure B.3: Wind pressure diagram for windward and leeward walls considering positive internal pressure.

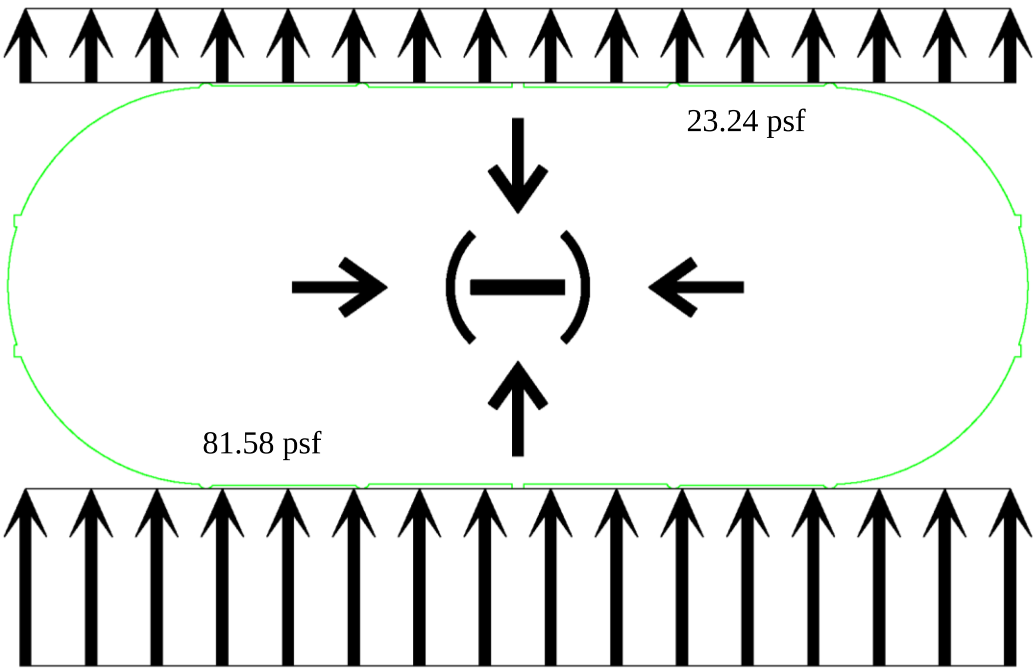

Figure B.4: Wind pressure diagram for windward and leeward walls considering negative internal pressure.

By adding the windward and leeward walls pressures the total pressure magnitude resulted in 104.82 psf. To obtain the total base shear due to wind load, the total pressure magnitude is multiplied to the projected area (windward or leeward walls surface area).

$$V_{base} = p_{net} * A_{wall-surface} = 104.82\,psf * \left(\frac{1Ksf}{1000\,psf}\right) * (130\,ft) * (69\,ft) = 940.2\,Kips$$

The total base shear due to the wind load resulted in 940.2 Kips, which will be eventually compared with the earthquake load base shear.

B. Earthquake Loads

The analytical procedure used to determine the earthquake loading was the equivalent lateral force analysis, which is presented below. For a Risk Category IV building, an importance factor of 1.5 was selected (See Table B.1). From Figure B.5 and Figure B.6, the maximum spectral acceleration for Aguada, PR, are S_s = 1.23 g and S_1 = 0.39 g.

Figure B.5: Spectral response acceleration at period 0.2 seconds, 5% of critical damping, recurrence of 2,475 years (probability of exceedance of 2% in 50 years).

Figure B.6: Spectral response acceleration at period 1.0 seconds, 5% of critical damping, recurrence of 2,475 years (probability of exceedance of 2% in 50 years).

From Section 3.7, the soil type for this area was cataloged as site class E - "soft clay soil". From Table B.8 and Table B.9, the site coefficients F_a and F_v have values of 0.9 and 2.44 respectively. The design spectral accelerations for short periods, S_{DS} and 1 second period, S_{D1}, were computed using Equations B.4 through B.7, resulting in 0.738 g, and 0.634 g respectively. According to Table B.10 and Table B.11, seismic design category D, prevailed for this particular case.

Table B.7: Site classification

Site Class	$\bar{v}_s$	$\bar{N}$ or $\bar{N}_{ch}$	$\bar{s}_u$
A. Hard rock	>5,000 ft/s	NA	NA
B. Rock	2,500 to 5,000 ft/s	NA	NA
C. Very dense soil and soft rock	1,200 to 2,500 ft/s	>50	>2,000 psf
D. Stiff soil	600 to 1,200 ft/s	15 to 50	1,000 to 2,000 psf
E. Soft clay soil	<600 ft/s	<15	<1,000 psf
	Any profile with more than 10 ft of soil having the following characteristics: - Plasticity index PI > 20, - Moisture content $w \geq 40\%$, and - Undrained shear strength $\bar{s}_u < 500$ psf		
F. Soils requiring site response analysis in accordance with Section 21.1	See Section 20.3.1		

Table B.8: Site coefficient, F_a

Site Class	Mapped Maximum Considered Earthquake Spectral Response Acceleration Parameter at Short Period				
	$S_S \leq 0.25$	$S_S = 0.5$	$S_S = 0.75$	$S_S = 1.0$	$S_S \geq 1.25$
A	0.8	0.8	0.8	0.8	0.8
B	1.0	1.0	1.0	1.0	1.0
C	1.2	1.2	1.1	1.0	1.0
D	1.6	1.4	1.2	1.1	1.0
E	2.5	1.7	1.2	0.9	0.9
F	See Section 11.4.7				

NOTE: Use straight-line interpolation for intermediate values of S_S.

Table B.9: Site coefficient, F_v

Site Class	Mapped Maximum Considered Earthquake Spectral Response Acceleration Parameter at 1-s Period				
	$S_1 \leq 0.1$	$S_1 = 0.2$	$S_1 = 0.3$	$S_1 = 0.4$	$S_1 \geq 0.5$
A	0.8	0.8	0.8	0.8	0.8
B	1.0	1.0	1.0	1.0	1.0
C	1.7	1.6	1.5	1.4	1.3
D	2.4	2.0	1.8	1.6	1.5
E	3.5	3.2	2.8	2.4	2.4
F	See Section 11.4.7				

NOTE: Use straight-line interpolation for intermediate values of S_1.

MCE Spectral Response Accelerations for Short Periods (S_{MS}) and at 1 sec. (S_{M1}), adjusted for Site Class Effects.

$$S_{MS} = F_a S_s \tag{B.4}$$

$$S_{M1} = F_v S_1 \tag{B.5}$$

$$S_{MS} = 0.9 * 1.23 = 1.11\ g$$

$$S_{M1} = 2.44 * 0.39 = 0.95\ g$$

Design Earthquake Spectral Response Acceleration Parameter at Short Period, S_{DS}, and at 1 sec. period, S_{D1}.

$$S_{DS} = \frac{2}{3} S_{MS} \tag{B.6}$$

$$S_{D1} = \frac{2}{3} S_{M1} \tag{B.7}$$

$$S_{DS} = \frac{2}{3} * 1.11 = 0.738\ g$$

$$S_{D1} = \frac{2}{3} * 0.95 = 0.634\ g$$

Table B.10: Seismic design category based on short period response acceleration parameter.

Value of S_{DS}	Occupancy Category		
	I or II	III	IV
$S_{DS} < 0.167$	A	A	A
$0.167 \le S_{DS} < 0.33$	B	B	C
$0.33 \le S_{DS} < 0.50$	C	C	D
$0.50 \le S_{DS}$	D	D	D

Table B.11: Seismic design category based on 1-second period response acceleration parameter.

Value of S_{D1}	OCCUPANCY CATEGORY		
	I or II	III	IV
$S_{D1} < 0.067$	A	A	A
$0.067 \le S_{D1} < 0.133$	B	B	C
$0.133 \le S_{D1} < 0.20$	C	C	D
$0.20 \le S_{D1}$	D	D	D

The seismic force-resisting system of the proposed building is a special reinforced concrete shear walls. In Table B.12, is specified a response modification factor of R = 5 for this seismic force-resisting system which for SDC D is permited for a building height up to 160 feet. However, as previously mentioned, it is expected that the refuge structure will survive the earthquake with limited structural and non-structural damage (continuing in service), and have adequate remaining strength to resist all tsunami induced loads. For this reason a system overstrength factor is considered by using a response modification factor of R = 2, even more conservative than the recommended value of 2.5 for this particular structural system. It is important to mention that overstrength factors are hidden in each of the steps for a given design procedure, (i.e., determination of section dimensions and selection of steel reinforcement configurations), where every structural element designed results with higher capacities than what is certainly needed according to the structural analysis. To calculate the fundamental period of the structure Equation B.8 was used, where the values of the parameters C_t and x were obtained from Table B.13, for the "All other structural systems" structure type. The values are C_t = 0.02 and x = 0.75. With these values and the height of the structure from base to the highest level (69 ft), a fundamental period of 0.48 seconds was obtained. The long-period transition period for Puerto Rico fom Figure B.7 has a value of 12 seconds. The seismic response coefficient, C_s, resulted in 0.554, and the total seismic base shear which is given by $V_{base} = C_s * W$, is 3,932.0 Kips.

Table B.12: Design coefficients and factors for seismic force-resisting systems.

Seismic Force–Resisting System	ASCE 7 Section where Detailing Requirements are Specified	Response Modification Coefficient, R^a	System Overstrength Factor, $\Omega_0{}^g$	Deflection Amplification Factor, $C_d{}^b$	Structural System Limitations and Building Height (ft) Limit[c]				
					Seismic Design Category				
					B	C	D[d]	E[d]	F[e]
A. BEARING WALL SYSTEMS									
1. Special reinforced concrete shear walls	14.2 and 14.2.3.6	5	2½	5	NL	NL	160	160	100

Approximate Fundamental Period (T_a), in seconds,

$$T_a = C_t h_n{}^x \tag{B.8}$$

Where h_n is the height in ft above the base to the highest level of the structure and coefficients C_t and x are determined from Table B.13.

$$T_a = 0.02 * 69\ ft^{0.75} = 0.48 \text{ s}$$

Table B.13: Values of approximate period parameters C_t and x.

Structure Type	C_t	x
Moment-resisting frame systems in which the frames resist 100% of the required seismic force and are not enclosed or adjoined by components that are more rigid and will prevent the frames from deflecting where subjected to seismic forces:		
Steel moment-resisting frames	0.028 (0.0724)[a]	0.8
Concrete moment-resisting frames	0.016 (0.0466)[a]	0.9
Eccentrically braced steel frames	0.03 (0.0731)[a]	0.75
All other structural systems	0.02 (0.0488)[a]	0.75

[a]Metric equivalents are shown in parentheses.

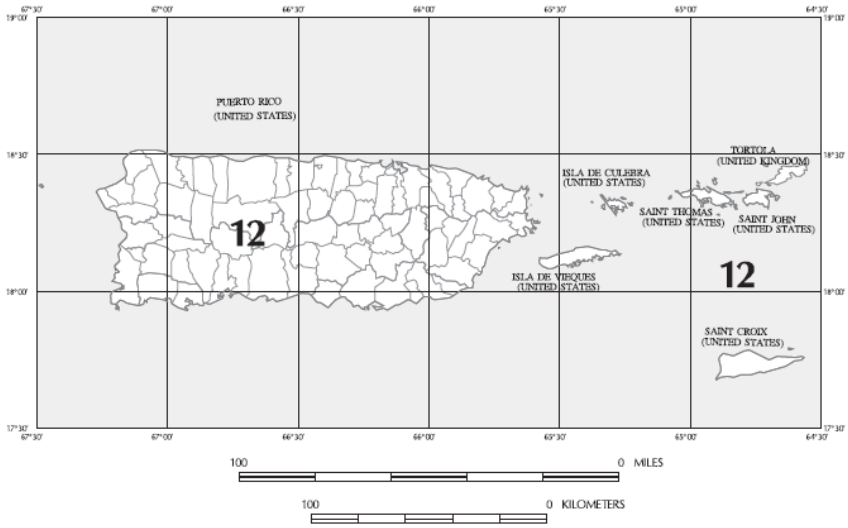

Figure B.7: Long-period transition period, T_L (sec.), for Puerto Rico, Culebra, Vieques, St. Thomas, St. John, and St. Croix.

The seismic response coefficient, *Cs* for $T < (S_{D1}/S_{DS})$

$$C_S = \frac{S_{DS}}{R/I} \tag{B.9}$$

$$C_S = \frac{S_{DS}}{R/I} = \frac{0.738}{2/1.5} = 0.554$$

The seismic base shear, V_{base} is obtained by the product of the seismic response coefficient and the total weight of the building,

$$V_{base} = C_s W_{building} \tag{B.10}$$

$$V_{base} = C_s W_{building} = 0.554 * 7{,}099.27 = 3{,}929.44\ Kips$$

The load distribution in each story is presented in Table B.14. A value of $k = 1$ was selected, since the fundamental period of the building is less than 0.5 seconds.

Table B.14: Lateral seismic loads distribution per story.

Story	W_i (kip)	h_i (ft)	$W_i * h_i^k$ (kip*ft)	F_i (kip)
6	139.18	69.00	9,181.87	152.52
5	1,259.63	57.50	69,385.62	1,152.59
4	1,425.12	46.00	62,949.84	1,045.69
3	1,425.12	34.50	47,356.47	786.66
2	1,425.12	23.00	31,706.87	526.70
1	1,425.12	11.50	15,970.27	265.29
Total	**7,099.27**		**236,550.95**	**3,929.44**

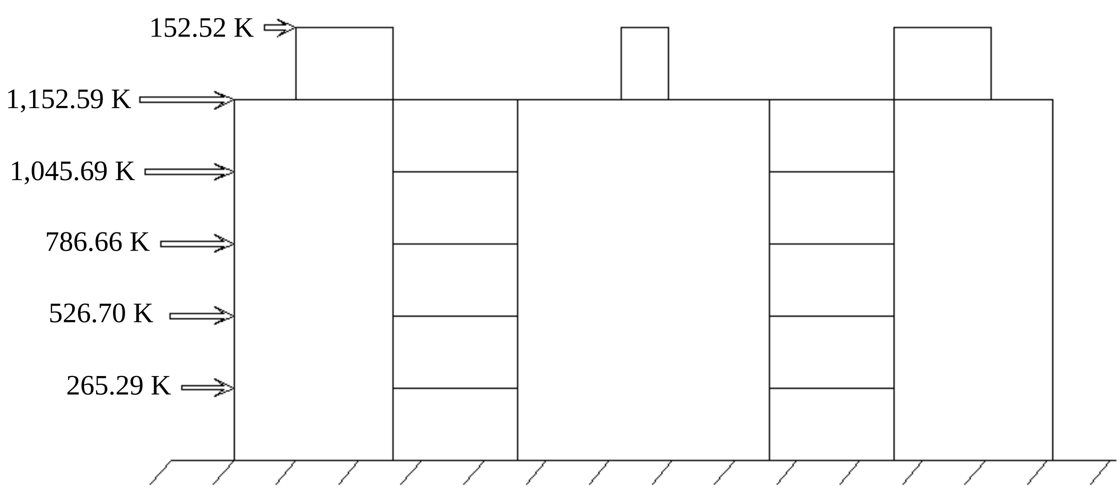

Figure B.8: Lateral seismic loads distribution per story.

APPENDIX - C STRUCTURAL DRAWINGS AND DETAILS

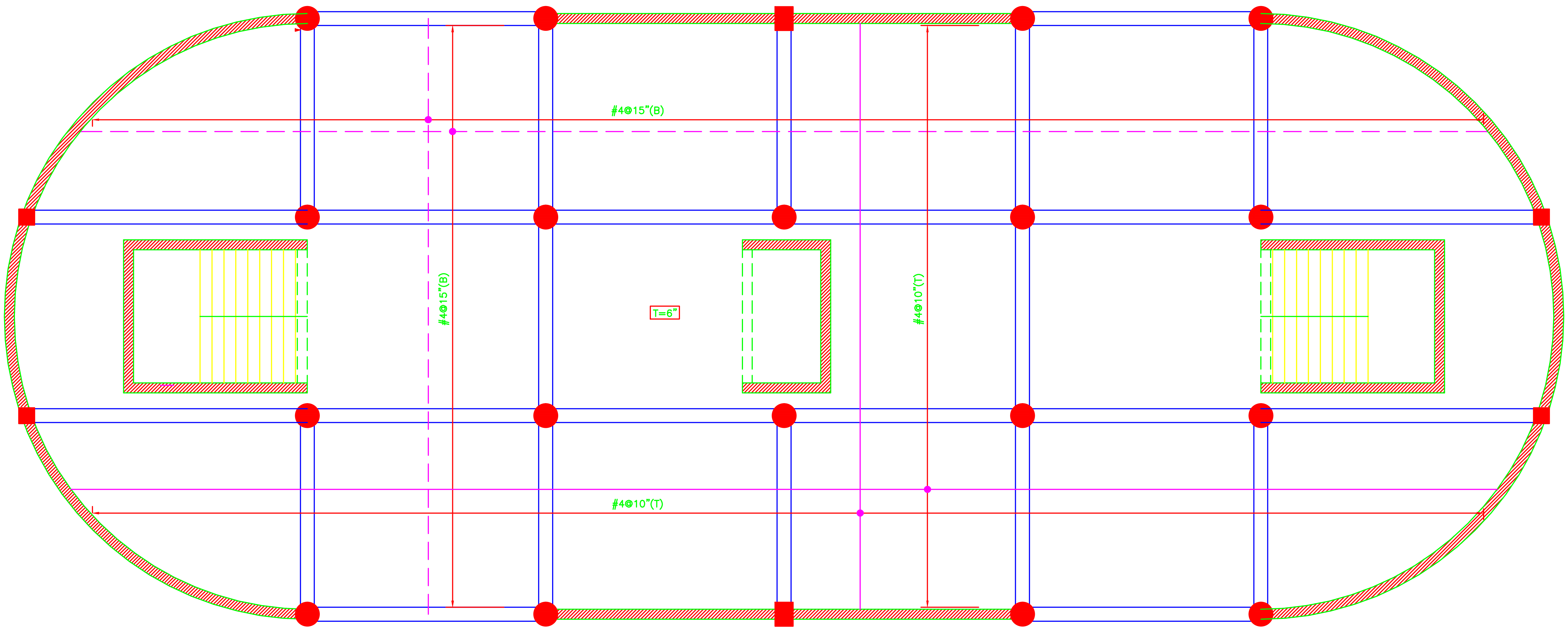

STRUCTURAL PLAN FOR STORIES 1 AND 2

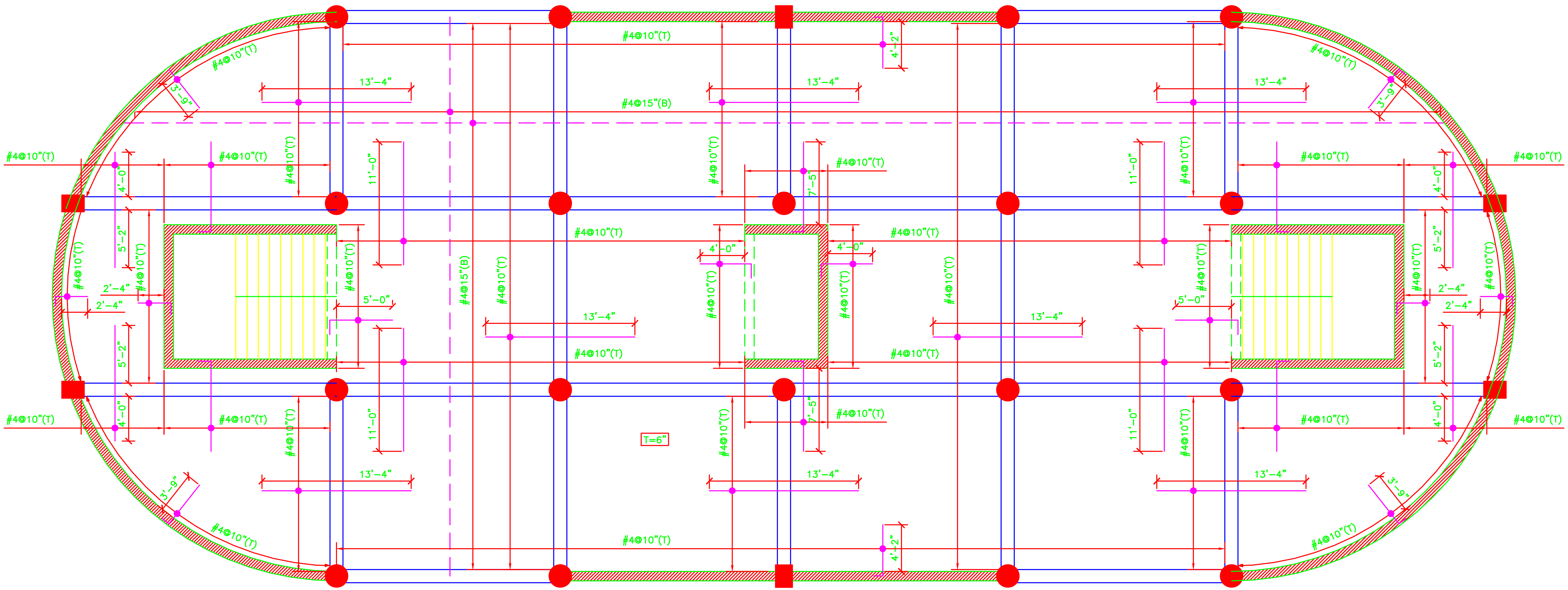

STRUCTURAL PLAN FOR STORIES 3 TO 5

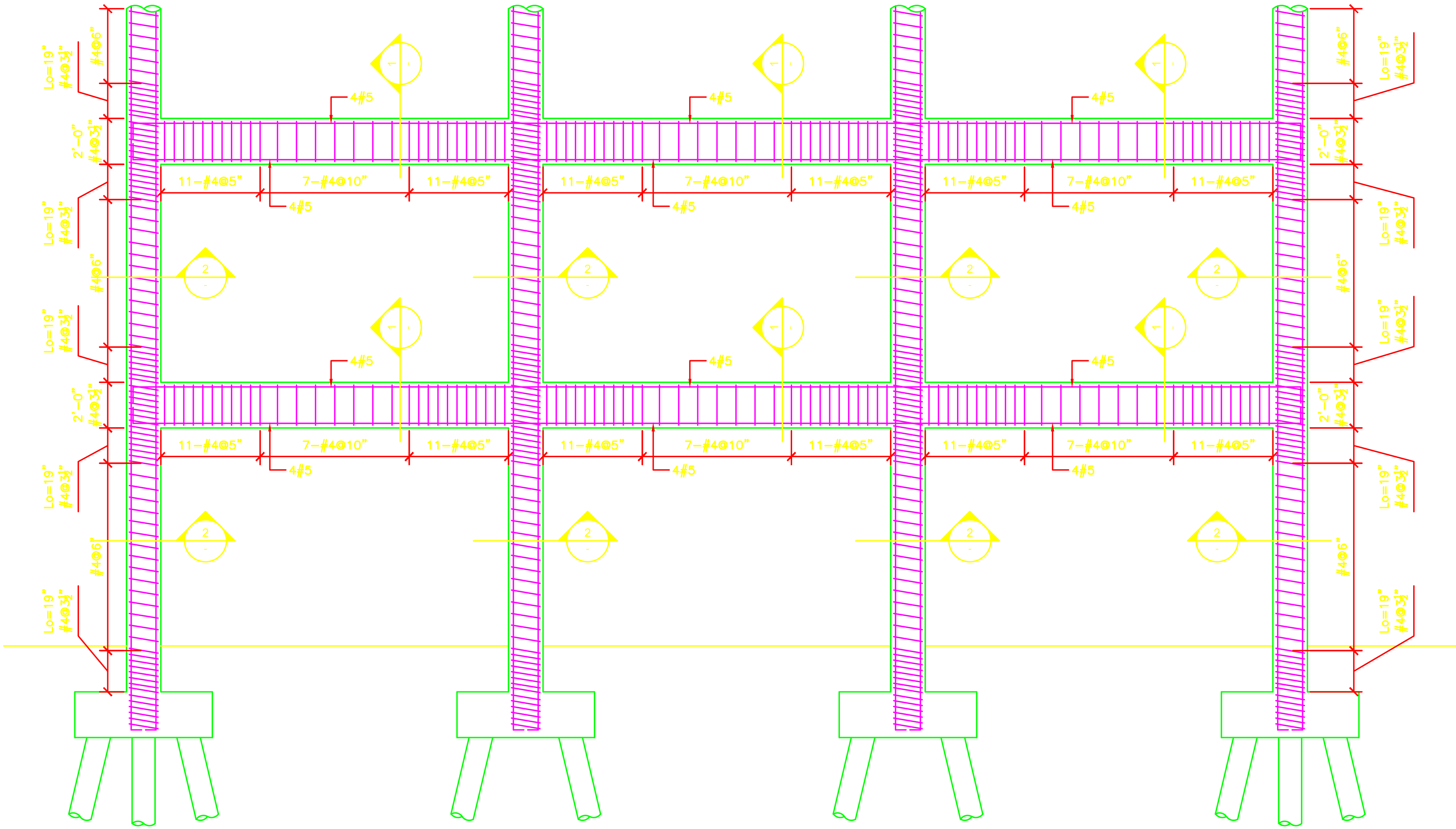

N-S PARTIAL FRAME STORIES 1 AND 2

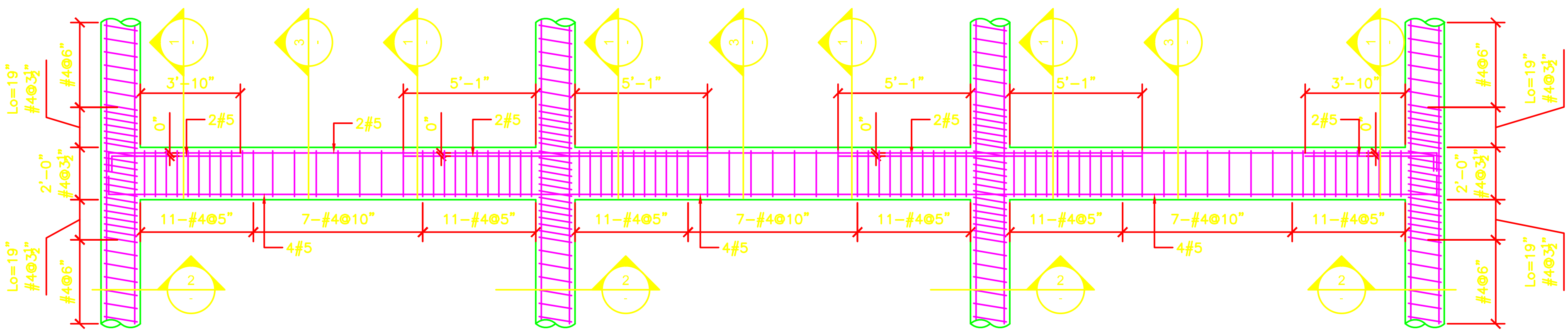

N-S DIRECTION BEAM ELEVATION FOR STORIES 3 TO 5

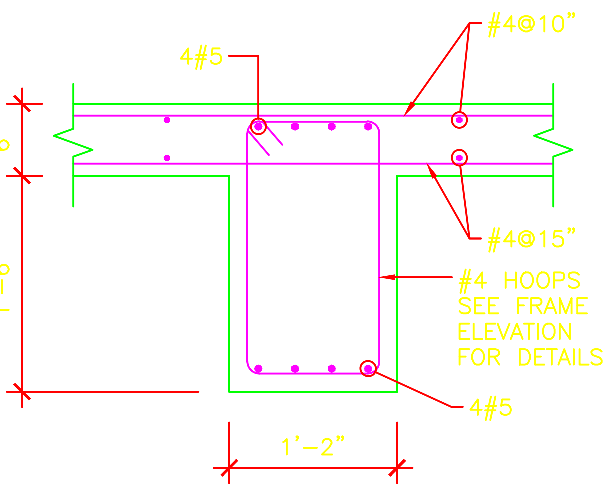

SECTION 1
SCALE: 3/4"=1'-0"

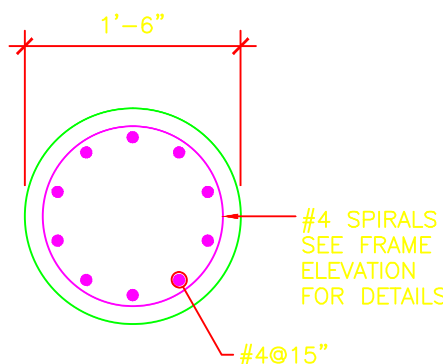

SECTION 2
SCALE: 3/4"=1'-0"

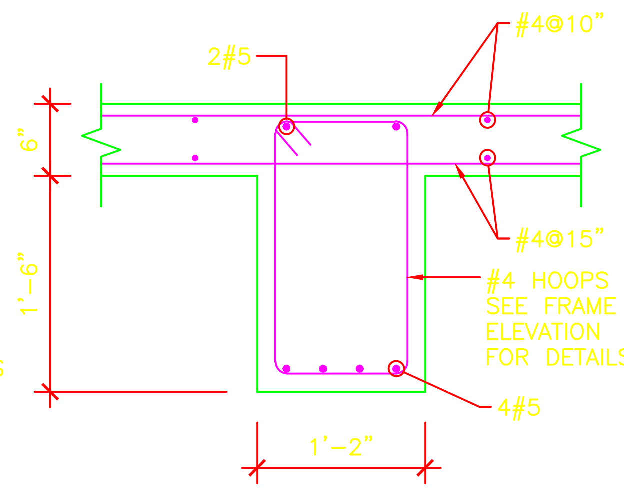

SECTION 3
SCALE: 3/4"=1'-0"

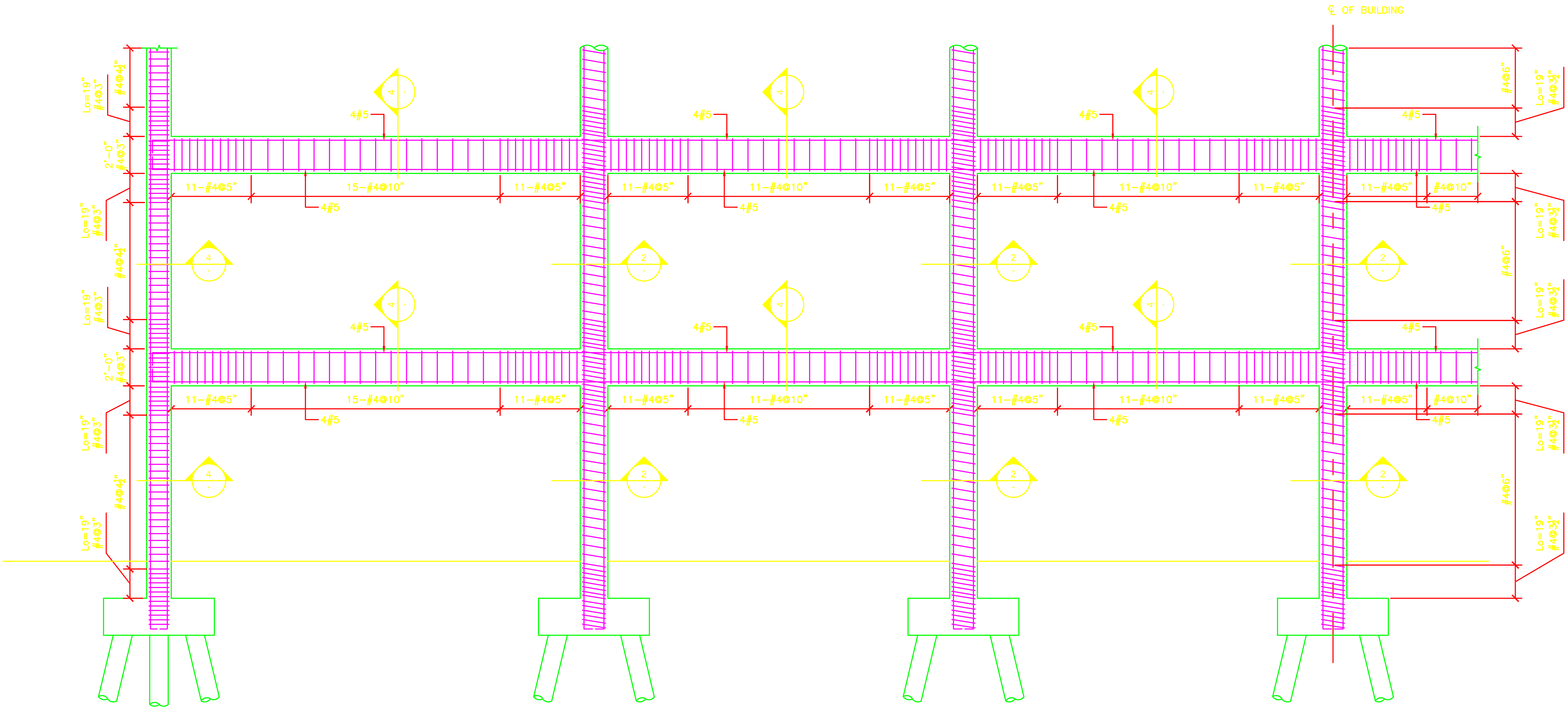

E-W DIRECTION BEAM ELEVATION FOR STORIES 1 AND 2

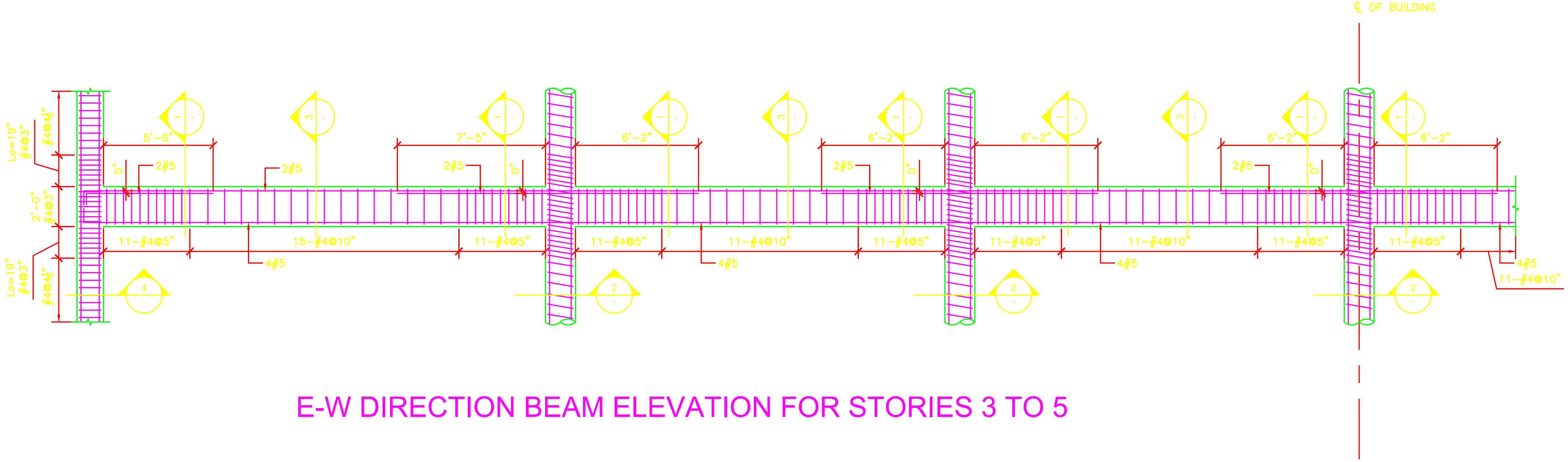

E-W DIRECTION BEAM ELEVATION FOR STORIES 3 TO 5

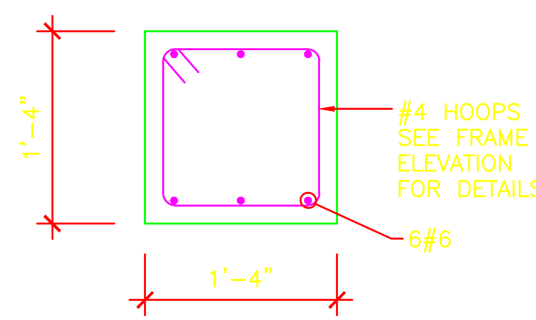

SECTION

SCALE: 3/4"=1'-0"

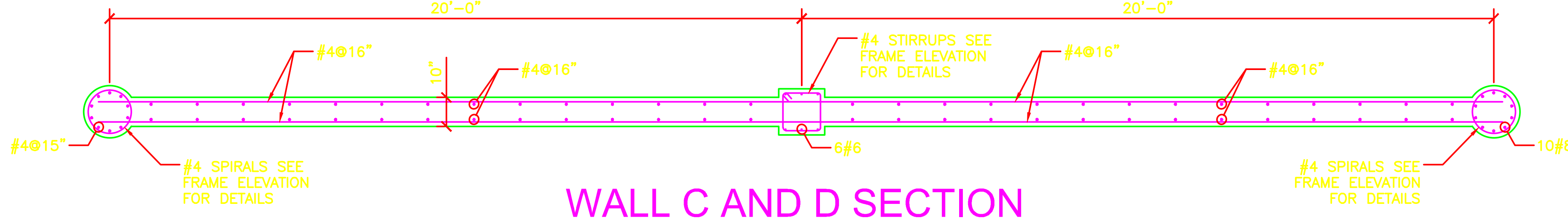

WALL C AND D SECTION

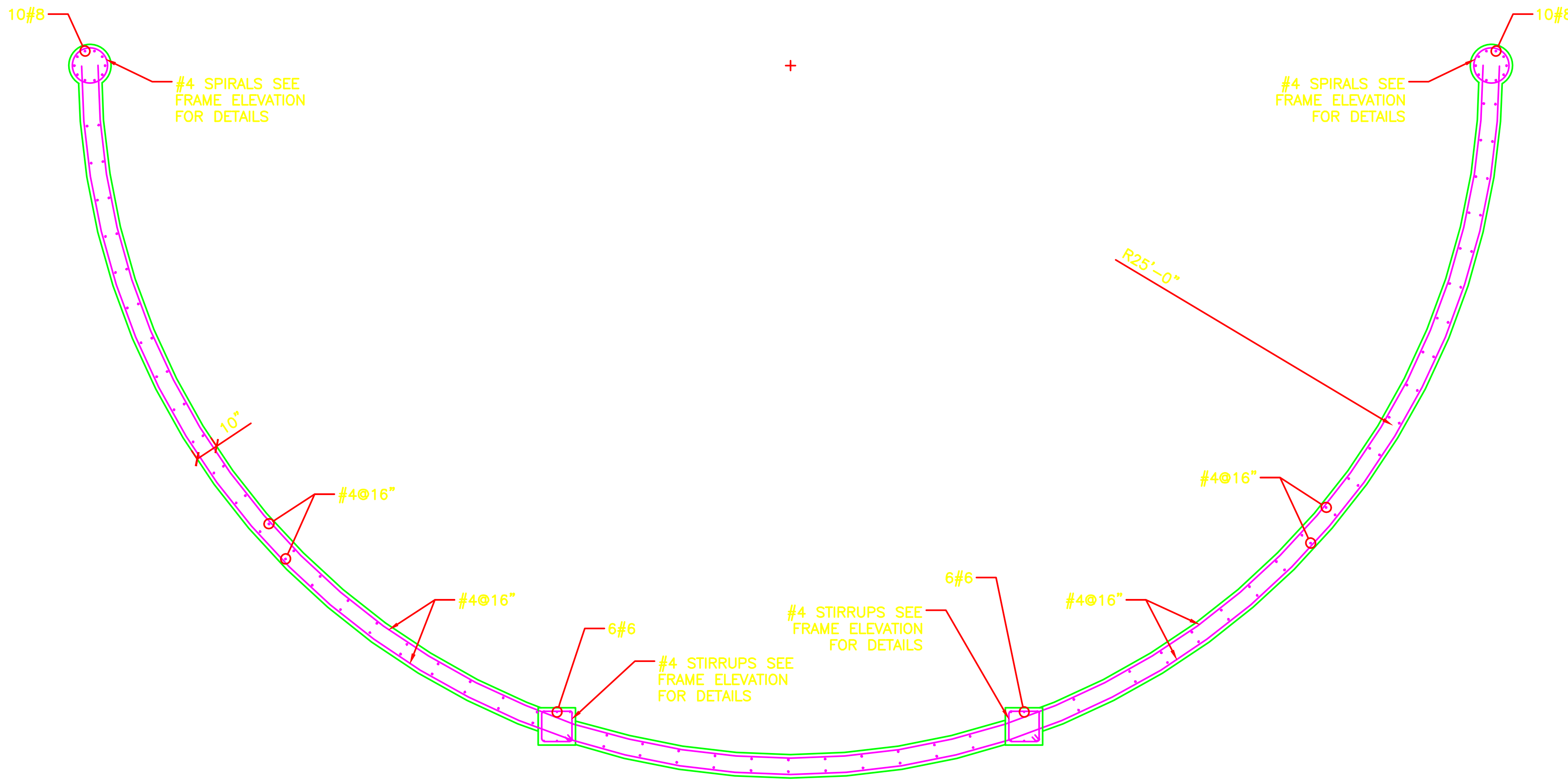

TYPICAL CURVE WALL SECTION

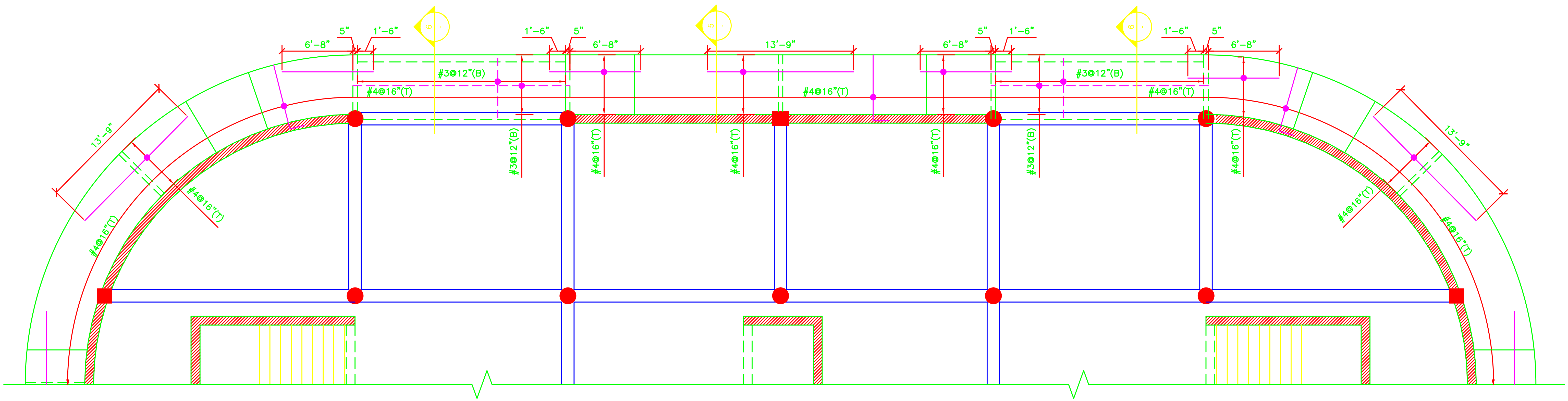

PARTIAL STRUCTURAL RAMP PLAN

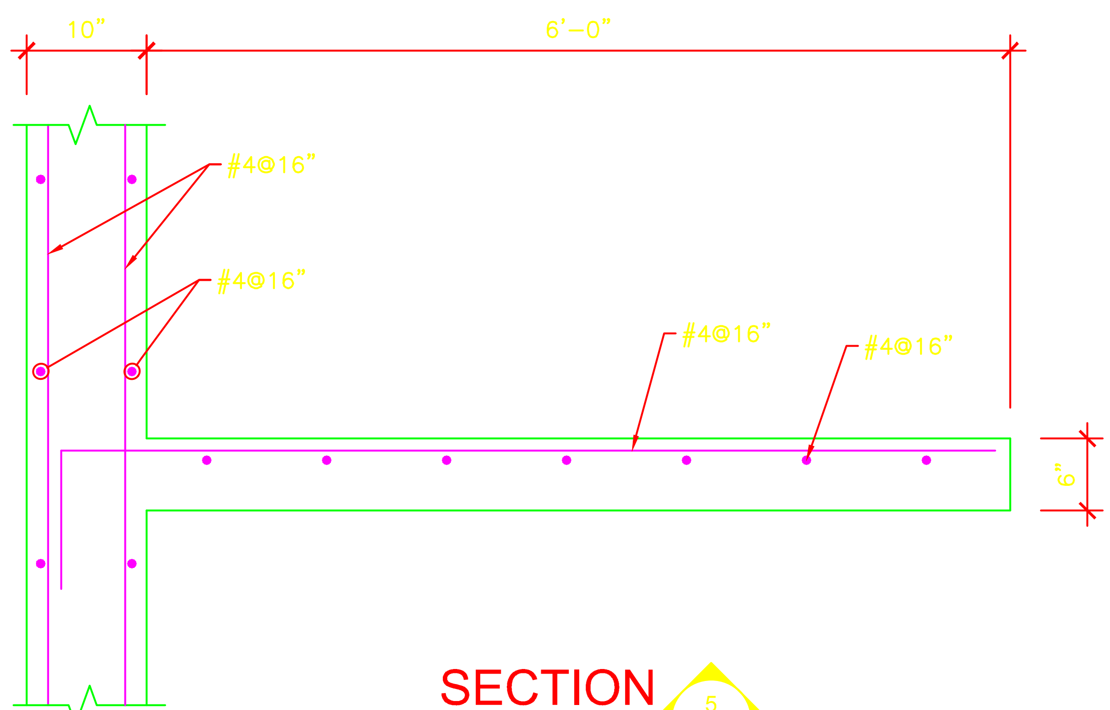

SECTION 5
SCALE: 3/4"=1'-0"

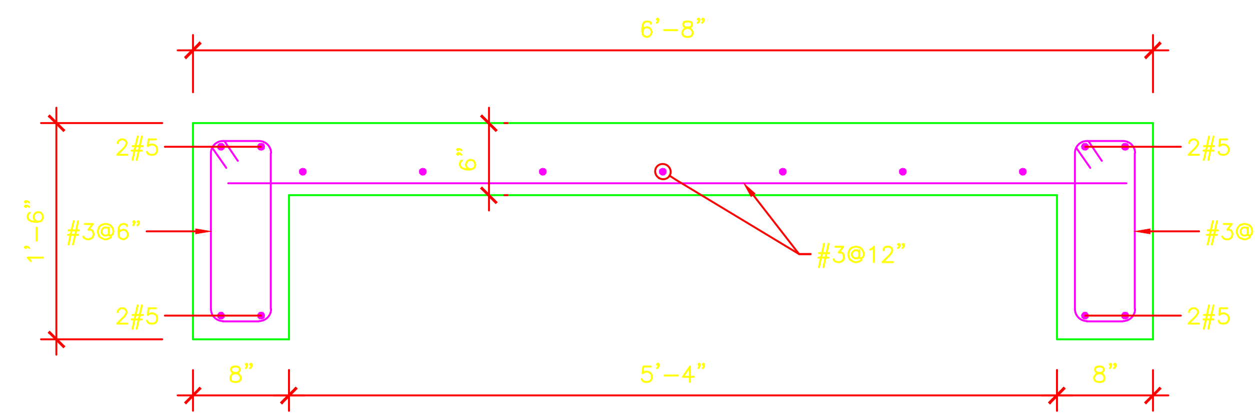

SECTION 6
SCALE: 3/4"=1'-0"

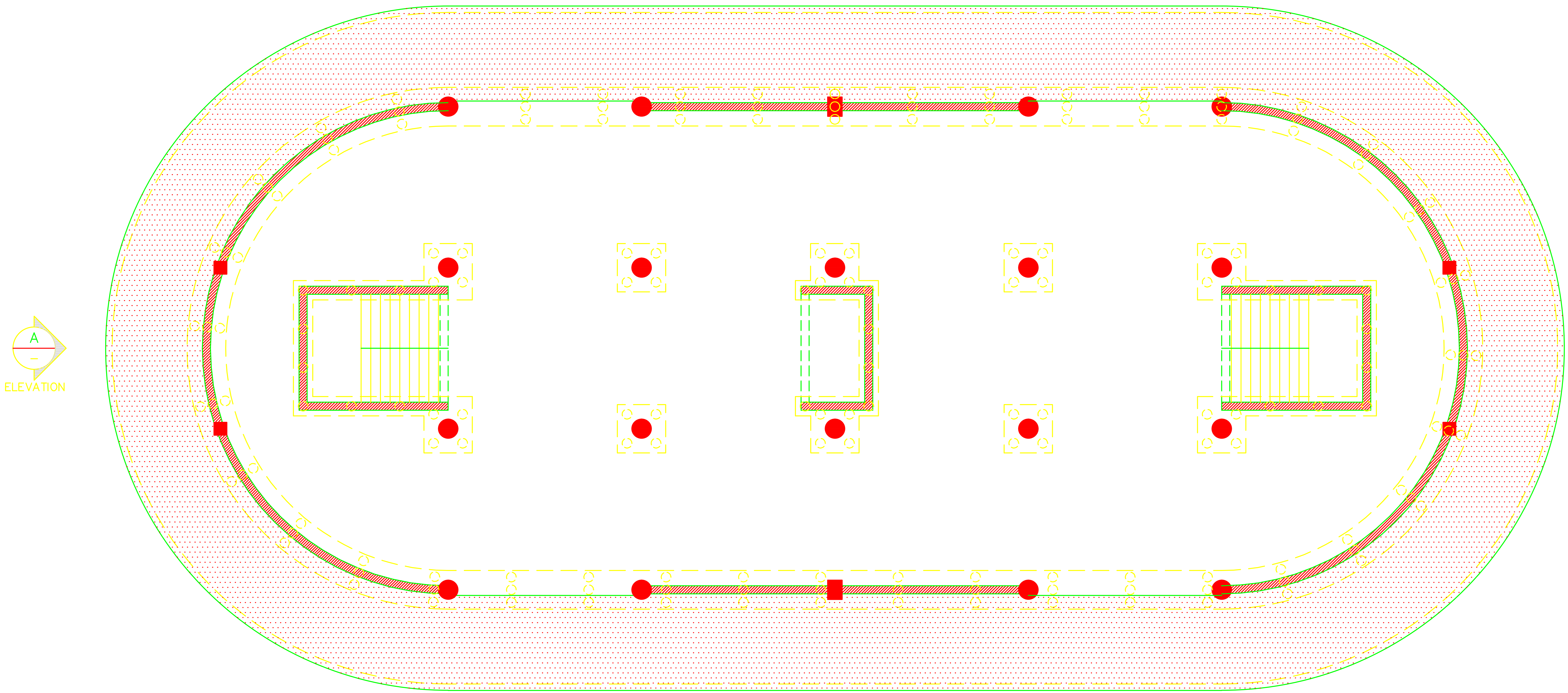

SUGGESTED FOUNDATION PLAN

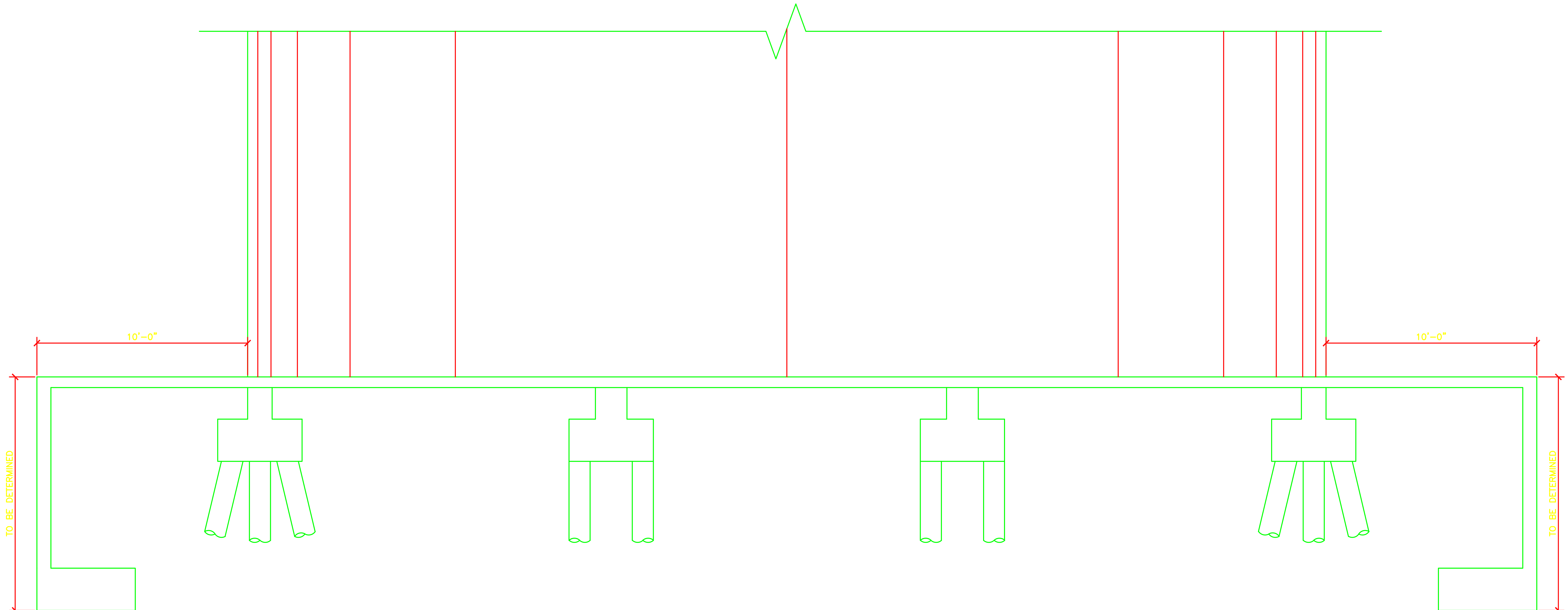

ELEVATION A